Durham E-Theses

Tectonic Evolution of the Prøven Igneous Complex within the Rinkian Fold-Thrust Belt, West Greenland: Investigation using 3D Photogrammetry

PHOEBE ROSE SLEATH

How to cite:

Use policy

Tectonic Evolution of the Prøven Igneous Complex within the Rinkian Fold-Thrust Belt, West Greenland: Investigation using 3D Photogrammetry

Phoebe Rose Sleath

This thesis is submitted as fulfilment for an MSc by Research in Geology, Department of Earth Sciences, Durham University, 2021

1

Contents

1. Abstract

The amalgamation of cratons and subduction of oceanic lithosphere in the Paleoproterozoic has formed linear orogenic belts worldwide, such as the little studied Rinkian fold-thrust belt on the west coast of Greenland. The Rinkian comprises a Paleoproterozoic shelf sequence formed on the margin of the Rae craton that was deformed by basement-core nappes in a high-grade deformation event at c. 1.82Ga. The northern part of the area affected by the Rinkian fold-thrust belt includes the Prøven Igneous Complex (PIC), a ca. 90 x 80 km large intrusive complex of orthopyroxene-bearing monzogranite to quartz monzonite, which was intruded between ca 1.87-1.9 Ga. The PIC was previously considered to be a syntectonic intrusion, so new work on the structural evolution is important. Here I use detailed photogrammetric mapping on 3D Stereo Blend at the GEUS Photogeological Laboratory in Copenhagen, combined with previous survey work, to identify the major deformation phases of the PIC and their associated structures. We found that the PIC formed as a large sheet intrusion which has been deformed by a westward verging thrust system, developing type II interference fold patterns. This is especially prevalent at the base PIC-metasediment contact, where incompetent rock – partially molten paragneisses and leucogranites – have resulted in more intense top to the west directed deformation. Furthermore, within the main PIC competent body a type I interference fold pattern has developed. Our results demonstrate that the PIC was likely emplaced in situ at shallow crustal levels, and then deformed by the Rinkian orogenic belt. This study has provided new insights into the deformation history of the Prøven Igneous Complex and the tectonic setting for the Rinkian fold-thrust belt overall. Furthermore, the project shows how remote mapping through photogrammetry can cover large areas in revealing detail.

2. Acknowledgments

3. Introduction

The North Atlantic and Rae Cratons are Archean crustal blocks accreted together in the Paleoproterozoic Eon, when the amalgamation of cratons and subduction of oceanic lithosphere formed linear orogenic belts worldwide (Fig. 3.1, St-Onge et al, 2009). Greenland contains many examples of Paleoproterozoic terranes, such as the little studied Rinkian on the west coast of Greenland (Figure 1A, St-Onge et al, 2009). The southern boundary of the Rinkian orogenic belt is the Disko Bugt suture just south of Disko Island, and the northern boundary is the margin with the Rae craton at Kullorsuaq (Escher & Pulvertaft, 1976).

Within the Rinkian Terrane is the Prøven Intrusive Complex (PIC), the largest magmatic intrusion by surface area in Greenland. The PIC is a 100km wide granitic intrusion emplaced at 1.90-1.87 Ga (Thrane et al 2005; Sanborn-Barrie et al 2017; Thrane, 2021 unpublished) into the Paleoproterozoic rocks of the Karrat Group, which overlie a basement of Archean orthogneiss, on the margin of the Rae Craton (Henderson & Pulvertaft 1987). Orientated NE from Disko Bugt to Melville Bugt, the Rinkian Fold Belt comprises of basement-cored nappes c. 1.83-1.82 Ga (Grocott & McCaffrey, 2017, Thrane et al 2005).

Understanding the origin and deformation history of the PIC, is key to understanding the plate tectonic model of the entire west coast of Greenland and across to Canada. Recent geochemical and geochronology results (Kokfelt et al 2021, unpublished), and fresh mapping of the area has spurred an effort to reinvestigate the origin and tectonic setting of the PIC based on systemic fieldwork undertaken by the Geological Survey of Denmark and Greenland (GEUS) from 2015-17 (Rosa et al. 2016; 2017; 2018).

This region was first mapped between 1967-79 at a scale of 1:100 000 by GEUS and detailed archive maps are available in the GEUS archives (T.C.R. Pulvertaft 1967; O. Stecher & J. C. Escher 1978-79; Grocott & Pulvertaft 1990,). Early work dated the PIC between 1.87 - 1.9Ga and established that the PIC was an A-type Granite (Sanborn-Barrie et al, 2017; Thrane et al, 2005). The PIC intrusion is an orthopyroxene-bearing granitic rock and so defined as charnockite which usually form in high-pressure settings (Frost & Frost, 2008).

The Upernavik-Prøven area spans from the Ikeq margin in the North to the southern coast of Kangeq 60km further South, and from Upernavik (settlement) in the West to the inland ice 95km to the East (Fig. 3.2). In this study, a new tectonic stratigraphy for the Upernavik-Prøven area is proposed and used to produce structural reconstructions of the subsurface, based on

state-of-the-art remote geological mapping. We present new photogrammetry data and interpretations relevant to the structural evolution of the PIC, both within the Rinkian Fold Thrust Belt and the tectonic setting of West Greenland.

Grenville orogen	Ice
Seal Lake Group	Palaeogene magmatic province
Ramah (RG) and Mugford (MG) groups	Phanerozoic orogens and basins
Mesoproterozoic plutonic suites	Gardar igneous province
Makkovik orogen	Mesoproterozoic basins including Thule basin (T)
Lac Lomier complex	Proterozoic basement
Lake Harbour Group	Julianehåb batholith
Tasiuyak gneiss	Ketilidian border zone and fore arc
De Pas batholith and basement	Prøven igneous complex
Burwell arc	Karrat and Anap nunâ groups
Labrador Trough	Inglefield mobile belt
Core zone, microcontinental fragment	Aasiaat domain
North Atlantic (Nain) craton	Rae craton
Superior craton	North Atlantic craton

Figure 3.1

A - Simplified geological map of Greenland modified from Escher & Pulvertaft (1995), showing principal tectonostratigraphic assemblages and structures discussed in the text. Extrapolation of geological boundaries beneath the Inland Ice (dashed lines) is constrained by the aeromagnetic data of Saltus & Gaina (2007). BaS, Baffin suture; BeS, Bergeron suture; DBS, Disko Bugt suture; NIS, Nordre Isortoq steep belt; SRS, Soper River suture; TgS, Tasiuyak gneiss suture. (St-Onge et al, 2009)

Figure 3.2

Geology of west-central Greenland adapted from Sanborn-Barrie et al, (2017)

(after Henderson and Pulvertaft, 1987 and modified from Connelly and Thrane, 2005)

DBS = Disko Bugt suture

SNF = Southern Nagssugtoqidian Front.

Inset map shows unreworked (dark grey) and reworked (light grey) Archean crust cut byPaleoproterozoic plutonic rocks of the Prøven (P), Qikiqtarjuaq (Q), and Cumberland (C) plutonic suites. NAC = North Atlantic craton; SUP = Superior craton; RAE = Rae craton

Red = Mapping Area

9

The objectives of this project are to fill a gap within the systematic mapping of West Greenland at 1:100,000 scale and to make detailed structural reconstructions to provide insight into; the internal deformation and structure of the PIC, the fold geometry and the original intrusion geometry, to establish if it is a pre-tectonic or post-tectonic intrusive complex. This is of crucial importance to developing structural reconstructions to understand the overall structural history of the area and to help constrain the Paleoproterozoic plate-tectonic model of the Canadian and Greenland margins of Baffin Bay. Mapping and petrology also provide context for the potential for economic geology opportunities in the area.

4. Geological Setting

The Prøven Intrusive Complex (PIC) is located on the West Coast of Greenland on the East side of Baffin Bay (Fig. 4.1). The PIC was first mapped in 1967 by T. C. R. Pulvertaft and then again from 1978-79 by J. C. Escher and O. Stecher of GEUS. Currently the GEUS 1:100000 published map series do not cover the main body of the PIC as shown in Figure 4.1, to the north is the Tassuisaq Map (Escher, 1981) and to the south the Pangnertôq map (1971).
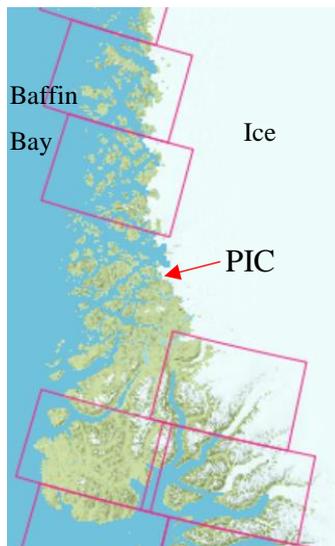
Figure 4.1 Current published GEUS 1:100,000 map sheets, missing coverage of the PIC

Originally the PIC was referred to as the Prøven Granite (Escher and Pulvertaft ,1968) and then renamed in 1978 as the Prøven Charnockite when fieldwork showed that it contained 5-15% hypersthene (Escher and Stecher, 1978). Most recently the term Prøven Igneous Complex has been adopted to cover the compositional variation within the units (Thrane et al, 2005). Initial dating suggested the PIC intruded into the Rae Craton at 1.9-1.87Ga, just before peak metamorphism in the Rinkian at c. 1.84 Ga (Connelly et al. 2006; Thrane, 2005; Sanborn-Barrie et al, 2017). This earlier commencement of intrusion casts doubt onto the previously

well-established model of a Cumberland-Prøven Intrusive Complex correlation across Baffin Bay, because the Cumberland Batholith has an age of 1.865-1.845Ga (Whalen et al, 2010). However new geochronology carried out in parallel with this project has found that the main components of the PIC were emplaced at c. 1870 Ma (Kokfelt et al, unpublished). Additionally, recent mapping and U-PB constraints have correlated the 1.90–1.88 Ga Qikiqtarjuaq plutonic suite on eastern Baffin Island with the PIC (Sanborn-Barrie et al, 2017). The PIC and the Cumberland Batholith are clearly very closely related within the large-scale Trans-Hudson Orogen (Fig. 4.4, Whalen et al, 2010; Kokfelt et al. 2021 (yet unpublished).
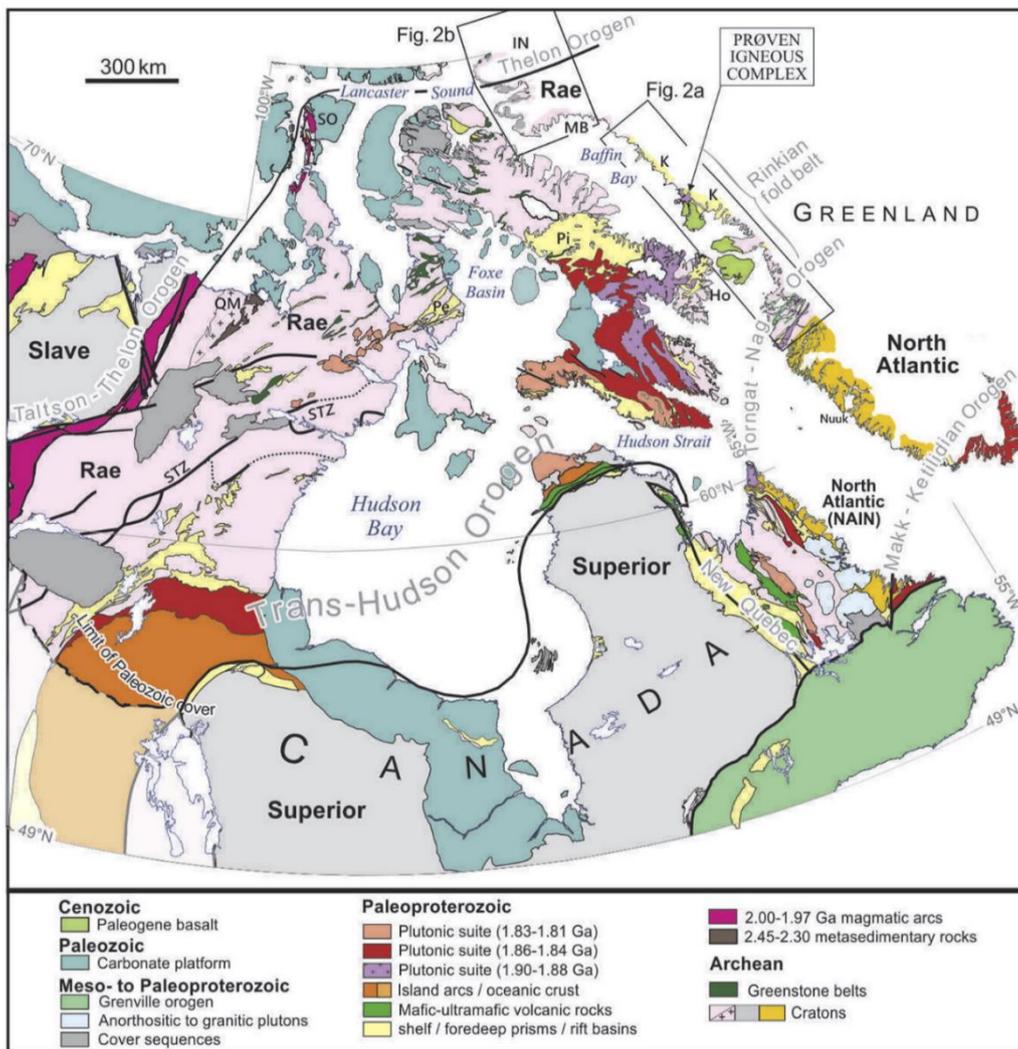
Figure 4.2 - Geological map of the Trans-Hudson Orogeny and the geological setting of the Rinkian Fold Belt and the Prøven Igneous Complex within Laurentia (Sanborn-Barrie et al, 2017)

Abbreviations: CB – Cumberland Batholith, Ho – Hoare Bay group, IN – Inglefield Mobile Belt, K – Karrat Group, Makk – Makkovik, MB – Melville Bugt; Nag – Nagssugtoquidian, Pe – Penrhyn Group, Pi – Piling Group, QM – Queen Maud granitoid suite; SO – Somerset Island, STZ – Snowbird tectonic zone.

The Trans-Hudson Orogen is a collisional belt across the top of North America separating the southern Superior Archean craton from an accumulation of smaller Archean cratons to the North such as the Rae Craton. (Hoffman, 1988; Lewry & Collerson, 1990) On the Eastern edge of the Rae craton lies the West coast of Greenland and the Rinkian fold-thrust belt (Whalen et al, 2010).

The Rinkian fold thrust belt is a Paleoproterozoic orogenic belt first recognised in 1976 by Escher and Pulvertaft. The host rocks of the distinctive Karrat Group were believed to have been deposited on the passive continental margin of the Rae Craton and lie to the South and North of the PIC (Escher & Pulvertaft 1976; Connelly et al. 2006). The Rinkian fold belt may be a continuation of the Nagssugtoqidian Orogen exposed to the south across Disko Bugt, which has a peak age of c. 1.84 Ga (Thrane et al 2003, Connelly et al. 2000; van Gool et al. 2002; (Connelly et al. 2006), suggesting the existence of an over 1000km wide Nagssugtoqidian-Rinkian Orogen (Connelly et al 2006). However, the interpretation of this combined large-scale orogeny is contested due variations in kinematic indicators between the two orogens (Grocott & McCaffrey, 2017). Transport direction within the Rinkian fold belt, indicated by regional stretching fabric, orientates WNW-ESE to WSW-ENE (Grocott & Pulvertaft, 1990). Transport direction in the Nagssugtoqidian trends N-S during convergence of the Rae and North Atlantic cratons, meaning the transport directions are perpendicular to each other (Grocott & Pulvertaft, 1990). There is also difference in structural style, the Nagssugtoqidian is more upright and intensely folded whereas the Rinkian shows an open dome and basin like structure (Grocott & McCaffrey, 2017). Significantly, the Nagssugtoqidian shows a reorientation of major structures during late strike-slip events at c. 1.84Ga, which are not present in the structural evolution of the Rinkian (Grocott & McCaffrey, 2017). The Rinkian was not formed by north-south convergence, and therefore does not continue the trend of Nagssugtoqidian structures to the north (Grocott & McCaffrey, 2017). Unlike the Rinkian, the Nagssugtoqidian Orogeny has been well studied and there have been many attempts to integrate it into the tectonic setting of North America and Greenland (Hoffman 1990; van Kranendonk et al. 1993; Corrigan et al. 2009; St.-Onge et al. 2009; Partin et al. 2014; Wodicka et al. 2014).

As the geology of the Upernavik Isfjord is investigated and the tectonic setting constrained, the relevance of understanding the PIC increases. Due to the large quantity of inland ice covering Greenland, and Baffin Bay across to Canada, only a small sliver of the geology along the West Coast of Greenland is exposed, and any potential subduction suture line is hard to constrain.

5. Methodology & Data Sources

When making a geological map, the survey needs to consider the three parameters of time, cost and quality. Fieldwork expeditions to Greenland are usually long, at least 2 months each year, and costly, with many resources spent on transport, accommodation and food. By reducing the length of time in the field to predominantly data collection and increasing amount of interpretation covered in the lab we reduce the overall cost of the map. The obvious way to do this is through photogrammetry.

This method was first used by the U.S Geological Survey (USGS) in 1904 by C.W. Wright and F. E Wright producing topographic surveys in Alaska (Thompson, 1952). By the 1950s practically all the USGS's mapping projects involved photogrammetry to some extent (Thompson, 1952). GEUS' first use of photogrammetry in Greenland was of the Paleoproterozoic Karrat Group in West Greenland (Henderson & Pulvertaft, 1987). This area was recently reassessed by GEUS as part of an effort to revise the geological map sheets and to assess the potential for photogrammetry across Greenland (Sørensen & Guarnieri, 2017).

5.1 Archive Maps

The GEUS archive maps were produced in 1967 by T.C.R. Pulvertaft and in 1978-79 by O. Stecher and J. C. Escher. They are a series 1:40,000 scale unpublished field maps of much of the area, especially along the west coast where the islands are more accessible than the remote mountains inland (Fig. 5.1).

There are a total of 11 archive maps, which have been scanned and are publicly available on the GEUS Greenland Portal (http://www.greenmin.gl/). As shown in Figure 4.1 the maps contain detailed coastal mapping, inland interpretations and notes in both English and Danish. Some terminology is out of date due to a substantial advancement in understanding since 1980. Often the notes by different geologists may contradict each other, so either the interpretation has been revised with photogrammetry or where this was not available the 1978-79 data was preferred. The maps are hard to read due to handwriting, crossing out and fading due to ageing (Fig. 5.1).
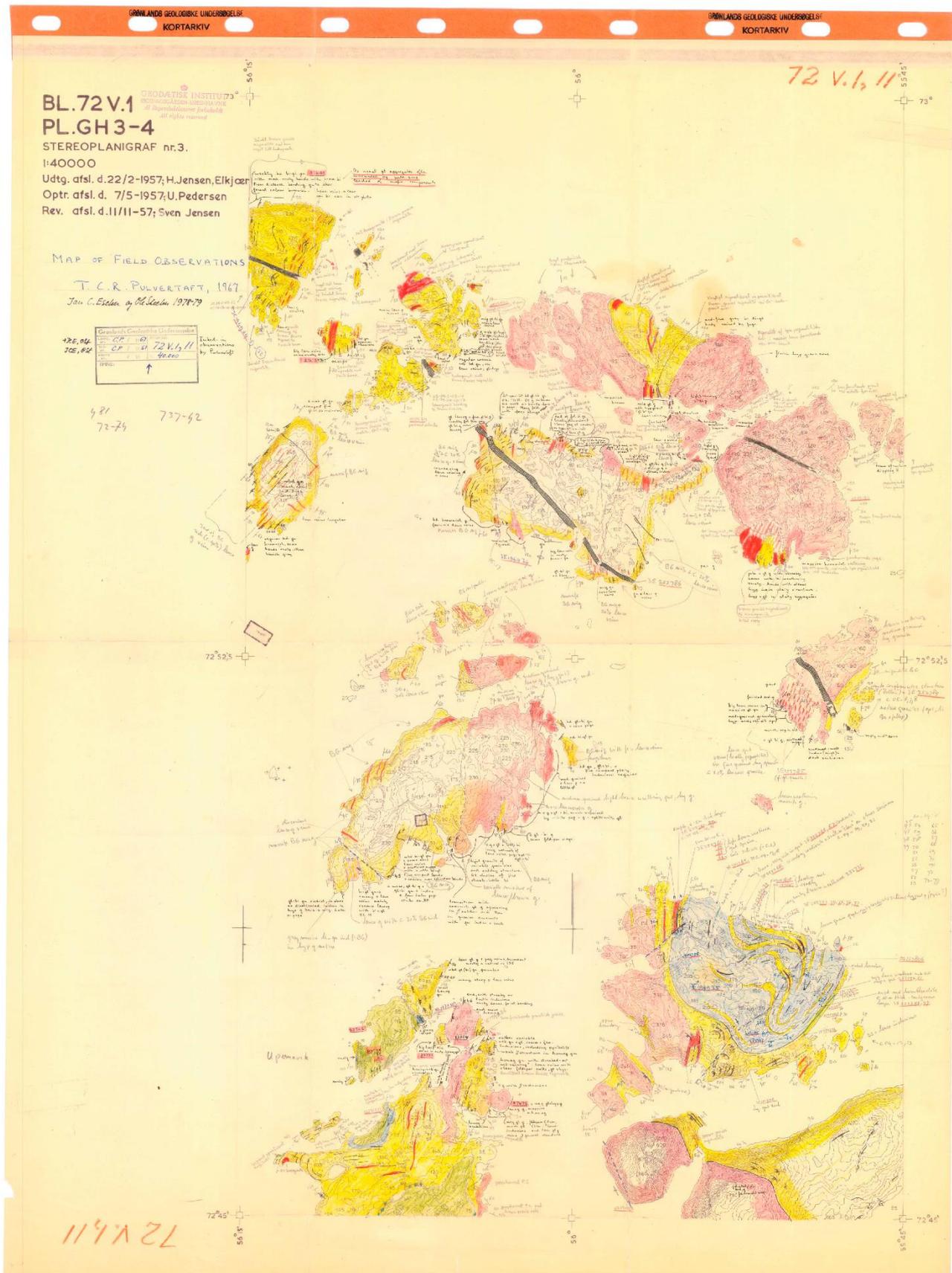
Figure 5.1 – Archive Map 72V1 011

T.C.R. Pulvertaft (1967) and O. Stecher & J. C. Escher (1978-79)

14

5.2 Aerial Images

From 28th August - 2nd September 2018, the GEUS field team took over 40,000 high-definition images across the area from a helicopter (Fig. 5.2). Each photo has geographical data and represents 50-60MB of raw data. Overall detail is excellent, foliation and bedding planes in the lithologies can be observed but small-scale mineral fabrics are too small.

Figure 5.2 – During field work new stereo imagery is normally collected from helicopters or boats but could also be collected from smaller fixed-wing aircraft, drones or while walking. (Sørensen & Dueholm, 2018)

5.3 Photogrammetry

Photogrammetry analysis was completed using the 3D Stereo Blend software package at the Photogeological Laboratory in the Department of Petrology and Economic Geology at the Geological Survey of Denmark and Greenland (GEUS). This study follows much the same workflow as the recently published paper reported by Sørensen & Dueholm (2018). In summary, the raw images taken by helicopter in 2018 have been compiled into flightlines and registered with Global Navigation Satellite Systems (GNSS) (Sørensen & Dueholm, 2018).
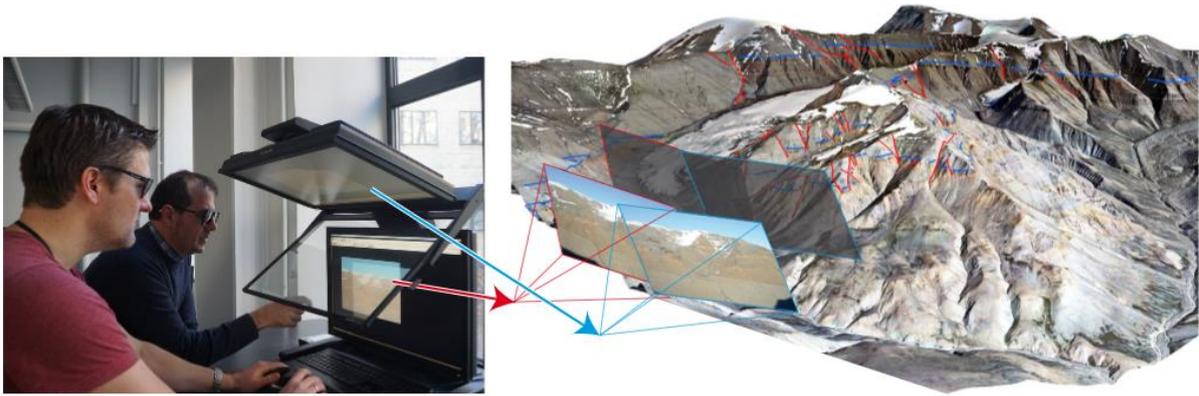
Figure 5.3 – The geologist at work in the Photogeological Laboratory. The stereoscopic model is displayed on a 3D monitor system that is well suited for full-day working. The stereoscopic model can be observed simultaneously by several viewers; this makes it easy to illustrate and discuss geological observations and ideas, which is beneficial for the geological interpretation. (Sørensen & Dueholm, 2018)

The images are then prepared by identifying the same points which overlap in different images and positioning the image in "real-world" space (Sørensen & Dueholm, 2018). A 3D model is produced in Agisoft Photoscan, and then placed into 3D Stereoblend (Sørensen & Dueholm, 2018). A standard workflow for processing the raw images for geological interpretation is outlined in Figure 5.4 (Sørensen & Dueholm, 2018). The model is then viewed two images at a time, to maintain image quality, and is available for geological interpretation by tracing features onto the model (Sørensen & Dueholm, 2018; Fig. 5.3). Outcrops can be viewed from different distances and angles, even from different flight lines in some places. The software can then calculate measurements such as strike, dip, length etc. Multiple features can be mapped and sorted into different groups of polylines such as lithological boundaries, dyke margins, foliation, bedding planes and deformation bands.
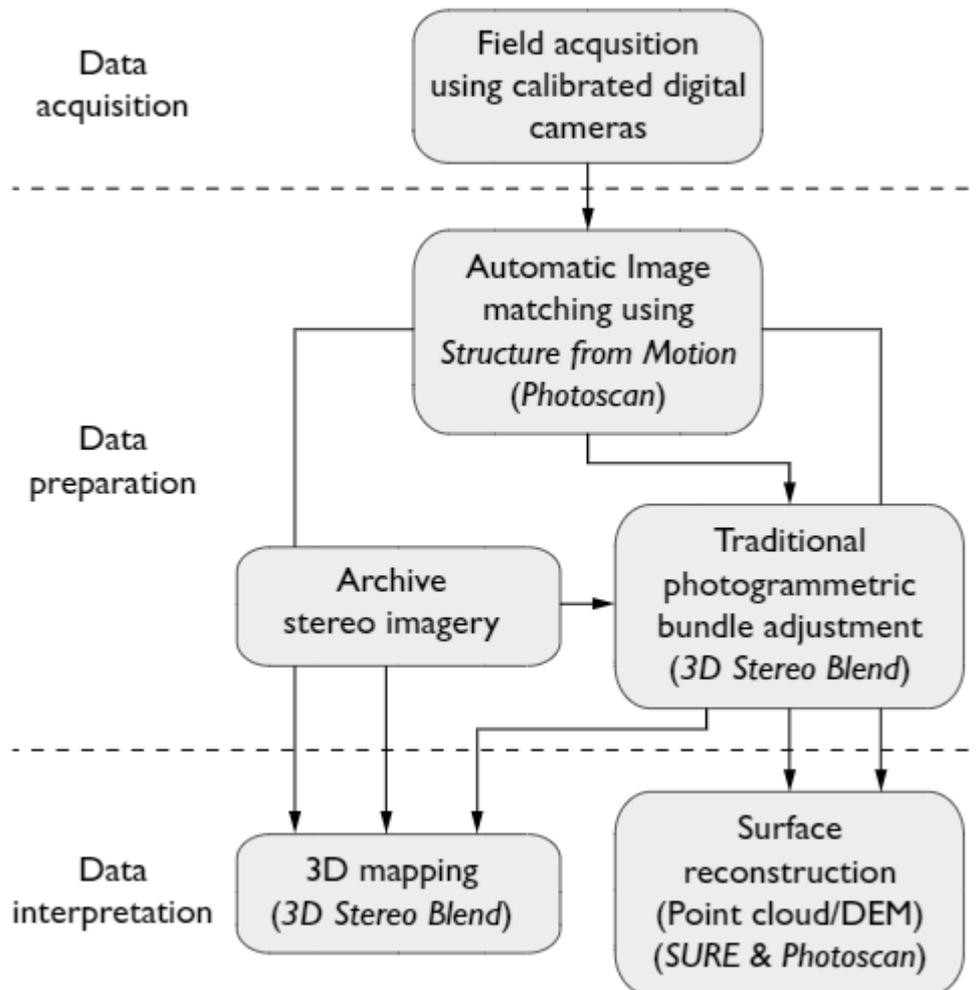
Figure 5.4 – Schematic flow diagram summarising the typical 3D-mapping workflow from data acquisition to photogrammetric data preparation and interpretation. (Sørensen & Dueholm, 2018)

5.4 GIS

The final geological map was compiled using ArcGIS Pro to form a large-scale 2D geological map by uploading the data produced from the photogrammetry and the aerial imagery. The ArcGIS Project is set up with the projected coordinate system of WGS_1984_Complex_UTM_Zone_22N. The extent of the base map is 8.8908357°N, 140.9695449°W, 38.9695449°E, 8.8908357°S. Polylines from the photogrammetry work were uploaded to base map and then used to produce boundaries. The photogrammetry derived polylines were then converted to structural measurements in useful positions for the map, and then integrated with archive measurements (Fig. 5.5).

Dataset Type	Number	Author
Archive Data	625	Selection from scanned maps by T.C.R. Pulvertaft (1967) and O. Stecher & J. C. Escher (1978-79)
Photogrammetry Data	288	Polylines converted to strike and dip measurements for map
Polylines from Photogrammetry	3345	Data produced on 3D Stereoblend

Figure 5.5 – Volume of each dataset produced to make the map

Satellite imagery was used to assist with mapping boundaries inland or where flight lines did not yield useful images due to visible changes in rock colour, weathering, aspect etc. These data were procured from the Sentinel-2 satellite system which is part of the European Space Agency's Copernicus Programme. Bands 2, 3 and 4 were merged on ArcGIS to form high-definition satellite imagery for the entire area. These images were instrumental in mapping inland, in areas where there was a lack of flight lines and large-scale fracture systems such as dykes and faults. The main limitation with the aerial imagery was spatial resolution, as the images are of exceptionally high quality and colour with no cloud coverage or snow (Fig. 4.6).

Dataset	Spatial Resolution
Sentinel-2 Aerial Imagery	10m
Google Earth Aerial Imagery	30m
GEUS Photogrammetry	Varies depending on distance between camera and outcrop. 14 mm at 100m distance

Figure 5.6 – Spatial Resolution for each dataset

5.5 Cross Sections

Cross sections were produced using both the 3D Stereo Blend software and traditionally hand drawn via ArcGIS Pro. On Stereo Blend a topographic profile needed to be produced as a polyline as the topography was not set on the system. This is then converted to a profile by the software. For the hand drawn sections, the topography was taken from the contouring on the archive maps which were overlain with the new updated geological map. Many cross sections

were drawn and coloured, and hand drawn was preferred as they can be produced away from the photogeological lab, easily edited and easy to extrapolate into the subsurface. These were used to decide the extent to which folds and thrust faults had produced the outcrop patterns in the PIC region. Cross sections were produced directly from measurements from the ArcGIS project and scaled onto the paper, which was very successful. Dip was calculated using the closest geological measurement and plotted using a protractor. As it was difficult to incorporate all the features into single straight cross sections, composite dog-legged section lines were drawn. The sections are drawn from generally in a west to east direction, which is perpendicular to the latest stage of folding. 2D sections do limit 3D understanding but 3D figures have been produced to help visually understand the complexity of the deformation. The cross sections were key in developing the map and inferred boundaries across fjords. They also helped to identify the location of thrust faults and other structural features such as anticlines and synclines, which allowed the map to be further fine-tuned.

The standard set of geometrical parameters were used to constrain geological style such as the geological rules of cross sections e.g., thrusts cut up section through a duplex structure justified by antiformal stack. Partial restorations were produced to test geological models and cross sections (Grocott & McCaffrey, 2017).

6. Tectonic Stratigraphy of Prøven-Upernavik

A regional tectonostratigraphy of the area from Karrat Fjord in the south, to Inugsulik Bugt in the north has been developed using a combination of mapping from fieldwork and photogrammetry interpretation (Fig 6.1; Fig 3.2). Many of the contacts were strongly tectonised during the Rinkian deformation events.
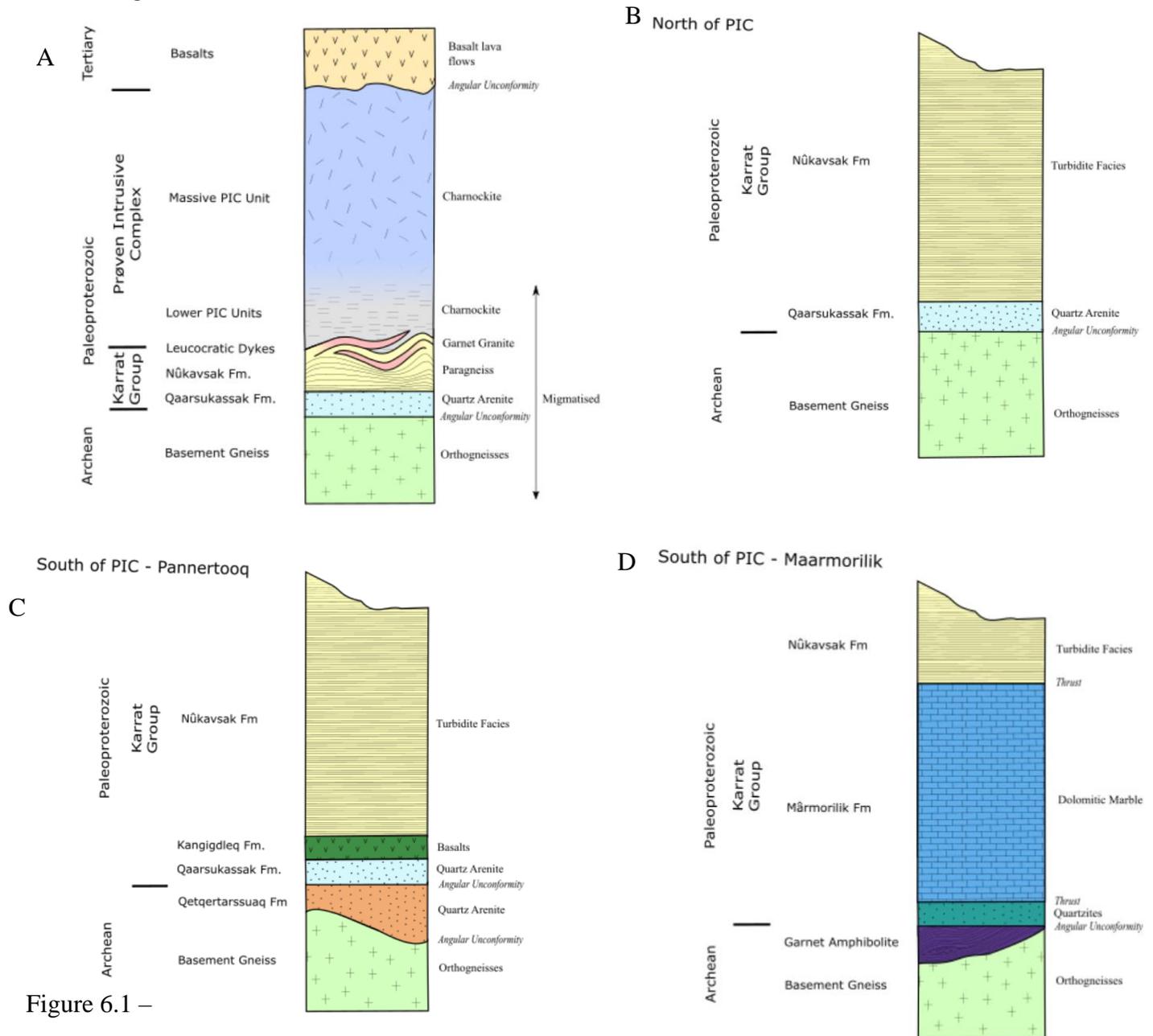
Figure 6.1 –

Tectonostratigraphic Columns Upernavik Isfjord based on proximity to the PIC

A – Central PIC area

B – North of the PIC

C – South of the PIC – Pannertooq

D – South of the PIC – Maarmorilik

B, C & D adapted from Tectonostratigraphic sections representing major tectonic units of the Rinkian Orogen in the Karrat area, Figu43 83, Rosa et al (2017)
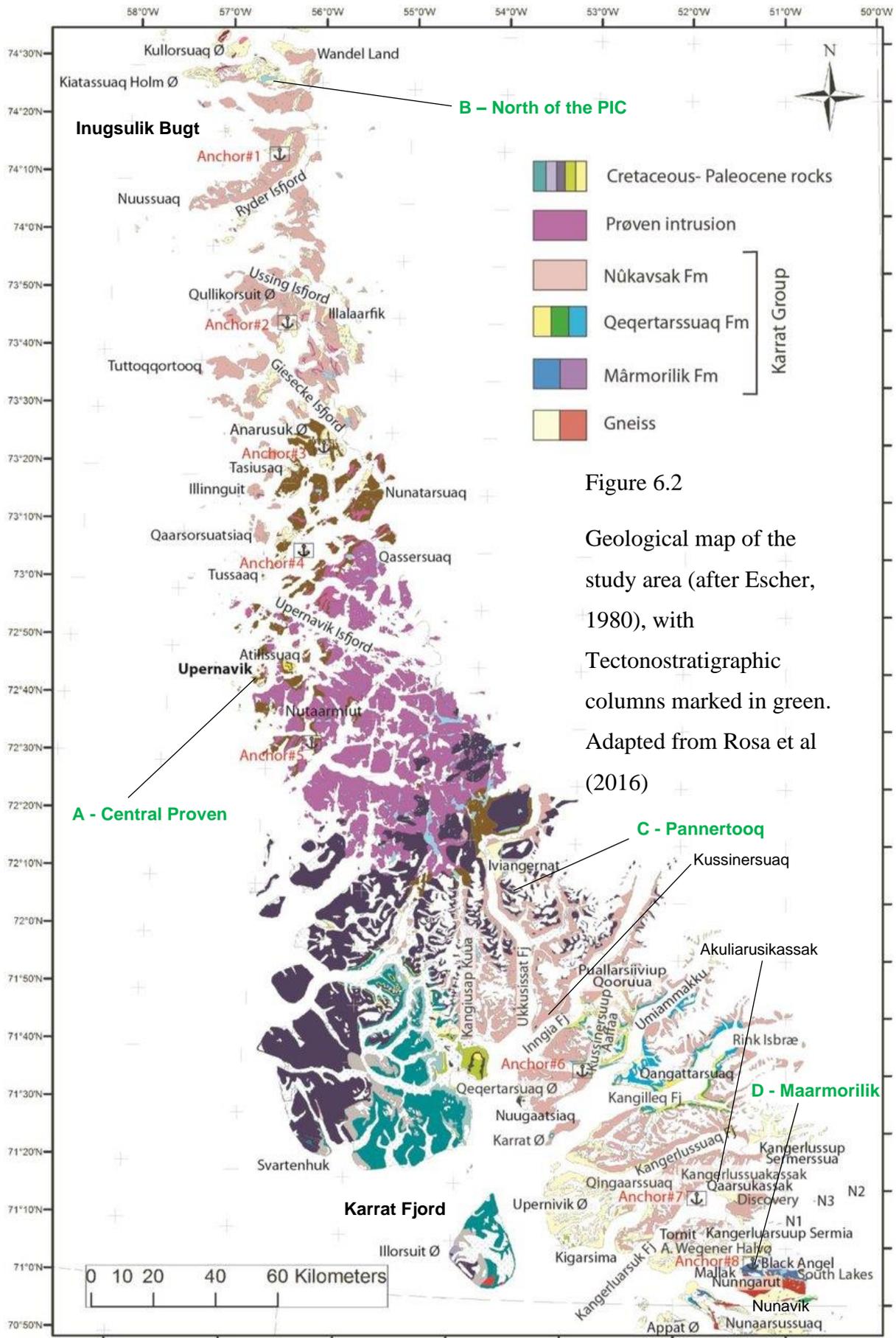
Figure 6.2

Geological map of the study area (after Escher, 1980), with Tectonostratigraphic columns marked in green. Adapted from Rosa et al (2016)

6.1 Archean Orthogneisses

The area from western Greenland to eastern Canada is assumed to be underlain by a basement of Archean orthogneisses belonging to the Rae Craton (Fig. 4.2). The orthogneisses are reworked from protoliths of biotite-hornblende tonalite, granodiorite, diorite, and amphibolite dykes (Sanborn Barrie et al 2017). The protoliths to these gneisses have been dated between 3.10–2.98 Ga (U-Pb; Thrane unpublished data; Connelly et al., 2006). Imprecise Rb-Sr whole rock dating of the orthogneisses at an age of *c*. 1.9 Ga has been interpreted as showing that the basement was strongly deformed and metamorphosed in the Rinkian belt to metatexite or diatexite migmatites (Kalsbeek, 1998). The melanosomes are amphibole-rich and the leucosomes contain plagioclase, quartz, hornblende, clinopyroxene and garnet (Rosa et al. 2017).

6.2 Archean Metasediments

Overlying the orthogneisses are a tectonically interleaved series of Archean orthogneisses and Paleoproterozoic metasediments (Fig. 6.1). These rocks have been metamorphosed to amphibolite facies increasing to granulite facies when proximal to the PIC (Grocott & Pulvertaft, 1990).

6.2.1 Qeqertarssuaq Formation

The Qeqertarssuaq Formation is found in the region to the south of the PIC (Henderson & Pulvertaft, 1987; Escher, 1995) (Fig. 6.1 C, Fig 6.2). An angular unconformity over the basement orthogneisses underlies a 500m thick sequence of paragneisses, schists and amphibolites developed from mostly quartz arenites with a few carbonates (Guarnieri et al. 2016; Henderson & Pulvertaft, 1967). The formation mainly crops out around Kangilleq and the peninsula between Umiammakku Isbræ and Inngia Fjord (Escher, 1995; Fig. 6.2). This formation is presumed not present in the region north of the PIC on lithostratigraphic grounds, due to the presence of carbonates in the quartz-arenite dominated lithologies. South of the PIC, a lack of Paleoproterozoic detrital zircons in the metasediments have led to its assignment to the Archean (Rosa et al. 2017).

6.3 Karrat Group

The Paleoproterozoic metasediments are known as the Karrat Group, which was first identified on Karrat to the south of the PIC (Fig. 6.2; Henderson & Pulvertaft, 1987). The Paleoproterozoic metasediments underlying the PIC and to the north show strong similarities and therefore the stratigraphy has been applied across the Central PIC region (Escher 1983;

Escher 1995). However, there are variations across the area which have been highlighted using the different tectonostratigraphic columns in Figure 6.1.

5.3.1 Karrat Group South of the PIC

South of the PIC, the Karrat Group consists of a base of either interlayered, dominantly quartz arenite, units – the Qaarsukassak Formation – or a dolomitic marble unit – the Mârmorilik Formation. These are overlain by a volcanic unit – the Kangilleq Formation – and then a thick cap of turbidite facies rocks (Henderson & Pulvertaft 1967; Escher & Stecher 1978, 1980; Fig. 6.1 – C & D).

5.3.1.1 Mârmorilik Formation

The Mârmorilik Formation is a 300m-thick shelf sequence of predominantly dolomitic marble, with horizons of semipelite, calc-silicate and orthoquartzite which crops out at Maarmorilik (Fig. 6.1, Fig 6.2), Akuliarusikassak, Nunaarsussuaq and Alfred Wegener Halvø (Henderson & Pulvertaft, 1967; Garde, 1978; Fig. 6.2). Originally the Mârmorilik Formation was presumed to be an Archean-age basement-cover sequence which had been strongly deformed and metamorphosed, erasing any unconformity with the orthogneisses below (Henderson & Pulvertaft 1967; Henderson & Pulvertaft 1987). However, as shown in Figure 6.1 - D, the discovery of an angular unconformity at the base of the Mârmorilik Formation reassigned the formation to the Paleoproterozoic Karrat Group (Garde & Pulvertaft, 1976).

5.3.1.2 Qaarsukassak Formation

In other places south of the PIC region, the angular unconformity over the basement orthogneisses underlies the Qaarsukassak Formation (Fig. 6.1 – C; Fig 6.2) (Guarnieri et al. 2016). The formation is 30-60m thick and comprises of the clastic sediments of a shallow-shelf formation; four interchanging units of quartz arenite and calcitic marble, with an overlying unit of meta-mudstone and siliciclastic rocks (Rosa et al 2016, Guarnieri et al 2016). Economically the Qaarsukassak Formation is of interest as it shows potential for base metal mineralisation and extraction of Pb-Zn mineralisation (Rosa et al, 2017).

 The Qaarsukassak Formation crops out in Kangerluarsuk, Tornit and Kangerluarsuup Sermia (Guarnieri et al 2016). In some places such as at Kussinersuaq the formation shows remnant crossbedding, which gives a right way-up younging direction (Rosa et al, 2017). It has been suggested that this unit correlates with the Mârmorilik Formation but has undergone less deformation (Guarnieri et al 2016).

5.2.1.3 The Kangigdleq Formation

The Kangigdleq Formation is the sole meta-volcanic unit of the Karrat Group and is predominantly formed of basaltic pillow lavas, lava flows, breccias and volcaniclastic tuff to breccias, metamorphosed to greenschist facies (Rosa et al. 2016; Rosa et al. 2017). The unit unconformably overlies the Qaarsukassak Formation and in some places the Qeqertarssuaq Formation (Fig. 6.1 - C). The Kangigdleq Formation has a transitional boundary with the overlying Nûkavsak Formation, and ranges in thickness between 5-50m (Rosa et al, 2017). It is solely recognised to the south of the PIC, from Kangilleq to Inngia Fjord (Escher 1995; Fig 6.2).

5.3.2 The Karrat Group South and North of the PIC

Two formations of the Karrat Group can be correlated across the PIC and into the Upernavik Isfjord region: a basement cover of the dominantly quartz arenite Qaarsukassak Formation (Section 6.3.2.1) and a cap of the greywacke turbidite facies rocks of the Nûkavsak Formation. (Henderson & Pulvertaft 1967; Escher & Stecher 1978, 1980; Henderson & Pulvertaft 1987; Fig. 6.1 – C and D).

5.3.2.2 The Nûkavsak Formation

The Nûkavsak Formation is an extensive uniform unit, at least 5000m thick comprising of metagreywacke, semipelites and pelite schists (Henderson & Pulvertaft 1967). It is interpreted as a deformed series of turbidite facies rocks; greywacke, sandstone, siltstone, and mudstone, due to the preservation of parts of Bouma sequences and flute clasts in eastern Nunavik and close to the village of Nuugaatsiaq, graded bedding, cross bedding and scour structures (Grocott & Vissers 1984; Rosa et al 2017; Fig 6.2). It has been highly deformed and metamorphosed to a stromatic metatexite, with some places showing high concentrations of coarse garnet (Fig. 6.3). In some areas to the south of Prøven, such as Nuugaatsiaq peninsula, the formation contains a volcanic unit (Rosa et al, 2017; Fig 6.2). The formation is the highest stratigraphic unit of the Karrat Group and has an unconformable contact with the Tertiary Basalts above (Fig. 6.1 - A). The unit is extensive across the west coast of Greenland from Alfred Wegener Halvø to Ukkusissat Fjord, into the northern Rinkian belt and even across Baffin Bay to Canada, where similar rocks crop out on Baffin Island and the Melville Peninsula (Escher 1985; Henderson & Pulvertaft 1987; Fig 6.2).

Figure 6.3 - Stromatic metatexite (Nûkavsak Fm.) near Tasiusaq. Image: Martin Hand

6.4 Tectonic Stratigraphy and Intrusive Rocks in the Prøven-Upernavik Region

Figure 6.4 –

Geological Map of Prøven-Upernavik Region (ArcGIS Pro)
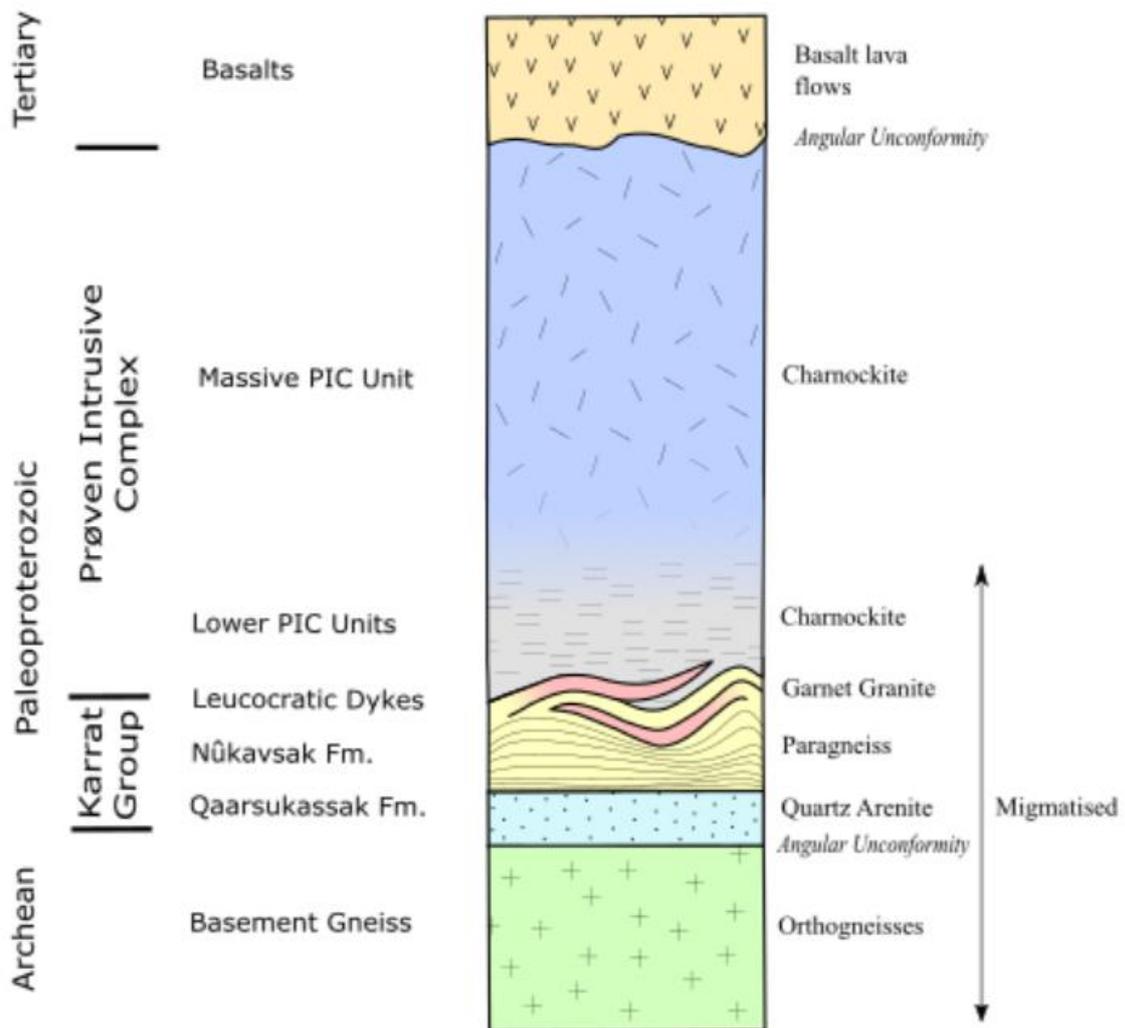
Figure 6.5 –

Tectonostratigraphic Column of the PIC region, developed for Figure 6.4 (Inkscape)

6.4.1 Basement Gneiss

Figure 6.6 –

A – Diatexite migmatite. Archaean Orthogneiss. Granulite facies hypersthene gneiss. Upernavik settlement (on the shore by the old town buildings) Image: John Grocott.

B –Diatexite migmatite. Archaean Orthogneiss. Granulite facies hypersthene gneiss. Upernavik settlement (on the shore by the old town buildings) Image: John Grocott.

The basement below the PIC is formed of metatexite and diatexite orthogneisses as described in Section 6.1 (Thrane et al, 2005). The basement is difficult to identify from photogrammetry as it varies in colour, and so has been mostly identified by fieldwork. Overall, the orthogneisses have a pale grey colour and form low lying knobbly platforms, classic of Archean gneisses in many other terranes (Fig. 6.5). They crop out on the very western fringes of the PIC region, normally in the core of refolded folds such as on Akia Island, where the largest outcrop is 1.8km wide (Fig. 6.4). The orthogneisses are also observed on small islands directly to the south and west of Akia, suggesting a structural continuity between the islands (Fig. 6.4). Structural reconstructions show that large-scale structural features, such as the Atilissuaq Dome Complex (Fig. 6.4), likely bring the basement very close to the surface in other areas, but it remains just below the overlying rocks (Fig. 6.7).

Figure 6.7 – Basement Gneiss below the PIC. Image: GEUS

6.4.2 Quartz Arenite Formation

Figure 6.8

A – Quartz arenite, Atilissuaq. Image: John Grocott

B – Quartz arenite, Atilissuaq. Image: John Grocott

Unconformably overlying the basement orthogneisses in the PIC region is a siliceous pale layer of predominantly quartz arenite but also contains thin calc-silicate, carbonate, ultrabasic and amphibolite horizons which are too small to be considered mappable units (Guarnieri, 2016; Fig. 6.5). The formation is the thinnest unit in the PIC area, between 2-50m thick (Rosa et al, 2017; Fig. 6.4, Fig. 6.5). The thickest outcrop of the quartz arenite can be found on Atilissuaq Island, due east of Upernavik, where the unit is up to 3km thick at the surface (Fig. 6.4, Fig. 6.9). Although the quartz arenite does not show evidence of migmitisation, the semi-pelitic marker horizons are clearly metatexite migmatite in texture showing strong evidence of partial melting like that of the overlying paragneisses (Rosa et al, 2018). The contact with the migmatised orthogneisses below has experienced high levels of deformation but is most likely to be unconformable.

Figure 6.9 – Quartz Arenite at Atilissuaq Image: GEUS

The quartz arenite shows strong lithostratigraphic similarities with the Qaarsukassak Formation to the South of Prøven (settlement), although it has not been formally correlated. Although there is no evidence that the same alteration of veining and sulphide mineralisation has taken place here there is still potential, and this is being investigated with a new analysis of the petrology.

6.4.3 Nûkavsak Formation (NF)

Figure 6.10 – Diatexite outcrop (Nûkavsak Fm.) Karrat (an island near Upernavik settlement). Image: John Grocott

In the PIC region the greywacke, sandstone, siltstone, and mudstone turbidite facies of the Nûkavsak Formation have been deformed to a paragneiss with migmatitic metatexite and diatexite textures (Fig. 6.4; Rosa et al, 2017; Grocott & Pulvertaft 1990; Escher & Pulvertaft 1976). Trails of garnet in a granite leucosomes highlight remnant lithological layering/bedding (Fig. 6.10). On Karrat (Upernavik), the formation potentially shows peritectic texture where almost complete melting has occurred (Fig. 6.11). The formation weathers to a strong brick red colour and is cut by thick leucocratic granite dykes which are bright white and interlinked (Fig. 6.18). The unit mainly crops out around the edges of the Atilissuaq Dome and in the core of subsidiary antiforms, which act as windows through the PIC to the base of the intrusion (Fig. 6.4). The formation is 2-5km thick, structurally thickening within the cores of large-scale folds as seen in cross sections (Grocott and Pulvertaft, 1990; Fig. 7.2). In places, such as Akuliaruseq,

mapping shows that small thrusts have raised the formation to be interleaved with the PIC (Fig. 7.1).

Figure 6.11–Diatexite (Nûkavsak Fm.) Karrat (an island near Upernavik settlement). Image: John Grocott

The boundary between the Nûkavsak Formation and the Qaarsukassak Formation has experienced strong deformation and so the exact nature of the contact is unknown but is most likely to be unconformable (Fig. 6.5).

The Nûkavsak Formation underlying the PIC and the lower units of the PIC have been intruded by abundant thick white leucocratic garnet granite dykes which align parallel with the remnant bedding and the intrusive contact (Rosa et al, 2018). The intrusive contact with the PIC has experienced strong tectonic deformation, and at Aappilattoq the Lower PIC units, enclaves of metasedimentary sandstones – most likely the Nûkavsak Formation - can be found indicating intrusion of the PIC into the metasediments (Fig. 6.12).

Figure 6.12– Meta-sandstone enclave in coarse hypersthene granite. Aappilattoq. Image: John Grocott

6.4.4. Prøven Intrusive Complex

Towards the east of the Prøven-Upernavik region the flat lying islands give way to steep, dark mountains sharply eroded by deep fjords all the way to the inland ice (Fig. 6.4). This indicates a change in rock type from the basement and metasediments to the Prøven Intrusive Complex (PIC) between c.72˚15´N and 73˚10´N (Rosa et al, 2017). For this study, the PIC has been separated into two broad phases: the upper undeformed Massive PIC Unit and the deformed Lower PIC units (Fig. 6.4, Fig. 6.5). The PIC is mainly formed of medium to coarse grained Charnockite – hypersthene granite - often with phenocrysts of K-feldspar (Escher & Pulvertaft 1976). There is a gradual change in mineralogy and fabric between the two phases, with no abrupt margin (Fig. 6.5). The PIC crops out at surface level in basins and synclines, whereas anticlines have been eroded (Fig. 6.4).

6.4.4.1 Massive PIC Unit (MPIC)

Across the area, steep dark grey-brown homogeneous cliffs rise sharply from the fjords, cut by glacial U-shaped valleys inland (Fig. 6.13). These are formed of the undeformed upper, massive PIC unit, which is the thickest unit of the PIC, a medium to coarse-grained, orthopyroxene bearing monzogranite to quartz monzonite (Thrane, 2005). The contact of the

MPIC with the lower PIC units below is gradational, which makes mapping the contact subjective (Fig. 6.4, Fig. 6.5)
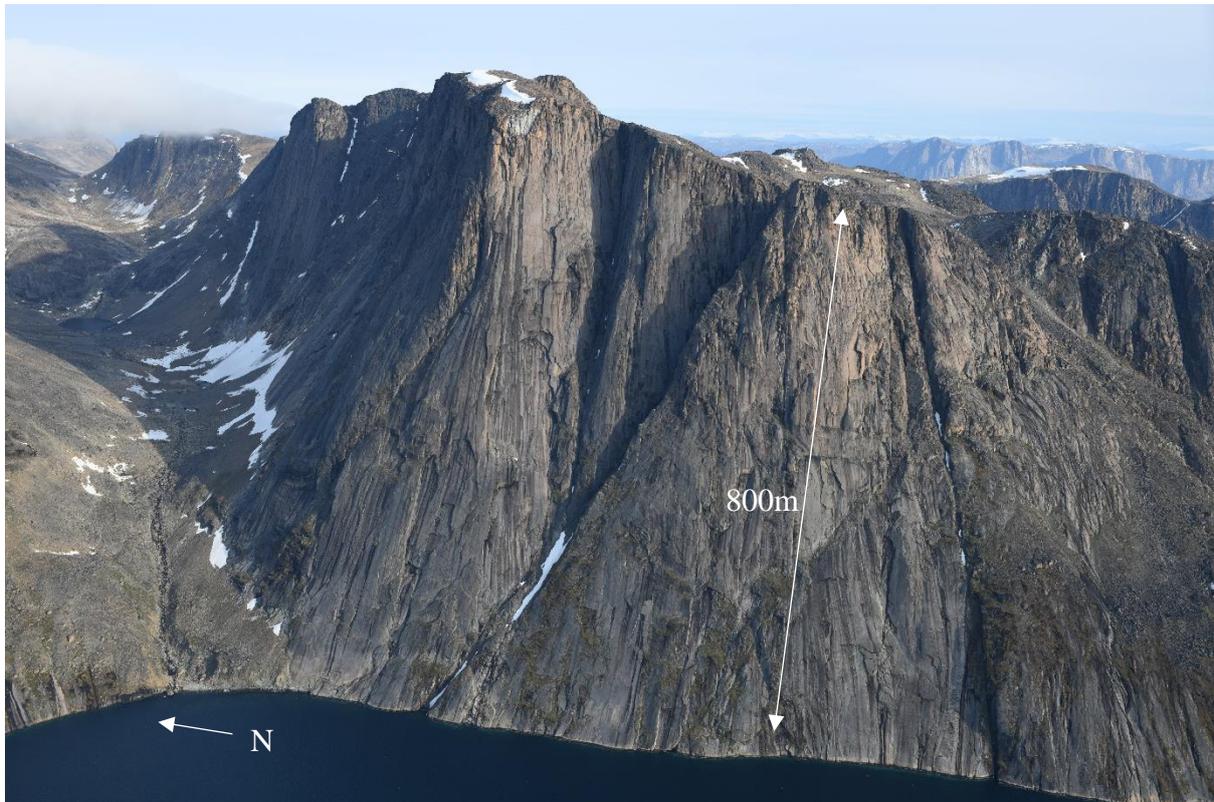
Figure 6.13 – Cliffs of MPIC at Itissaarsuaq, SW Nutaarmiut Image: GEUS

Extensive granulite facies metamorphism across the entire PIC obscures most internal structures and igneous textures, although in some localised places crystal plastic fabrics indicate transport direction and aligned large orthoclase feldspar phenocrysts and hypersthene can still be seen (Rosa et al, 2017; Fig. 6.14). Tectonic foliation is strongest at the margins and weakly present in the internal parts of the intrusive body (Thrane, 2005).

Figure 6.14 – Orthoclase phenocrysts in the Massive PIC unit. Maniisoq, NE of Upernavik Isfjord. Image: John Grocott

6.4.4.2 Lower PIC Units (LPIC)

Stratigraphically below the MPIC, the cliffs are a paler grey in colour and show distinctive horizontal white layers, parallel to the intrusive contact with the Nûkavsak Formation below (Fig. 6.4, Fig. 6.5, Fig. 6.15).

Figure 6.15 – Cliffs of LPIC, SE Akuliaruseq Image: GEUS

Petrologically the LPIC is a migmatised charnockite - hypersthene granite - with crystal-plastic fabrics parallel to the base of the intrusion, emphasised by the leucocratic granite sheets (Thrane, 2005). It is rich in garnet and in some places pheonocrysts of orthoclase feldspar have survived recrystallisation and indicate a protolith of porphyritic granite of the MPIC (Figure 6.16). The layers in the PIC are garnet rich leucogranite but have been much less deformed than those in the metasediments below, described in 6.4.5 (Thrane, 2005). Overall, the leucocratic sheets decrease in thickness and number away from the lower contact with the Karrat Group (Fig. 6.4, Fig. 6.5). The LPIC is made up of multiple units due to the presence of diorite enclaves, flattened by tectonic deformation, which show variation in original composition of the intrusion (Fig. 6.17).

Figure 6.16 – Lower Unit PIC with Orthclase Feldspar Phenocryst highlighted. Atilissuaq

Images: John Grocott

Figure 6.17 – Diorite enclaves in the Lower Unit PIC showing strong tectonic foliation.
Appallit (NW tip of Qaarsorsuatsiaq) Image John Grocott.

The LPIC varies in thickness across the area and is normally around 1km thick, thickening to 5km in the core of folds such as on Sanningasoq (Fig. 6.4, Fig. 7.28). Cross sections produced show that the presence of LPIC within MPIC reflects a raised dome or anticlinal structure, or if within the metasediments or basement the outcrop highlights a lowered basin or synclinal structure such as on Akia (Fig. 6.4). The LPIC crops out across the entire area, where the base of the PIC is raised, but can be inferred to always be below exposure level where the MPIC crops out, such as towards the inland ice (Fig. 6.4).

6.4.5 Leucocratic Intrusions

Figure 6.18 – Southern Limb of anticline highlighted by Leucocratic Dykes intruded into the Nûkavsak Formation Image: GEUS

All along the intrustive conact below the PIC the already strongly foliated metasediments of the Nûkavsak Formation and the lower PIC units have been heavily intruded by a series of pale, highly deformed sheets roughly parallel to foliation (Grocott & Pulvertaft 1990, Figure 6.18). They can be found across the entire area and increase in density towards the contact (Fig. 6.4). The sheets are between 1-20m in width and thicken within the core of folds such as within the Sanningasoq Anticline where it crops out up to 2.7km (Fig. 6.4).

Fieldwork identified the intruded sheets as garnet leucogranite - out-of-source leucosome derived by partial melting of the underlying metasedimentary rocks and intruded into the lower PIC (Grocott & Pulvertaft 1990, Fig. 6.19). In some places within the PIC the sheets of leucogranite appear to have formed in situ during partial melting of a screen of metasediment within the lower PIC, this is especially common on the southern peninsular of Nutaarmiut (Fig. 6.20). The sheets are discordant, strongly folded and often boudinaged, indicating that they are syn- to post-tectonic intrusions in a high-temperature zone of intense ductile deformation (Fossen, 2016; Rosa et al, 2017).

Figure 6.19 – Leucocratic Dyke within lower unit PIC. NE Aappilattoq Image: John Grocott

Figure 6.20 – Leucocratic Dyke formed in situ from a screen of metasedimentary rock within the LPIC Units. NE Aappilattoq Image: John Grocott
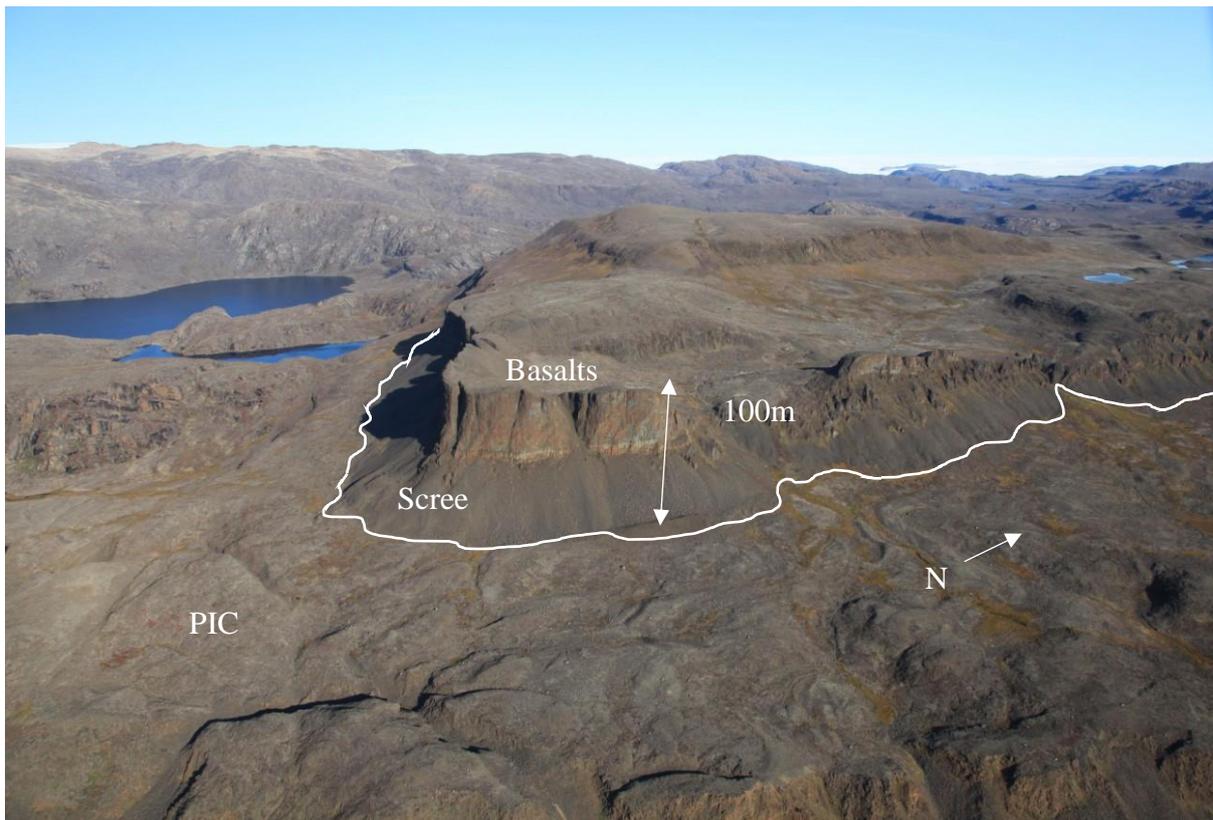
6.4.6 Tertiary Basalts

Figure 6.21 - Tertiary basalt lava flow resting unconformably on PIC. Nuna J.P. Koch. Image John Grocott.

Towards the south of the area the high plateaus underlain by the PIC are covered with a steep cap of dark orange-brown rocks, surrounded by a large skirt of scree (Fig. 6.21). This is the unconformable contact between the MPIC and the Tertiary basaltic lava flows, and the indicative scree slope means that the contact can be clearly mapped from aerial imagery (Fig. 6.4)

6.4.7 Dykes

Across the area, visible in photogrammetry and aerial images, are a network of around 100m wide dark dyke sets, likely basaltic in composition. There are 3 main large-scale sets, numbered according to age relationships, which crosscut the entire stratigraphy except the Basalts which they pre-date (Fig. 6.4).

Figure 6.22 – View NW of set 2 Dyke (Melville Bugt Dyke Swarm) from Nutaarmiut

Image: John Grocott

6.4.7.1 Set 1

This dyke set trends WNW-ESE and the dykes are around 150m wide (Fig. 6.4). The largest dyke is 70km long and can be traced all the way along the northern boundary of the area, as much of the outcrop is coastal, from Assaquataq Island in the North West to Suilaasartoq in the North East (Fig. 6.4). The other major dyke in this series is 26km to the south and not so easy to identify across the area which is mostly inland and highly weathered (Fig. 6.4). This set generally tends to erode out to form small gullies.

6.4.7.2 Set 2

The most prominent dyke set across the area trends NE -SW (Fig. 6.22). The dykes up to 250m wide and the longest dyke cross cutting this area can be mapped for 120km (Fig.6.4). This set seems to be less easily eroded than Set 1 and forms ridges and points which are useful identifying features along coastline. Although sets 1 and 2 do crosscut in the island to the north west, but this point is underwater so a definite age relationship can only be defined through geochronology (Fig. 6.4). There are three major parallel dykes defining this set which have been mapped across the area spaced between 15-7km apart (Fig. 6.4). This set can be correlated with and has already been mapped as part of the Melville Bugt Dyke Swam (Nielson, 1990).

The Melville Bugt Dyke swarm can be mapped for over 1000km from Thule on the north coast of Melville Bugt to Disko Bugt and which has been dated to 1645Ma (Nielson, 1990).

6.4.7.3 Set 3

These dykes trend E-W and are much thinner than the first two sets and at around 50-60m across (Fig. 6.4). They are much harder to view in the aerial imagery and best mapped using the photogrammetry at the coastlines, therefore the longest dyke mapped is only 15km in length but likely to be much larger (Fig. 6.4). There are at least 4 of these dykes mapped, mainly on the southern end of Nutaarmiut Island in the centre of the area, and always within the Prøven Igneous Complex, cross cutting both the Lower Layered and the MPIC (Fig. 6.4).

On the Nerrittut Peninsular at the very south eastern tip of Nutaarmiut Island a regional dyke is clearly visible in the aerials and photogrammetry. It is around 200m across and at least 1km in length. It is clearly of a very different composition to the dark dykes of Set 1-3 as it is a pale white suggesting a much more silicic composition, perhaps relating to that of the PIC.

7. Structural Geology

To analyse the geology of the Rinkian fold-thrust belt six regional cross sections orientated W-E have been produced (Fig. 7.2), constrained by accurate photogrammetric geological mapping, and validated by restoration. This validation technique is extremely useful for structural analysis as it imposes geometrical discipline on cross-section construction. It allows complete or partial restoration of the deformed cross-section as a test of geometrical validity and enables easy visualisation of the geological history.
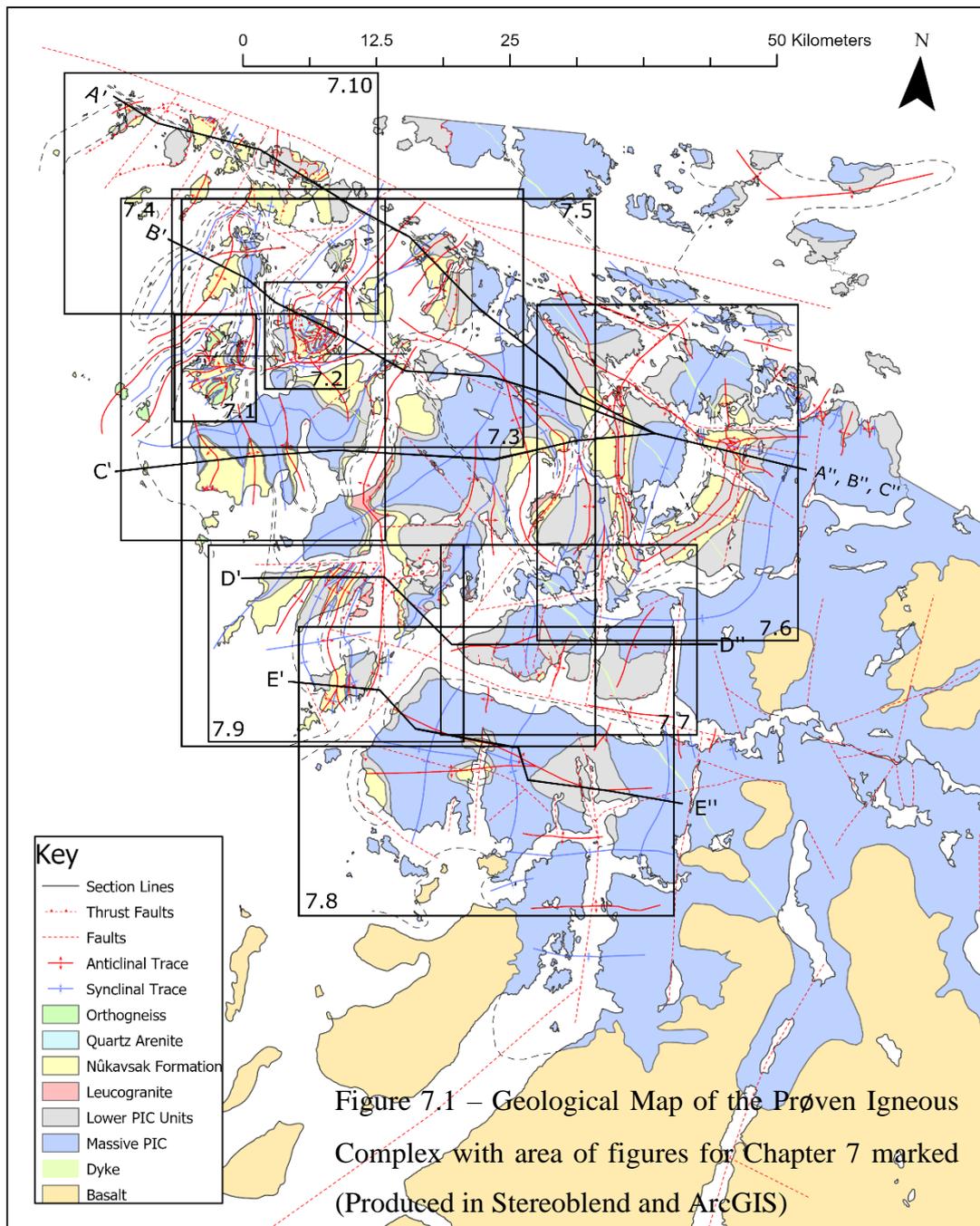

Figure 7.1 – Geological Map of the Prøven Igneous Complex with area of figures for Chapter 7 marked (Produced in Stereoblend and ArcGIS)

Figure 7.2 – Cross Section Compilation (produced on ArcGIS Pro and Inkscape)

Key
- Massive PIC
- Lower PIC Units
- Leucogranite
- Nûkavsak Formation
- Orthogneiss

Sanningasoq Fold

Akornat Anticline

Ikeq Margin Thrust Belt

?

Appilatoq

Nutaarmiut

Sanningasoq

W

E

0km   10km   20km

7.2a A'-A'' – Ikeq to Sanningasoq

Key
- Massive PIC
- Lower PIC Units
- Leucogranite
- Nûkavsak Formation
- Quartz Arenite
- Orthogneiss

Atilissuaq Dome Complex

?

Atilissuaq

Karrat

Akornat Anticline

Sanningasoq Fold

Nutaarmiut

Sanningasoq

W

E

0km   10km   20km

7.2b B'-B'' – Karrat to Sanningasoq

Key

- Massive PIC
- Lower PIC Units
- Leucogranite
- Nûkavsak Formation
- Orthogneiss

?

W

Qaarsorsuatsiaq

Akornat Anticline

Nutaarmiut

Sanningasoq Fold

Sanningasoq

E

0km   10km   20km

7.2c C'-C'' Qaarsorsuatsiaq to Sanningasoq

Key

- Massive PIC
- Lower PIC Units
- Leucogranite
- Nûkavsak Formation
- Orthogneiss

Akornat Anticline

Annertusoq

Nutaarmiut

Akuliaruseq

Amarortalik

W

E

Thrust

0km   10km   20km
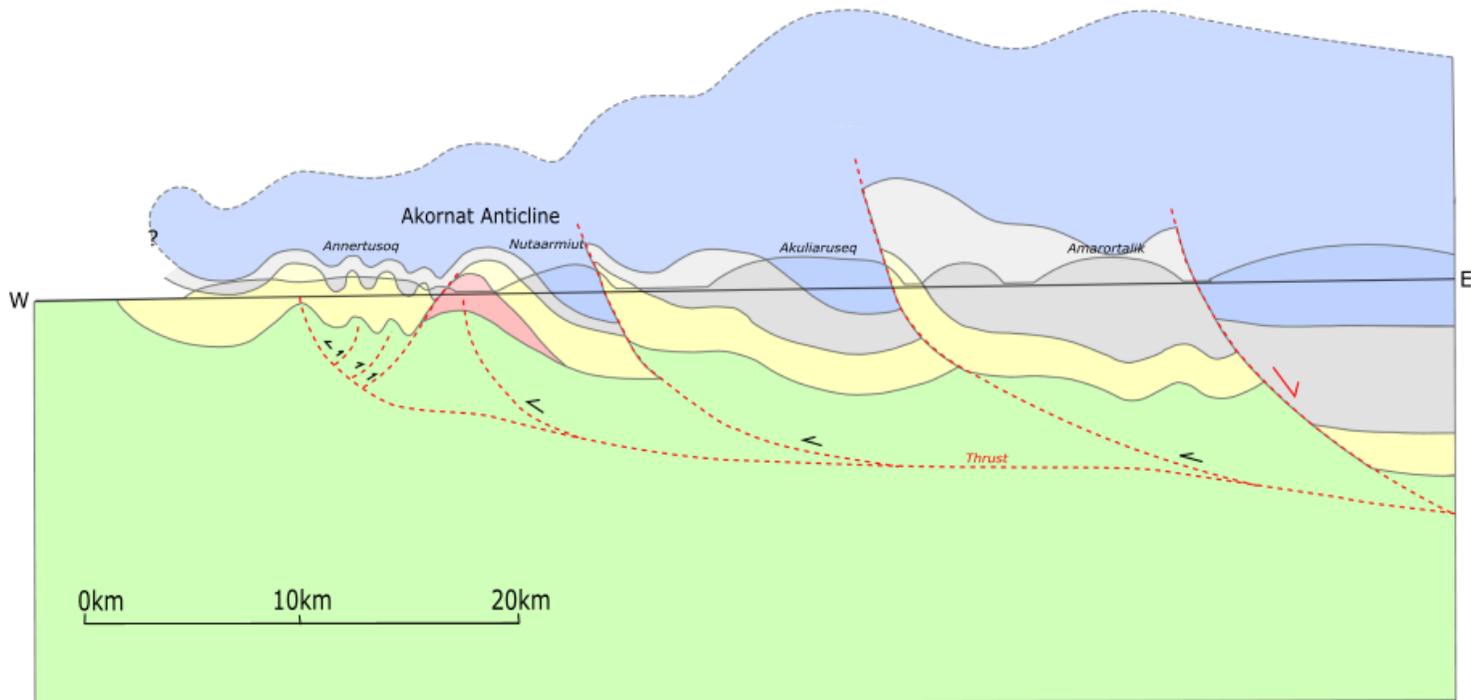
7.2d D'-D'' – Annertusoq to Amarotalik

Key

- ▨ Massive PIC
- ▨ Lower PIC Units
- ▨ Nûkavsak Formation
- ▨ Orthogneiss

W — E

?

Iperaq

Kangeq

Kangerlussuaq

Kangeq

Mallap Avannaa

0km   10km   20km
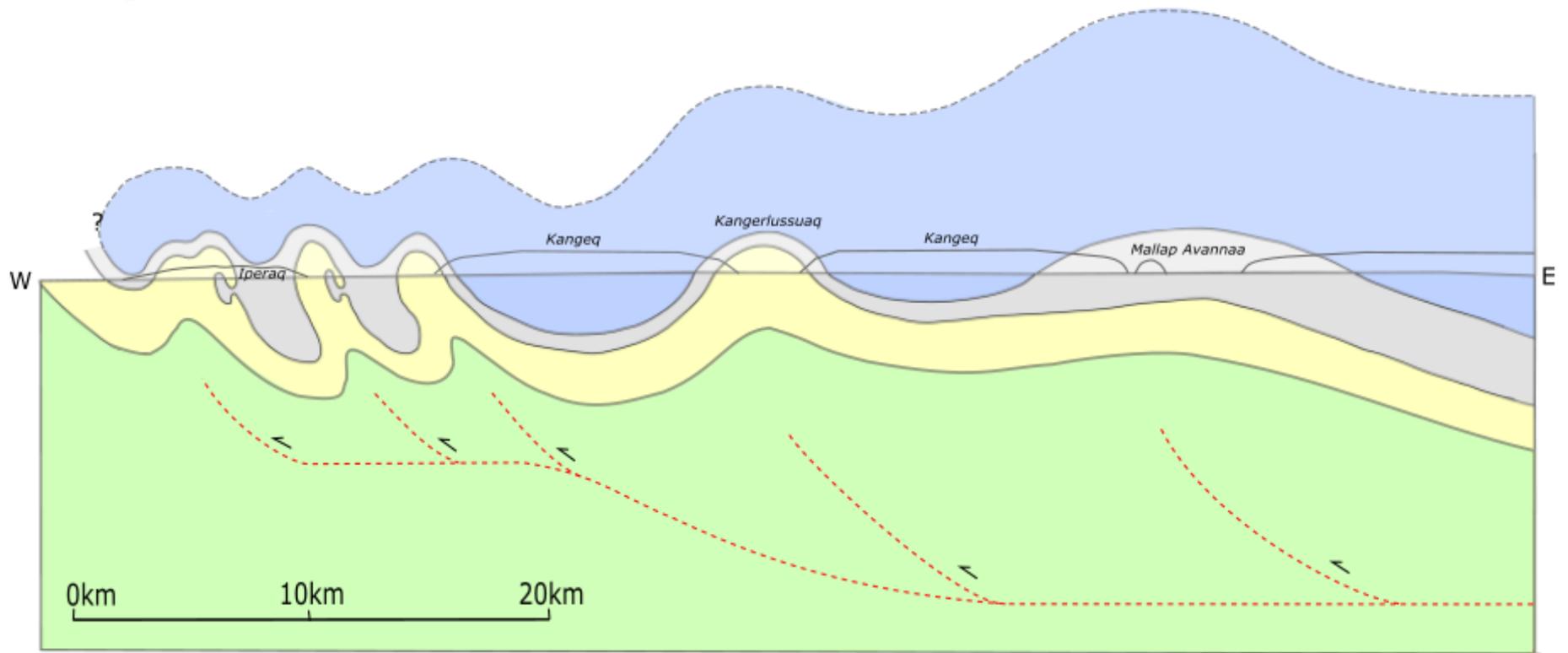
7.2e E'-E'' – Iperaq to Mallap Avannaa

7.1 Akia (Lange Ø)

7.1.1 Descriptions

Figure 7.3 – SE Akia Red – Anticlinal axial trace, Blue – Synclinal axial trace. Image: GEUS

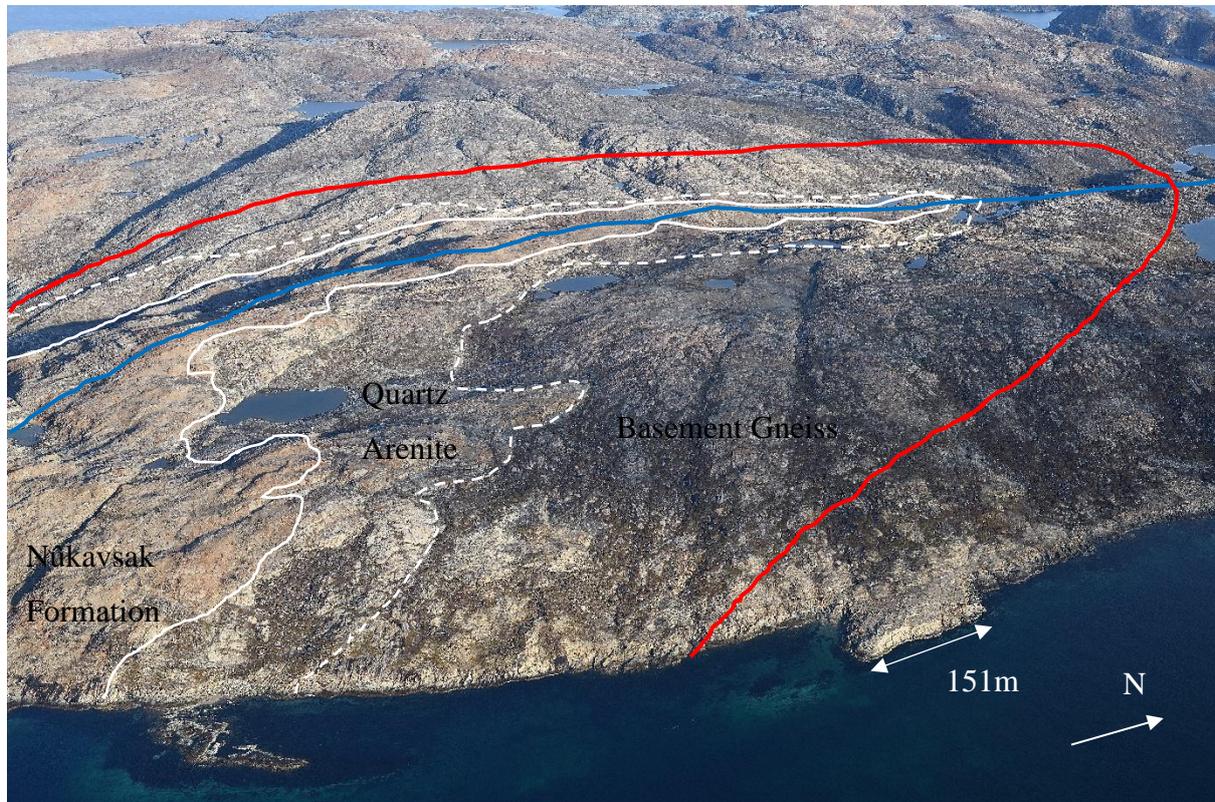Akia is a small island 5km in width and 6km in length located immediately due south of Upernavik (Fig. 7.1). The rocks are well exposed, and the island is relatively flat lying allowing for accurate geological mapping from the photogrammetry (Fig. 7.1).

On Akia, a clear unconformity between basement orthogneisses and the overlying Nûkavsak Formation metasediments crops out (Fig. 7.3). At the base of the metasedimentary rocks, a thin unit of Quartz Arenite measuring 40m across in map view is mapped continuously around this unconformity (Fig. 7.3, Fig. 7.4). The map pattern shows two 3km long boomerang-shaped outcrop patterns on the east coast of Akia, directly exposing the unconformable contact between the basement gneiss and the Quartz Arenite (Fig. 7.3). In the central northern section, a narrow strip of Lower PIC units is connected from a smaller island to the east of Upernavik onto Akia (Fig. 7.4).
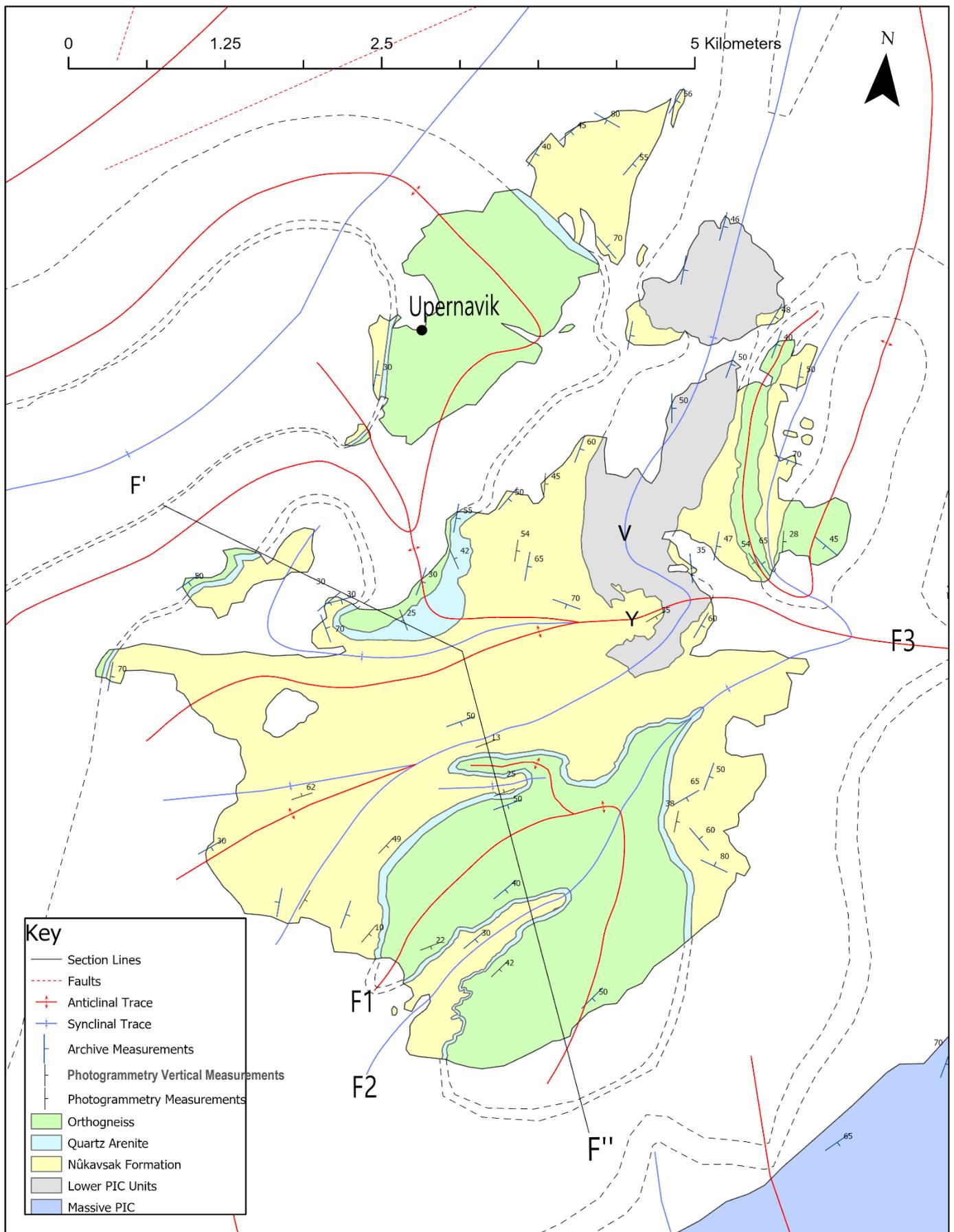
Figure 7.4 – Geological Map of Akia (ArcGIS Pro)

The map pattern and structural measurements reveal three major fold structures (Fig. 7.4). The boomerang map patterns reveal the fold hinge of a central antiform which has been folded around a large-scale tight fold (Fig. 7.4). The axial trace of the primary folds is around 1.8km in length and the trend varies from SE-NW on the western limb to SSE-NNW on the eastern limb of the secondary fold (Fig. 7.4). The direction of the boomerang highlights the 8km axial trace of two second phase folds, that trend N-S and plunge towards the SE and have limbs that dip towards the east (Fig. 7.5). An overprinting third phase major fold structure is highlighted in the map pattern at the centre of Akia, with an E-W orientated axial trace which can be mapped for about 6km across the island and plunging moderately to the west. Discrepancies in the map pattern highlight the fold hinge at the contact between the Nûkavsak Formation and the Lower PIC units, marked Y on Figure 7.4. On the northern limb the contacts strike N-S and dip to the east, reflecting the earlier fabrics of the F2 fold style. However, on the southern limb the contacts dip to the south, indicating a tight overprinting F3 structure.

Figure 7.5 Stereonet of fold in SE of island n=12 Red = East limb Blue = West limb
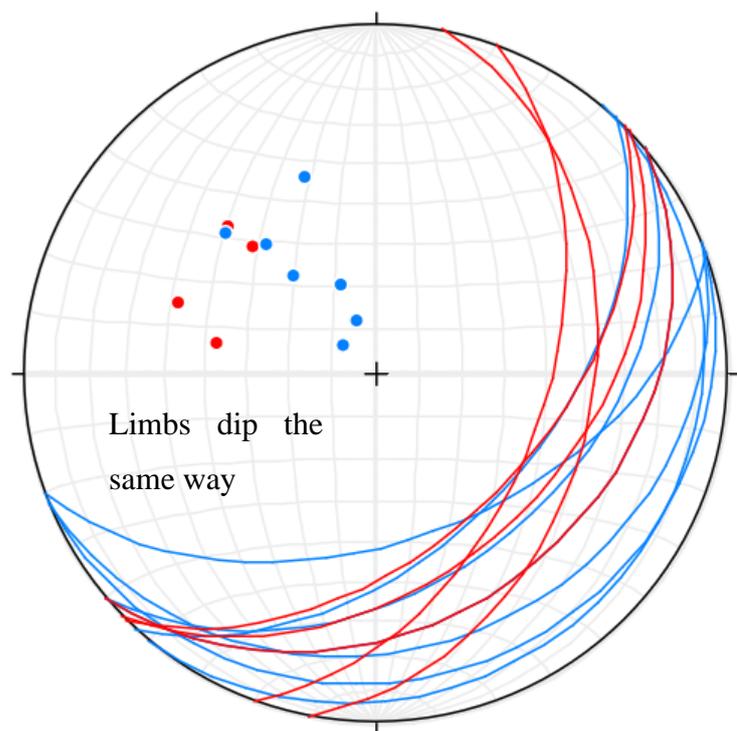
Using data from the geological survey maps and supplementing them with field observations and photogrammetry has allowed production of detailed cross sections of Akia (Fig. 7.6).

Observations show that the basement gneiss within the boomerang fold cores appears to be structurally above the metasediments (marked X on cross section), however the units are downwards facing in the exposed limb of an F1 fold which has been inverted over the metasediments (Fig. 7.6). Coupled with the map pattern, this indicates that the structure is an interference patterns where F1 folds have been folded by F2 folds that are inclined to the east.
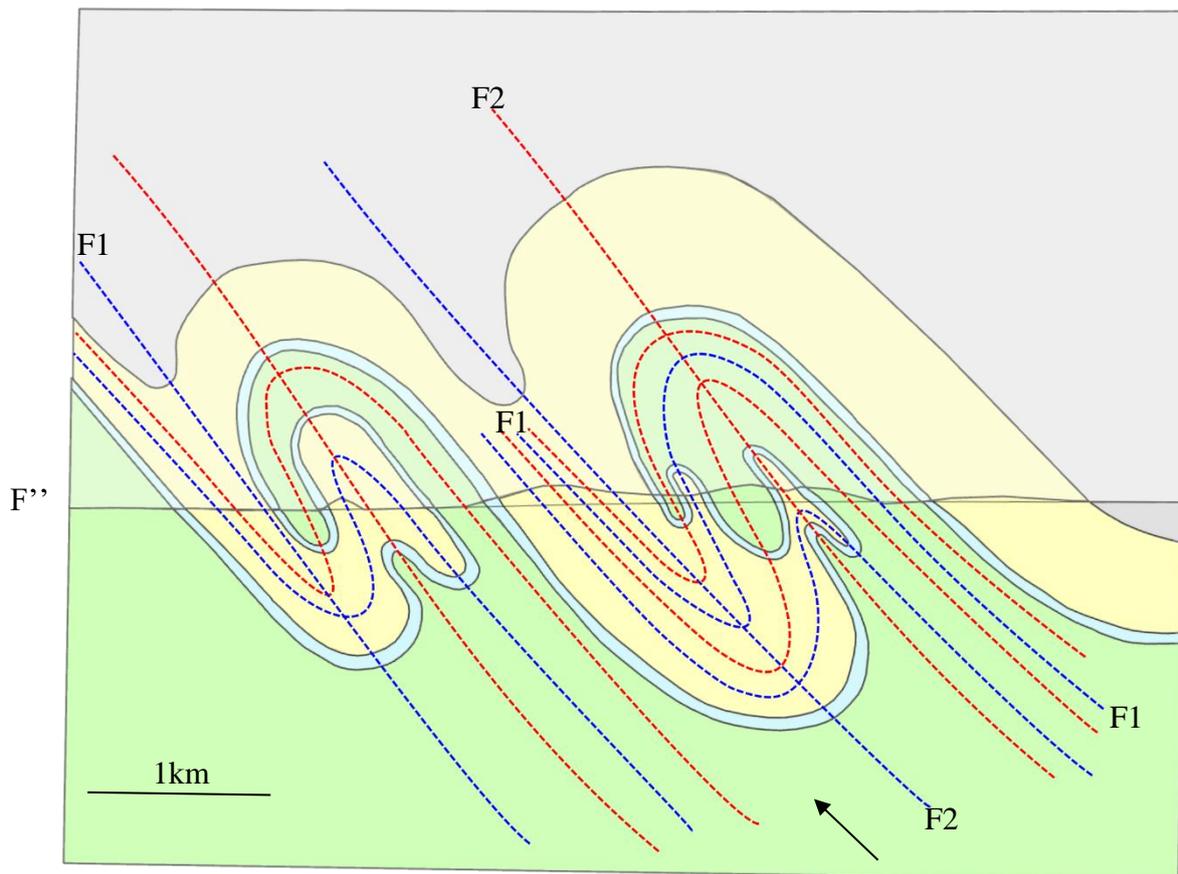
Figure 7.6 – Cross section of Akia

In the cross section the F1 axial traces are parallel, indicating isoclinal folds (Fig 7.6). F2 folds are orientated approximately N-S, highlighted by the strip of PIC units in a syncline (marked V on the map) and inclined to the east. This has produced a Type 2-fold interference pattern – so called "dome-crescent-mushroom style" interference patterns (Ramsay, 1967; Ramsay and Huber 1987). Both these folds have been overprinted by F3 folds, which are not shown in the cross section (Fig 7.4).

7.1.2 Interpretations

The mapped boundaries shown in Figure 7.4 are interpreted to be the result of at least 3 stages of folding (Fig. 7.7). Original orientation of axial trace and shape of folds has been restored using the cross sections (Fi. 7.9).

Phase	Restored Description	Deformed Description	Restored Orientation of Axial Trace
F1	Upright open folds	Isoclinal recumbent folds	E-W
F2	Close to tight folds	Tight folds with axial trace bent towards the east	N-S
F3	Open folds		E-W

Figure 7.7 – Table of Folds mapped on Akia

On the island there is no evidence for duplication of units by thrusting or any other significant structural thickening, because the thin unit of Quartz Arenite is mapped continuously around the unconformity between the metasediments and the basement orthogneisses (Fig. 7.3).

Through restoration we can interpret the evolution of the F1 folds (Fig. 7.7). It is likely that they were originally upright open folds or recumbent folds (Fig. 7.8). The restoration implies an intense period of regional horizontal shear during ductile thrusting which produced the eventual recumbent isoclinal F1 folds.

Phase	Associated structures	Strain Regime
D1	F1 Upright open folds	Ductile thrusting
	F1 Isoclinal recumbent folds	Intense horizontal shear
D2	F2 tight folds	E-W Contraction
D3	F3 Open folds	N-S Contraction

Figure 7.8 – Table of Deformation on Akia

Contact between Basement Orthogneisses and metasediments

Open F1 Folds

Progressive rotation by horizontal shear

F1 recumbent isoclinal folds

Upright F2 folds inclined to E fold F1 folds
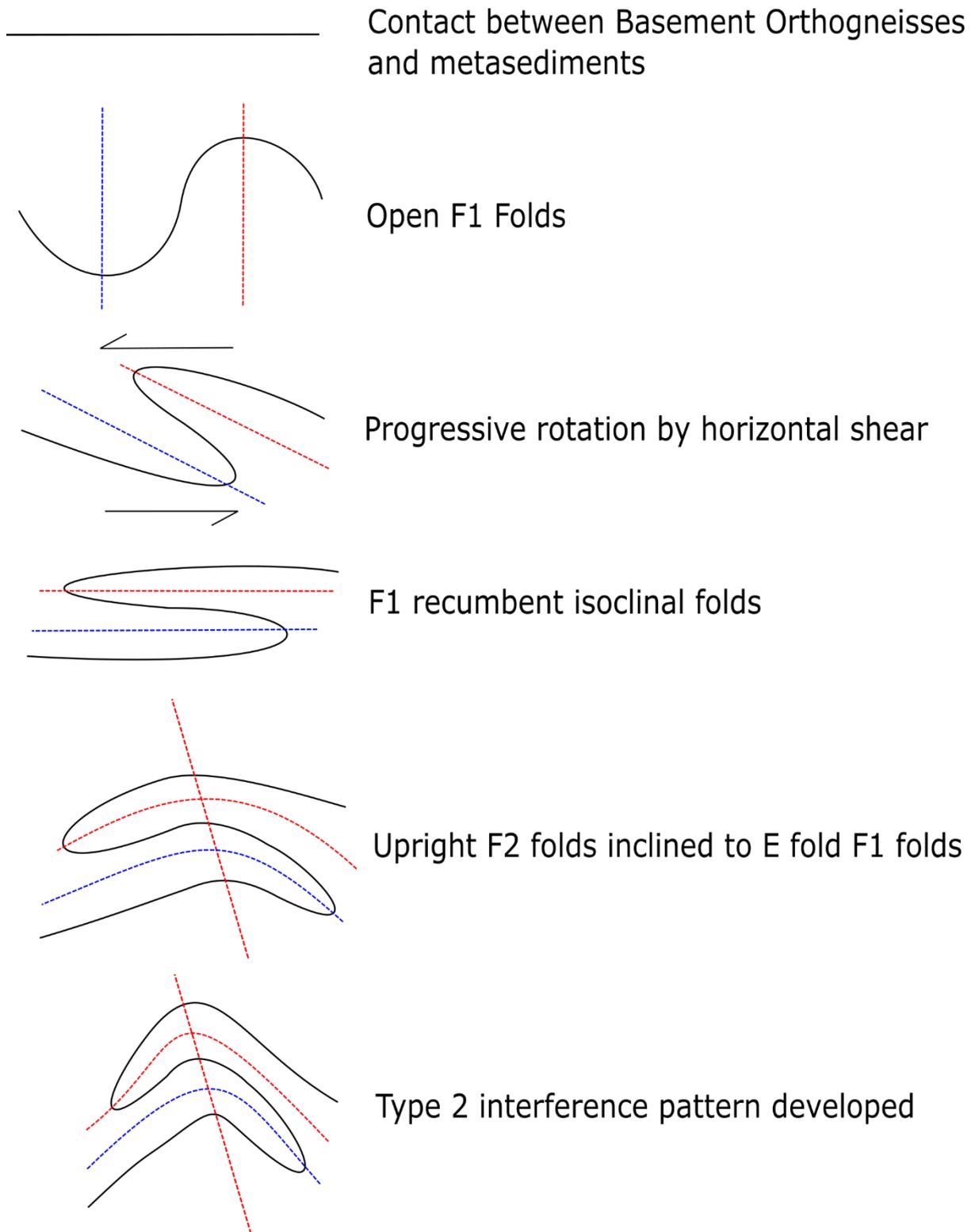
Type 2 interference pattern developed

Figure 7.9 – Schematic diagram of evolution of tight isoclinal F1 folds during D2 deformation
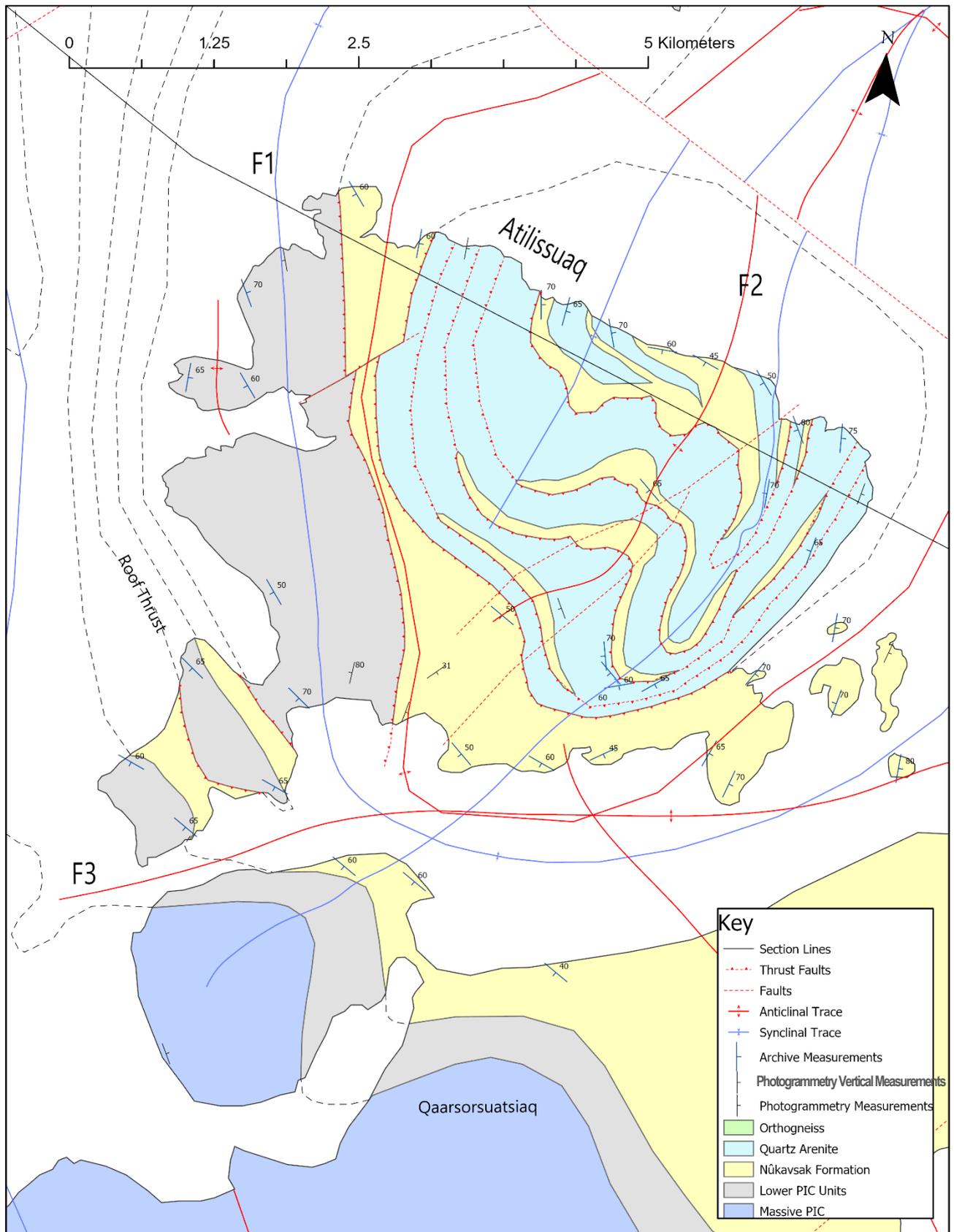
7.2 Atilissuaq Island

Figure 7.10 – Geological Map of Atilissuaq

7.2.1 Descriptions

Figure 7.11 – View of East Atilissuaq with contact between Nûkavsak Formation and Quartz Arenite highlighted Image: GEUS

To the east of Akia, separated by a deep fjord, lies the low-lying island of Atilissuaq. Here the metasediments display a contrasting structural style to Akia (Fig. 7.10). The east of Atilissuaq is predominantly a sub-circular outcrop of Quartz Arenite, within which 100-150m wide screens of folded Nûkavsak Formation are repeated on approximately 150m scales (Fig. 7.11). On the west coast are repeated strips of Nûkavsak Formation and Lower PIC units with contacts trending N-S, sub parallel to the Quartz Arenite outcrop contact (Fig. 7.11). These units all dip to the east, and the Nûkavsak Formation appears to be both above and below the Lower PIC units (Fig. 7.11).

The map pattern and structural measurements reveal three major fold structures, that can be correlated with those on Akia (Fig. 7.4).

On the west coast the leucogranite layers within the Lower PIC Units show close, upright isoclinal folds with axial traces orientated N-S (Fig. 7.11). On the south east coast within the Nûkavsak Formation, similar close, upright isoclinal folds trend SW-NE (Fig. 7.10). These fold axial traces can be linked by following the direction of the Quartz Arenite – Nûkavsak

Formation contact, which they run parallel to (Fig. 7.11). This suggests that they are associated with the formation of the Quartz Arenite outcrop and are the primary phase of folding (F1).

The obvious folds in the map are highlighted by the pattern of Nûkavsak Formation within the Quartz Arenite outcrop and are tight to close, upright isoclinal folds (Fig. 7.11). The axial trace of these folds is around 3km in length and the overall trend is SSW to NNE, plunging towards the south (Fig. 7.11). These folds are a secondary deformation phase (F2).

An F2 fold on the island of Qaarsorsuatsiaq to the south of Atilissuaq can be extrapolated across the fjord to connect with the equivalent folds on Atilissuaq, but this would involve a large 90-degree bend (Fig. 7.11). This implies the existence of a E-W trending fold with an axial trace along the fjord between Qaarsorsuatsiaq and Atilissuaq (Fig. 7.11). The map pattern shows that the contacts towards the west bend towards the supposed axial trace, implying the presence of a tertiary fold hinge at the contact between the Nûkavsak Formation and the Lower PIC units (F3) (Fig. 7.11).

7.2.2 Interpretations

The mapped boundaries in Figure 7.11 are interpreted as a result of three distinct phases of deformation (Figure 7.12). Original orientation of axial trace and shape of folds has been restored using the cross sections (Fig 7.2B, Fig 7.6, Fig 7.9).

Mode	Descriptions	Orientation of Axial Trace
F1	F1 tight upright isoclinal folds, antiformal stack	E-W
F2	Close to tight F2 folds	N-S
F3	F3 folds open, km-scale wavelength	E-W

Figure 7.12 – Table of stages of deformation on Atilissuaq

The map pattern on this island is complicated and shows intense tectonic activity which has created a complex tectonostratigraphy (Fig. 7.12). Several contacts here can be interpreted as thrust contacts, as the map pattern shows that the previously understood stratigraphy shown in Figure 6.4 has been reordered (Fig. 7.11). On the west coast the Nûkavsak Formation is above the Lower PIC units, requiring a thrust contact at the base of the Nûkavsak Formation (Fig.

7.11). In the large Quartz Arenite outcrop, the thin screens of Nûkavsak Formation mark the thrusts which have thickened the Quartz Arenite into an unusually large outcrop (Fig. 7.11).

Cross sections of the island show that the central structure is made up of a series of Quartz Arenite horses with a thin layer of Nûkavsak Formation on the upper boundaries between a series of duplex thrusts cutting up-section to the W (Fig 7.2B). It is proposed that these horses initially developed as an antiformal stack with the youngest thrusts in the centre. As this developed further imbrication folded the roof thrust sharply into a dome but not the floor thrust which detaches on the basement gneiss (Fig 7.2B). Structural reconstructions show that the basement orthogneisses are likely to be located very close to the surface here, at the internal core of the antiformal stack, but do not crop out on the island (Fig 7.2B).

Bent around the antiformal stack, it is interpreted that the tight isoclinal F1 folds formed synchronously with the antiformal stack during D1 and indicate the shape of the large-scale dome (Fig 7.2B). Later the obvious F2 NE-SW folds highlighted by the Nûkavsak Formation screens deformed the dome, creating the clear fold in the centre of the dome seen in the cross section (Fig 7.2B). These folds likely connect to the F2 folds on Qaarsorsuatsiaq across the fjord (Fig. 7.11). This interpretation implies the existence of F3 folds orientated E-W in the fjord between Atilissuaq and Akia (Fig. 7.11).

Phase	Associated structures	Strain Regime
D1	D1 Thrust Faults	Ductile thrusting E-W
	F1 Upright isoclinal folds	Ductile thrusting E-W
D2	F2 tight folds	E-W Contraction
D3	F3 Open folds	N-S Contraction

Figure 7.12 – Table of stages of deformation on Atilissuaq and Akia

This structural history can be correlated with the deformation seen on Akia, and 3 early stages of deformation are beginning to emerge across the area (Figure 7.12).
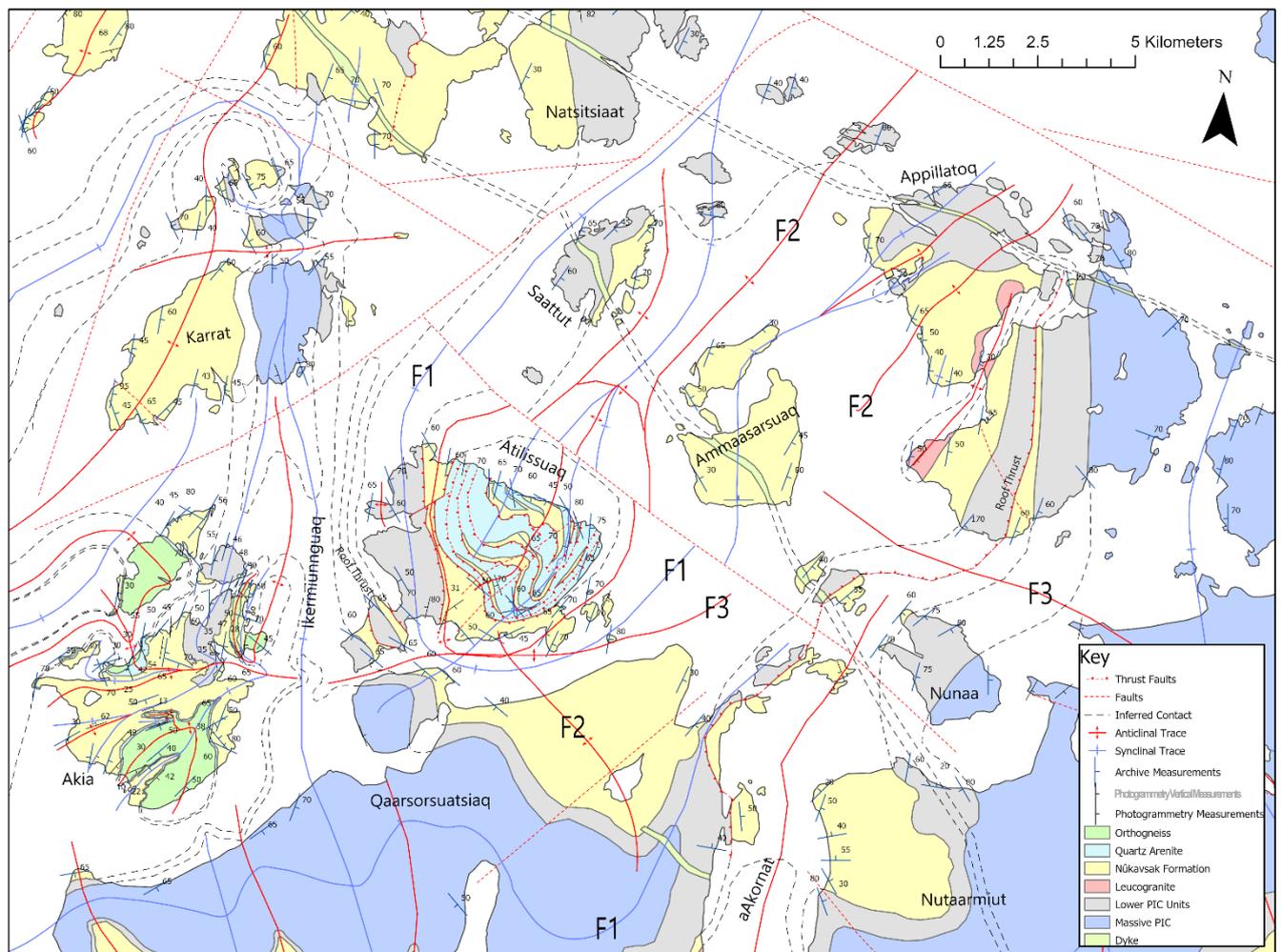
7.3 Wider Atilissuaq Dome Complex

Figure 7.13 – Geological Map of Atilissuaq Dome Complex

7.3.1 Description

The map pattern in the geology of the islands in the NE of the mapping area shows a 15 km diameter sub-circular map pattern - between Ikeq and the islands of Qaarsorsuatsiaq and Nutaarmiut (Fig. 7.13). This is highlighted by the contact between the Lower PIC Units and the Nûkavsak Formation which can almost be continuously traced across the islands (Fig. 7.13). On Atilissuaq the contact strikes N-S and can be mapped south onto Qaarsorsuatsiaq where there is a clear 90-degree bend in the map pattern (Fig. 7.13). The contact is then mapped east onto Nutaarmiut and again bends north up to Apilliatoq in the NE, where the map pattern shows another 90-degree bend across the island as the contact is striking west on the west coast of Aappilatoq (Fig. 7.13). From Aappilatoq the contact reappears on the island of Saattut where it has a strong SW strike and can be extrapolated back to Atilissuaq (Fig. 7.13).

Structural measurements show the limbs of this ring all dip outwards, except where it has been overprinted by later deformation, indicating a large-scale dome structure (Fig 7.2B). Atilissuaq exposes the central core of this dome, which is best exposed on the islands of Atilissuaq and Aappilatoq (Fig. 7.14). The axial surface trace broadly trends NE-SW with an asymmetrical shape centred over Atilissuaq (Fig 7.2B). On Aappilatoq a repeated sequence of Lower PIC Units and metasediments reflect the identified thrust contact on Atilissuaq (Fig 7.2B). Cross sections show this is likely the same roof thrust as already identified on Atilissuaq, inverted over the dome (Fig 7.2B). Down the

Figure 7.14 Stereonet of Atilissuaq Dome Complex n=18

Red = East limb Blue = West limb

Pink = North limb Green = South Limb

centre of Aappilatoq a 600m wide strip of Leucogranite striking NE-SW marks the axial plane of the Akornat Anticline (Fig 7.2B).
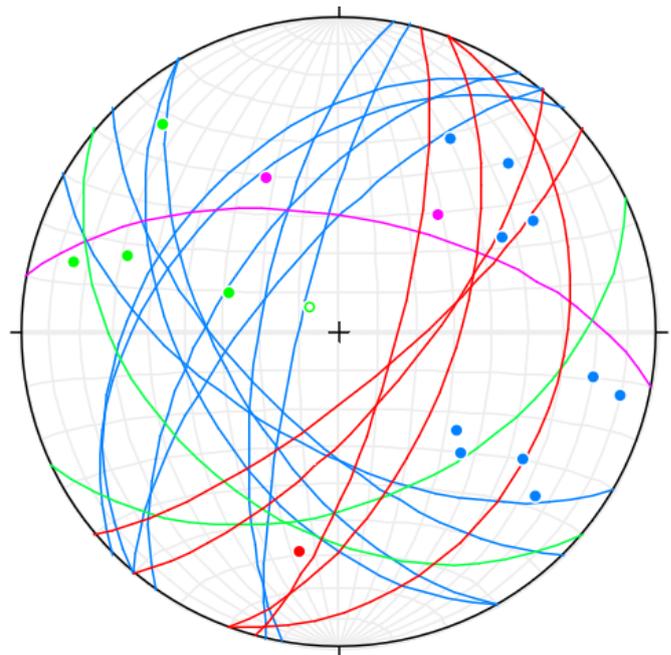
Surrounding the dome, parallel to the contact between the Lower PIC Units and the Nûkavsak Formation are a series of isoclinal folds (Fig. 7.13). As already identified on Atilissuaq these folds are likely related to initial deformation as the dome formed (F1).

On Aappilatoq the map pattern shows that the contacts and F1 structures have clearly been deformed by a different phase of deformation (Fig. 7.13). The associated structures are tight folds with axial traces trending NE-SW and hinges plunging steeply at around 70 degrees to the south (Fig. 7.13). The hinges of these folds are clear in the archive maps and in the aerial photographs. Their axial traces have a similar directional trend as the F2 folds on Atilissuaq (Fig. 7.13). Similar orientated but larger, more open folds bound the dome on either side – shown by the outcrops either side of the Akornat and Ikermiunnguaq fjords (Fig. 7.13). These folds (addressed in Sections 7.3 and 7.4) deform the edges of the dome and shown by the map pattern on Aappilatoq as a strip of leucogranite trending NE-SW (Fig. 7.13). Altogether this associates these folds with a secondary phase of deformation (F2).

The other major fold structure in the area is suggested to the east by the dips on the islands of Aappilatoq and Nunaa which show that outer rim of the dome has been deformed (Fig. 7.13). This implies the existence of a third fold structure with an E-W trending axial plane plunging towards the east (Fig. 7.13). This is an overprinting third phase of deformation (F3).

It is also noted that between Akia and Aappilatoq the F2 axial traces vary slightly in orientation (Fig. 7.13). On Akia the axial traces are in a N-S orientation, as opposed to the NE-SW orientation on Aappilatoq meaning that the axial traces rotate anticlockwise by 45 degrees to a NE strike (Fig. 7.13).

7.3.2 Interpretations

Mode	Descriptions	Orientation of Axial Trace
F1	F1 tight upright isoclinal folds	Parallel to the edge of the dome
F2	Close to tight F2 folds	NE-SW
F3	F3 folds	E-W

Figure 7.15 – Table of stages of deformation on Akia and Atilissuaq

The mapped boundaries and structural measurements for this area further imply a sequence of 3 phases of deformation (Fig. 7.15). Original orientation of axial trace and shape of folds has been restored using the cross sections (Fig 7.2B).

Phase	Associated structures	Strain Regime
D1	D1 Thrust Faults	Ductile thrusting E-W
	F1 Upright isoclinal folds	Ductile thrusting E-W
D2	F2 Tight folds	E-W Contraction
D3	F3 Open folds	N-S Contraction

Figure 7.16 – Table of stages of deformation on Akia and Atilissuaq

During early deformation, intense thrust imbrication formed an antiformal stack on Atilissuaq with synchronous isoclinal F1 folds developing around the dome, parallel to the dome sides (Fig. 7.16). The thrust contact on both Atilissuaq and Aappilatoq represents the roof thrust of the imbrication and causes the repetition in units (Fig 7.2B).

The dome was then folded by larger scale tight to closed F2 folds orientated SW-NE, up to 20km in length, which are extensions of the folds clearly highlighted by the screens of paragneiss on Atilissuaq (Fig. 7.14). The dome is bound by two large scale F2 synclines, to the west the Ikermiunnguaq syncline and to the east the Nutaarmiut syncline (Fig. 7.14). These synclines trend N-S and are marked by a return in exposure to the MPIC ((Fig 7.2B, Fig. 7.12). A large bend on the eastern edge of the dome is a strong indication of an F3 E-W Fold (Fig. 7.14).

The reorientation in the direction of the F2 axial traces indicates this deformation has occurred as part of D3 as a phase after the formation of the dome and subsequent deformation (Fig. 7.14).

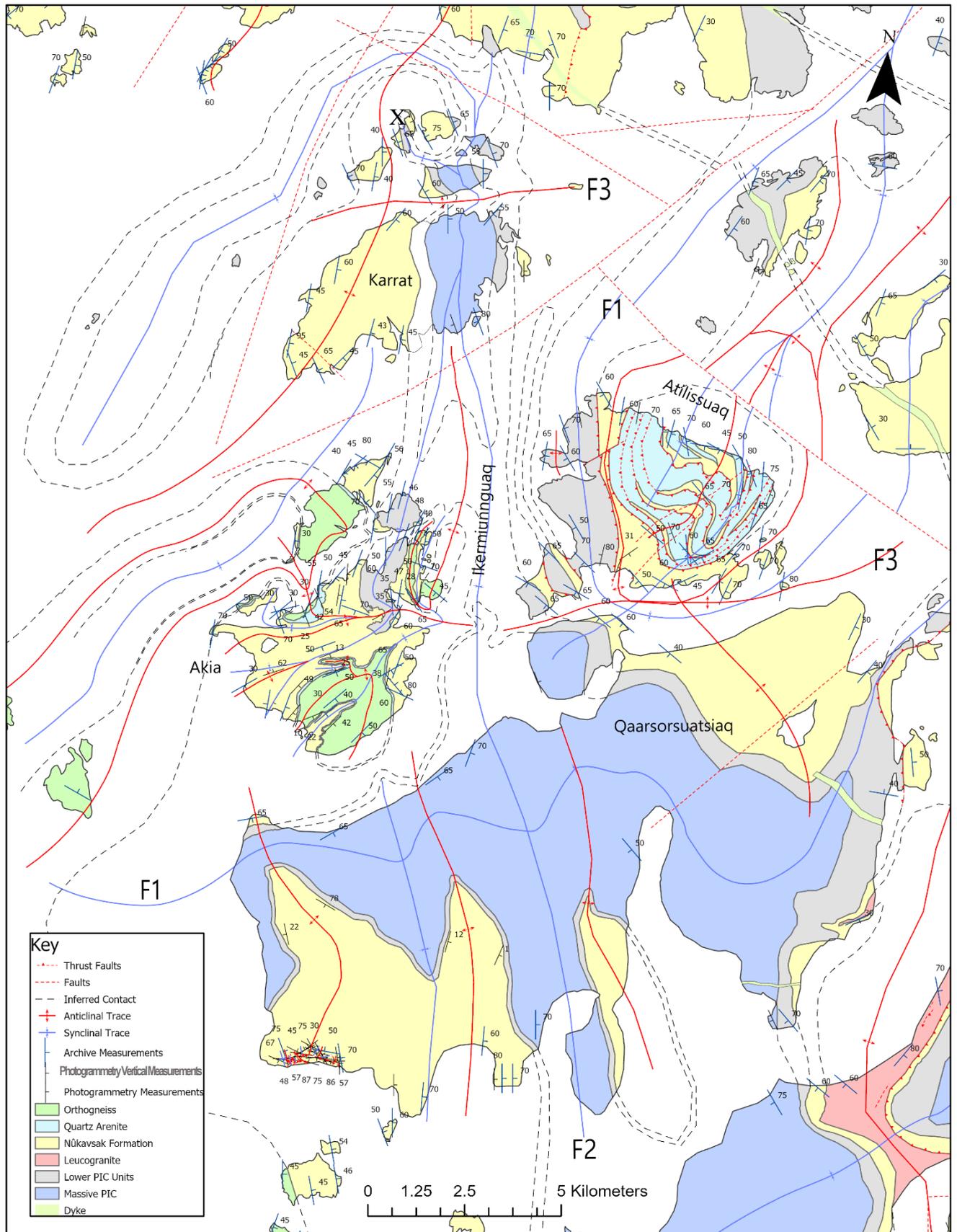## 7.4 Ikermiunnguaq and Qaarsorsuatsiaq

Figure 7.17 – Geological Map of the Ikermiunnguaq fjord

7.4.1 Descriptions

From the north coast of Qaarsorsuatsiaq the Ikermiunnguaq fjord stretches north to the island of Karrat, passing between the islands of Akia and Atilissuaq (Fig. 7.1). The contact between the Lower PIC Units and the Nûkavsak Formation can be mapped on Akia and Atilissuaq either side of the fjord (Fig. 7.17). Structural measurements show that the contact strikes to the north and dips inwards on either side (Fig. 7.17). Further North, on Karrat, the Upper PIC Unit crops out along the east coast of the island bounded on either side by Lower PIC Units (Fig. 7.17).

The map pattern indicates a major structure in this area - the Ikermiunnguaq Syncline – a 3.5km wide fold with a N-S orientated axial trace with a shallow plunge to the north (Fig. 7.17). This syncline is the largest in a series of large-scale linear folds with axial traces-oriented N-S which run parallel down Qaarsorsuatsiaq (Fig. 7.2C). It lies on the western boundary of the Atilissuaq Dome Complex (Fig. 7.14, Fig. 7.2D).
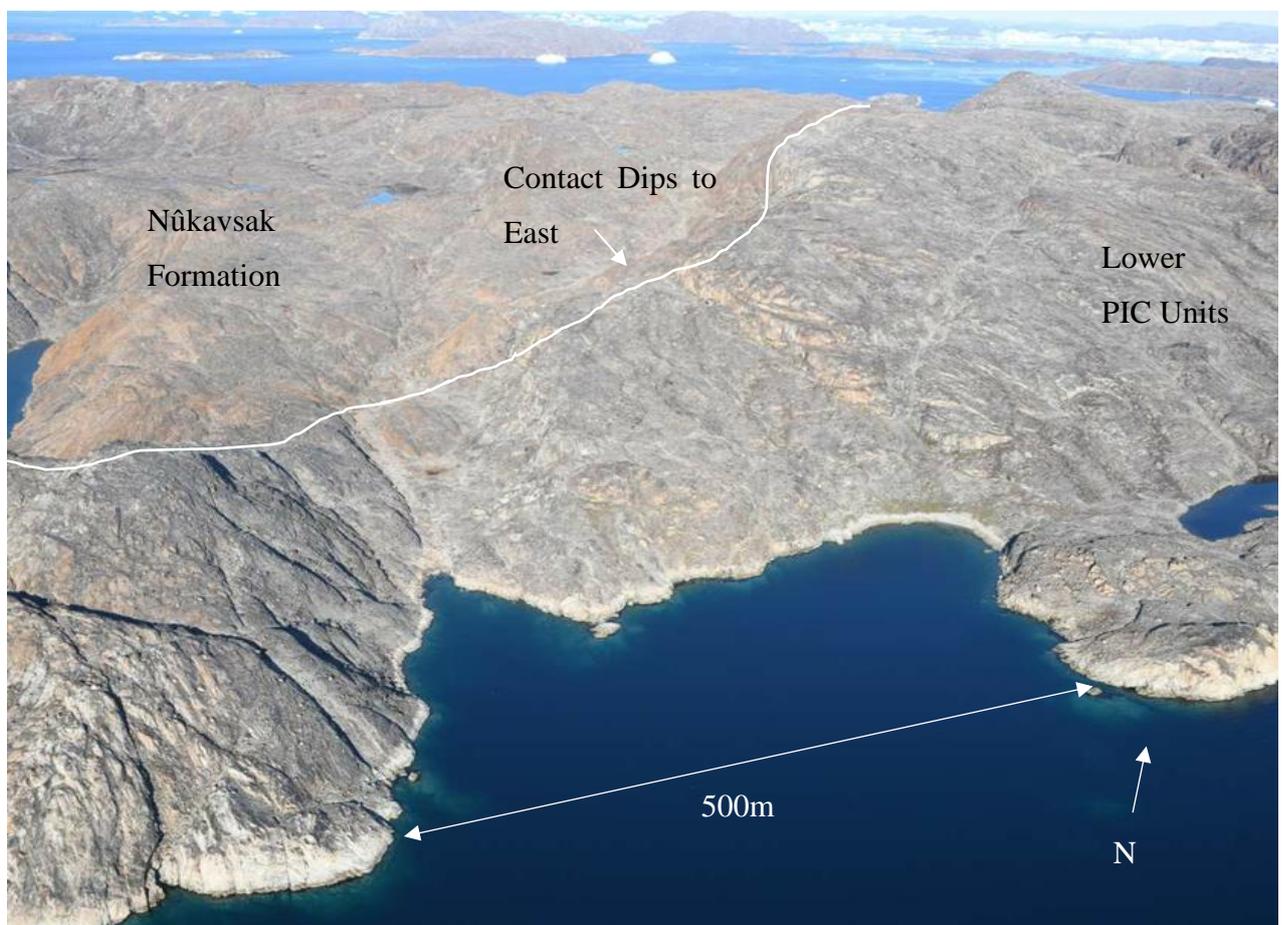

Figure 7.18 – West Limb of Ikermiunnguaq syncline on Karrat, with contact between Nûkavsak Formation and Lower PIC Units highlighted Image: GEUS

On Qaarsorsuatsiaq the Upper PIC Units are the dominant outcrop on the island, but the map pattern of the exposed Lower PIC Units and Nûkavsak Formation highlights 3 hinges up to 2km wide (Fig. 7.17). Structural measurements and cross sections produced show that this outcrop pattern is not a topographic effect on the contact, but these are a series of tight box folds plunging very shallowly to the south, with axial traces orientated N-S (Fig. 7.17, Fig. 7.2D).

On the east coast of Qaarsorsuatsiaq the map pattern shows a fold hinge in the contact between the base PIC and Nûkavsak Formation, with a clear axial trace-oriented NE-SW (Fig. 7.17). This trace can be extrapolated E-W across Qaarsorsuatsiaq within the upper PIC units (Fig. 7.17). This is likely related to early stage folding (F1) and is heavily overprinted by the N-S orientated (F2) folds (Fig. 7.17).

On the southern coast of Qaarsorsuatsiaq at Tunua, superb outcrops of small-scale detachment folds are visible highlighted by leucogranite sheets in the Nûkavsak Formation ((Fig. 7.17, Fig. 7.19). This shows buckling of leucogranite dykes within the more ductile paragneiss.

Figure 7.19 – Detachment Folds highlighted by Leucocratic dykes on Tunua Coast Image: GEUS

Further north from Karrat, in the Ikeq Margin Thrust System, the syncline is unmappable using photogrammetry as it has been intensely deformed (Fig. 7.17).

On Karrat the map pattern at the north of the islands and on the small cluster of islands north of Karrat clearly shows a bend in the contact Lower PIC Units and Nûkavsak Formation towards the east (Fig. 7.17). This indicates that the F2 Ikermiunnguaq Syncline is overprinted by an E-W anticline (F3), plunging to the west (Fig. 7.17).

On smaller islands just to the north the map pattern here also shows a small strip of Lower PIC Units separate to the Upper PIC Units, marked X on the map, implying the presence of a small parasitic syncline (Fig. 7.17). This, coupled with outcrops of Lower PIC Units to the west, indicates a hook like shape which bends the axial trace in the north of the syncline to a NE orientation (Fig. 7.17). The fold limbs dip towards the east indicating an interference pattern of non-cylindrical folding developing during progressive deformation (Fig. 7.20). The refolded structure reflects the Type 2 "dome-crescent-mushroom style" as on Akia as the F2 Ikermiunnguaq Syncline overprints F1 folds (Ramsay, 1967; Ramsay and Huber 1987; Fig. 7.6).

Cross sections show that this syncline is likely the tip and thinnest part of the PIC sheet intrusion, folding over and back on itself around the Atilissuaq Dome Complex (Fig. 7.2B).
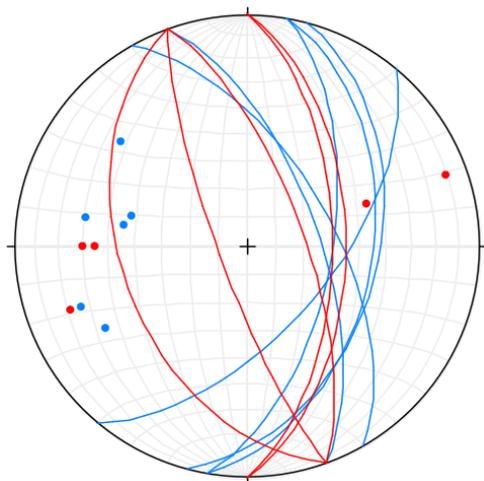

Figure 7.20 Stereonet of Ikermiunnguaq Syncline   n=11
Red = East limb Blue = West limb

Both limbs dip inwards overall indicating cylindrical syncline with multiple hinge lines. Sub horizontal plunge towards S.

7.4.2 Interpretations

The mapped boundaries and structural measurements for this area further imply a sequence of 3 phases of deformation (Fig. 7.21). Original orientation of axial trace and shape of folds has been restored using the cross sections (Fig 7.2B, Fig. 7.2C).

Mode	Descriptions	Orientation of Axial Trace
F1	F1 folds	E-W

F2	Close to tight F2 folds	N-S
F3	F3 folds	E-W

Figure 7.21 – Mapped folds related to the Ikermiunnguaq Syncline

Cross sections and structural measurements show that the F2 folds on Qaarsorsuatsiaq are steep sided detachment folds – "box folds", reflecting the small-scale outcrops at Tunua (Fig. 7.2C). This implies that the PIC overlies a below erosion level thrust system facing to the west (Fig. 7.18).

Phase	Associated structures	Strain Regime
D1	D1 Thrust System	Ductile thrusting E-W
	F1 Upright folds	Ductile thrusting E-W
D2	F2 Tight folds	E-W Contraction
D3	F3 Open folds	N-S Contraction

Figure 7.22 – Table of stages of deformation related to the Ikermiunnguaq Syncline

The Ikermiunnguaq Syncline formed after initial ductile thrusting and the formation of the Atilissuaq Dome Complex. It is part of a series of large scale tight, with a sub horizontal plunge F2 folds which trend N-S across the area (Fig. 7.2C). The Ikermiunnguaq Syncline has much larger wavelength than the F2 folds on Akia, and this variation in fold wavelength and thickness appears to change systematically across the area (Fig. 7.2).
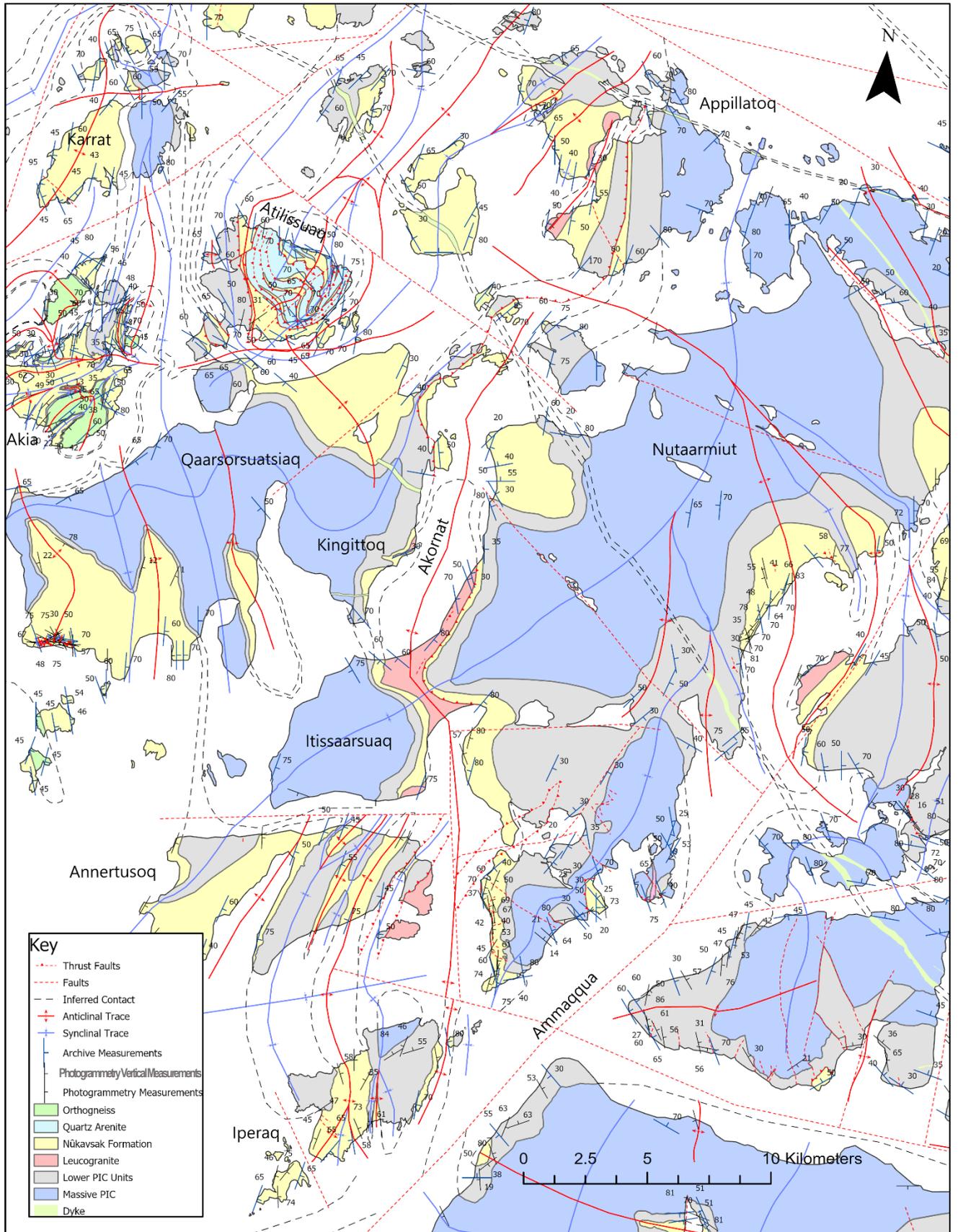
7.5 Akornat and Nutaarmiut

Figure 7.23 – Geological Map of Akornat and Nutaarmiut

To the east of the Atilissuaq Dome Complex the Akornat Fjord stretches 23 km from Aappilatoq in the north to Itissaarsuaq in the south (Fig. 7.23). Leucogranite and Nûkavsak Formation is predominantly exposed along the coastline of the fjord, especially between the islands of Nutaarmiut and Qaarsorsuatsiaq (Fig. 7.23). The contact between the Nûkavsak Formation and the Lower PIC Units can be mapped along the cliffs of the fjord for much its length (Fig. 7.23). Structural measurements show that the contact on the west coastline dips to the west between 80-50 degrees and the contact on the east coastline dips to the east between 70-60 degrees (Fig. 7.23). This indicates that each side of the fjord is on the opposing limb of a sub-horizontally plunging cylindrical anticline (Fig. 7.24). The fjord marks the axial plane of the 40km N-S trending F2 Akornat Anticline (Fig 7.23).

The Akornat Anticline axial trace can be mapped from Aappilatoq in the north to Iperaq in the south (Fig 7.23). It is characterised by an outcrop of steeply dipping leucogranite in the core of the anticline (Fig. 7.23). Cross sections show the leucogranite cross cuts the Nûkavsak Formation all along the hinge zone of the anticline (Fig 7.23). On the east coast of Qaarsorsuatsiaq, at Kingittoq, the outcrop pattern appears to either indicate a small interference pattern within the folding or a feature of an intrusive contact (Fig 7.23). The anticline is broad with a very shallow, sub-horizontal plunge reflecting the similar geometry of the F2 Ikermiunnguaq syncline (Fig. 7.24).
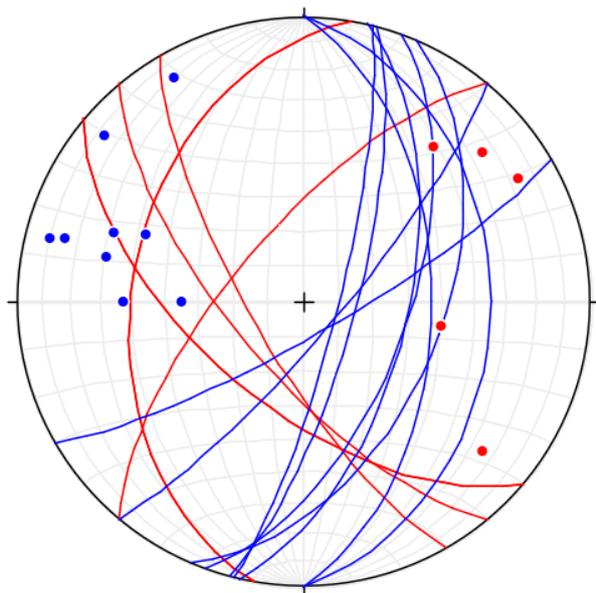

Figure 7.24 Stereonet of Akornat Anticline   n=16

Red = East limb Blue = West limb

Both limbs dip outwards indicating an anticline.

On Aappilatoq in the north, the stratigraphy is very complex (Fig. 7.23). The map pattern on the east limb shows repeated Lower PIC units and Nûkavsak Formation, with leucogranite in

the hinge of the fold (Fig. 7.23). This indicates the presence of an exposed thrust system described previously in section 7.3.1. Further to the south on the peninsula of Itissaarsuaq this anticline is best exposed where the steep cliffs cut straight down into the hinge, exposing the pale white leucogranite (Fig. 7.25). Here it is noted that the Nûkavsak Formation thins close to the contact with the Lower PIC Units, suggesting an intrusive relationship between the leucogranite and the anticline (Fig 7.23). Further south the anticline is less traceable and is cut heavily by thrusts, it likely crops out across Iperaq but is much smaller in wavelength than to the north (Fig. 7.23).
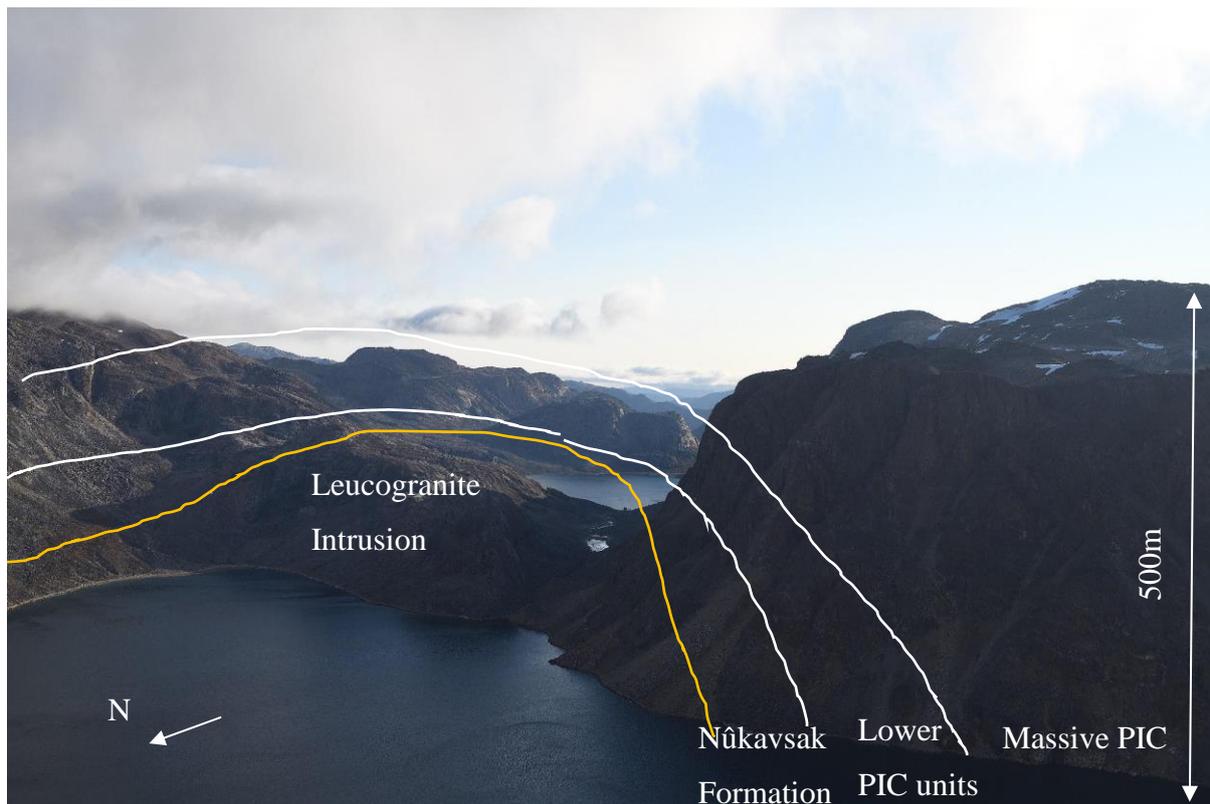

Figure 7.25 – Akornat Anticline at Itissaarsuaq

Akornat runs parallel to the western coastline of the island of Nutaarmiut, which is about 36km long and 13km wide (Fig. 7.23). Nutaarmiut is predominantly formed of the Upper PIC Unit with outcrops of Lower PIC Units and Nûkavsak Formation along the coastline, especially on the east and west coast (Fig. 7.23). This map pattern and structural measurements indicate a syncline with axial trace orientated N-S down the island (Fig. 7.23; Fig 7.2C). Using the photogrammetry data and archive data two synclinal traces are revealed: a tight N-S orientated syncline down Nutaarmiut and a NE-SW trending syncline from the centre of Nutaarmiut to Itissaarsuaq (Fig. 7.23). The NE-SW orientated syncline is heavily overprinted by the F2 Akornat Anticline, indicating that it is an F1 syncline – the Itissaarsuaq Syncline (Fig. 7.23). At Itissaarsuaq the two fold traces intersect perpendicular to each other (Fig. 7.23).

As the other main syncline – the Nutaarmiut Syncline – trends broadly N-S parallel to the Akornat Anticline and the Ikermiunnguaq Syncline, and it overprints the F1 Itissaarsuaq Syncline, we can assume this is an F2 syncline (Fig. 7.23). The Nutaarmiut Syncline is open and has a very shallow plunge, reflecting the geometry of other large scale F2 folds such as the Akornat Anticline (Fig. 7.23).

Across the island several fold traces are orientated broadly E-W, revealed by the map pattern and structural measurements (Fig. 7.23). These overprint the F2 Nutaarmiut Syncline and so are F3 folds (Fig. 7.23).

7.5.2 Interpretations

The map pattern supports the indication of three main phases of deformation.

Mode	Descriptions	Orientation of Axial Trace	Associated Structures
F1	F1 folds	E-W	Itissaarsuaq Syncline
F2	Close to tight F2 folds	N-S	Akornat Anticline, Nutaarmiut Syncline
F3	F3 folds	E-W	Many folds across Nutaarmiut

Figure 7.26 – Mapped folds related to the Akornat Anticline

Phase	Associated structures	Strain Regime
D1	D1 Thrust System	Ductile thrusting E-W
D2	F2 Open folds	E-W Contraction
D3	F3 Open folds	N-S Contraction

Figure 7.27 – Table of stages of deformation related to the Akornat Anticline

The Itissaarsuaq Syncline is the oldest structure in this area and related to ductile E-W thrusting synchronous with the formation of the Atilissuaq Dome Complex (Fig. 7.2B).

The Akornat Anticline and Nutaarmiut Syncline appear to be the same age as each other and a product of E-W contraction around the Atilissuaq Dome Complex (Section 7.3). The map pattern indicates that the leucogranite has crosscut the Nûkavsak Formation.
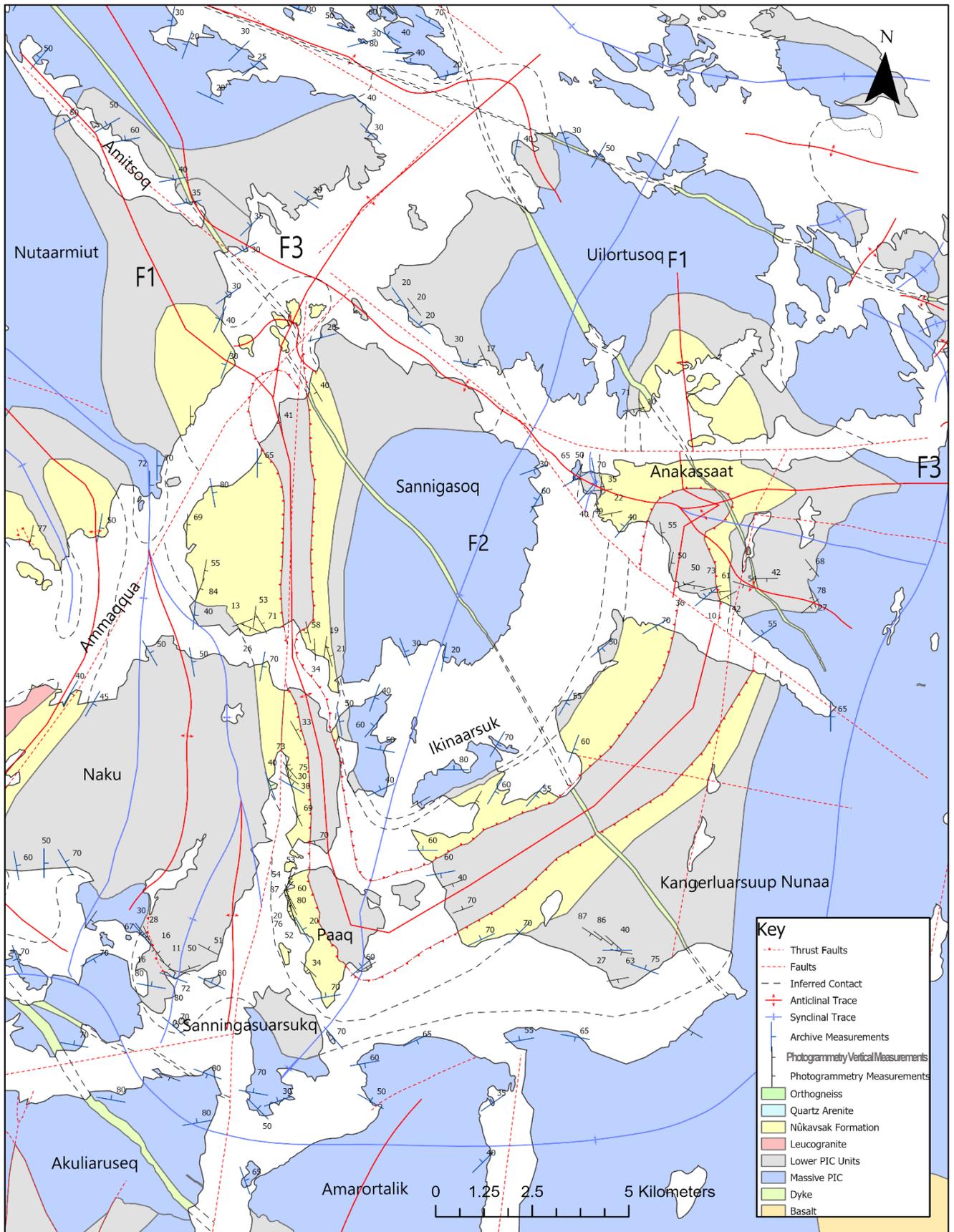
7.6 Sanningasoq Fold

Figure 7.28 – Geological Map of Sanningasoq Fold

Away from the Atilissuaq Dome Complex, the map pattern shows that the Massive PIC becomes much more dominant at outcrop with only smaller localised outcrops of Lower PIC Units and Nûkavsak Formation (Fig. 7.1).

At the Amitsoq fjord in the north of Nutaarmiut the lower PIC units crop out in a semi-circular hinge map pattern, dipping to the NW along the fjord (Fig. 7.28). Following the Amitoq to the SE to the east coast of Nutaarmiut the Nûkavsak Formation crops out, also dipping to the NW (Fig. 7.28). This indicates the presence of an anticlinal hinge with axial trace orientated NE-SW and plunging gently to the west (F1) (Fig. 7.28). Across the 50km long NE-SW orientated Ammaqqua fjord, a major feature of the mapping area, on the island of Sanningasoq the lower units again crop out (Fig. 7.28). However here there is a central outcrop of Lower PIC Units down dip of Nûkavsak Formation along with outcrop up dip of Nûkavsak Formation (Fig. 7.28). The Nûkavsak Formation is sandwiched between Lower PIC Units, contrasting the established stratigraphy, and creating a repeated pattern indicating a thrust contact which has been folded within the anticline creating an inverted limb (Fig. 7.28). These units all dip to the east and strike due south and can be mapped directly down Sannigasoq, onto the islands of Naku and Paaq (Fig. 7.28). On the south coast of Paaq the leucogranite sheets within the Nûkavsak Formation and Lower PIC Units suddenly dip to the north and strike to the NE (Fig. 7.28). Just to the south of Paaq, on the island of Sanningasuarsuk, the map pattern shows a 90-degree bend in the contact between the Lower PIC Units and the Upper PIC, this is clear from the aerial imagery and in the archive mapping (Fig. 7.28). This indicates the presence of a later stage synclinal fold hinge which has folded the anticline on a SSW-NNE axis (F2) (Fig. 7.29; Fig. 7.25).
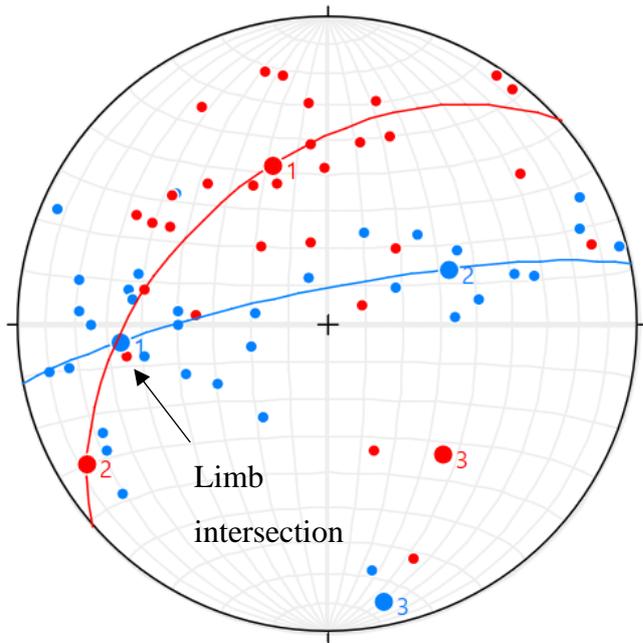
Figure 7.29 Stereonet of Sanningasoq Fold n=65
Red = East limb
Blue = West limb

Extrapolating to the north east the contacts all repeat the same sequence on the mainland peninsula of Kangerluarsuup Nunaa and continue straight along strike to the peninsula of Anakassaat further north (Fig. 7.28). On Anakassaat the contacts are deformed in hinge like shapes towards the east and the central strip of Lower PIC Units does not crop out along the northern coastline of the peninsula (Fig. 7.28). This indicates the presence of several later stage small overprinting E-W orientated folds (F3) (Fig. 7.28). Further to the north on the island of Uilortusoq a clear anticlinal hinge zone can be mapped shown in Figure 7.30, with Nûkavsak Formation and Lower PIC units outcropping below Upper PIC Units in a semi-circular outcrop pattern (F1) (Figure 7.28). This means that the primary F1 anticlinal axial trace can be mapped for over 90km from Amitsoq to Uilortusoq (Fig. 7.28).

This complicated outcrop pattern required extensive investigation through cross sections, but excellent exposure such as at Ikinaarsuk, allows detailed mapping and the structural evolution of the area to be defined (Fig. 7.31, Fig. 7.2A, Fig. 7.2B, Fig. 7.2C).

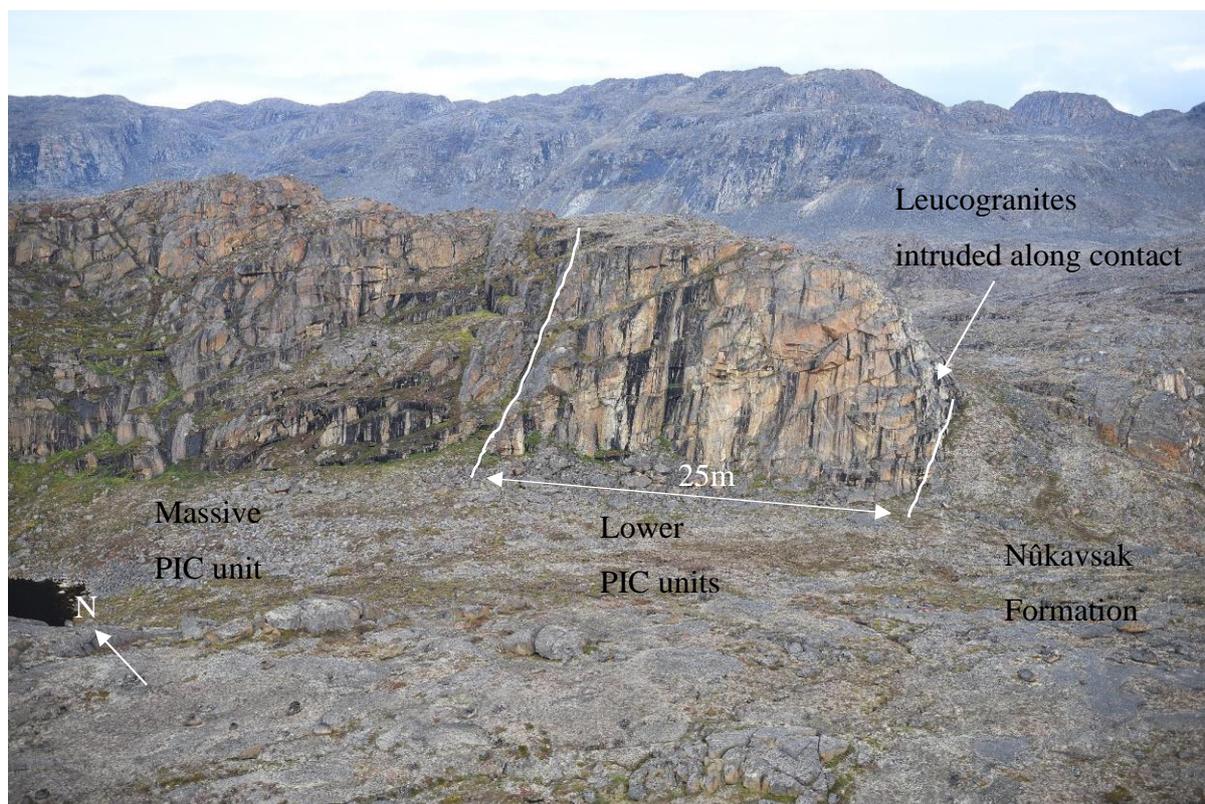Figure 7.30 – Hinge of Anticline at Uilortusoq Image: GEUS

Figure 7.31 – Outcrop at Ikinaarsuk on Northern limb of Sannigasoq anticline Image: GEUS

7.6.2 Interpretations

Using cross sections and reflecting the geology seen to the west of Sanningasoq we can identify the main structures and their order of formation (Fig. 7.32).

Mode	Descriptions	Orientation of Fold Axial Trace
D1	D1 Thrust Boundary	
F1	F1 Central Anticline	E-W
F2	F2 Syncline	SSW-NNE
F3	F3 Folds	E-W

Figure 7.32 – Table of stages of major structures within the Sanningsoq Fold

The deformation phases here, although very different in map pattern, can be easily correlated with the structural evolution and strain regime of the Atilissuaq Dome Complex to the west. (Fig. 7.28)

Phase	Associated structures	Strain Regime
D1	D1 Thrust System F1 Tight anticline	Ductile thrusting E-W
D2	F2 Open folds	E-W Contraction
D3	F3 Open folds	N-S Contraction

Figure 7.33 – Table of stages of deformation related to the Sanningasoq Fold

The map pattern strongly indicates that the stratigraphy has been repeated by a D1 thrust, the same as seen on Aappilatoq within the Akornat Anticline - likely the roof thrust of the Atilissuaq Dome Complex (Fig. 7.2B). This thrust repeated stratigraphy has been folded into a large-scale F1 anticline which was likely originally orientated E-W much like the F1 folds on Nutaarmiut and Akia (Fig. 7.1). Later the F1 anticline has been folded into a Type II "dome-crescent-mushroom style" interference pattern by a large-scale NNE-SSW orientated F2 syncline plunging to the SE noted in the Stereonet (Fig. 7.29) (Ramsay, 1967; Ramsay and Huber 1987). Finally, smaller E-W trending F3 folds have overprinted the northern section of the fold - this is especially clear on the Anakassaat peninsular (Fig. 7.28).
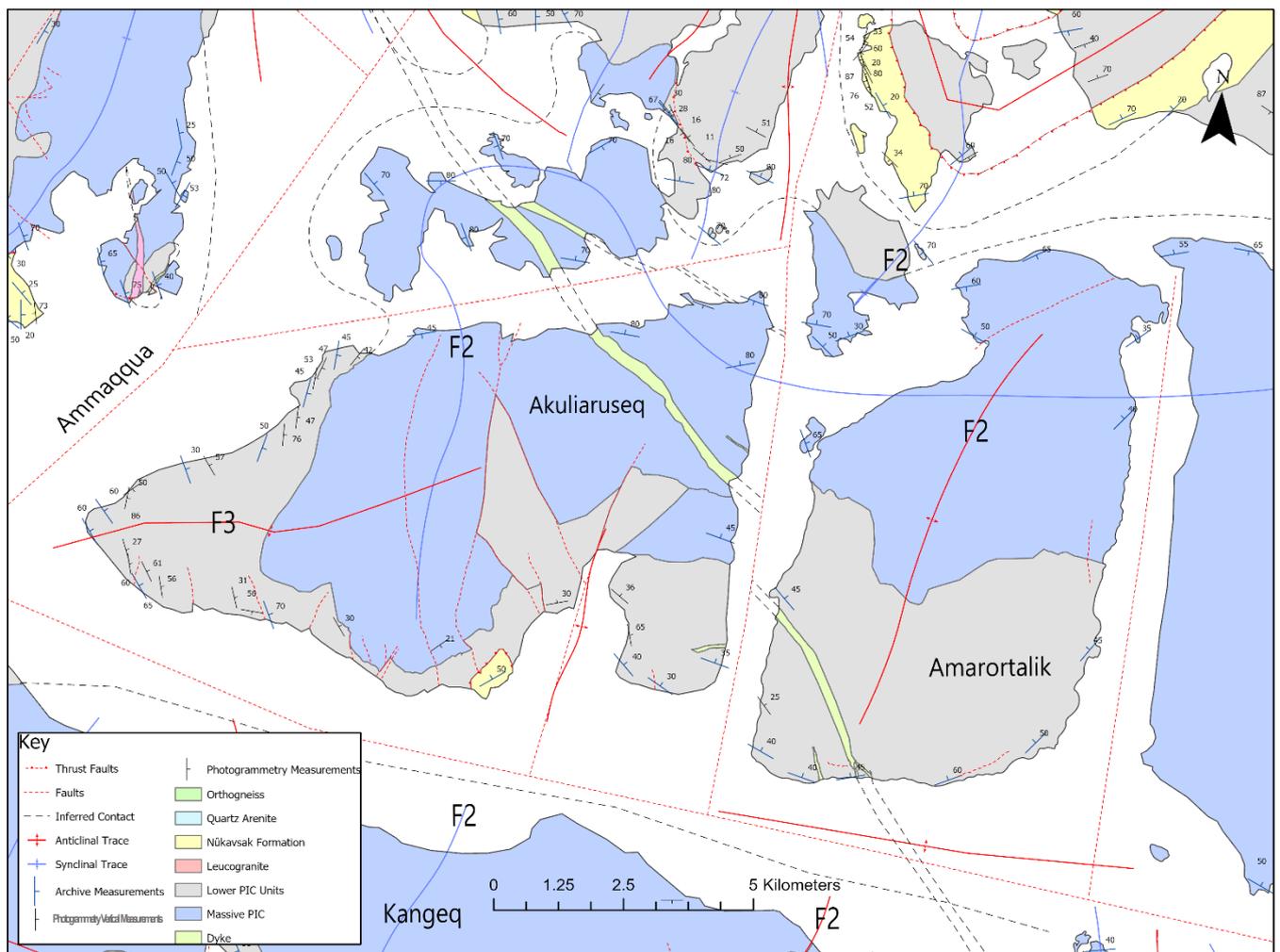
7.7 Akuliaruseq and Amarortalik

Figure 7.34 – Geological Map of Akuliaruseq and Amarortalik

7.7.1 Descriptions

To the South of the Sanningasoq Fold the islands of Akuliaruseq and Amarortalik are predominantly formed of Upper PIC units in the north and Lower PIC Units along the southern coastline (Fig. 7.34).

Structural measurements on the western peninsular of Akuliaruseq reveal that on the southern coastline the layering within the Lower PIC Units dips gently to the SE, and on the northern coastline the layering dips to the NE (Fig. 7.34). This indicates the presence of very open, non-cylindrical anticline with an axial trace orientated E-W (Fig. 7.35).

Two other anticlines can be mapped here, with axial traces orientated N-S, plunging gently to the south east and overprinting the older E-W anticline (Fig. 7.34). Where synclines are likely

present the fjords have eroded, suggesting the PIC acts as a protective erosional cap and anticlines are therefore more likely to be preserved (Fig. 7.34).

7.35 Stereonet of Akuliaruseq Antiform

n=19

Pink = North limb Green = South limb
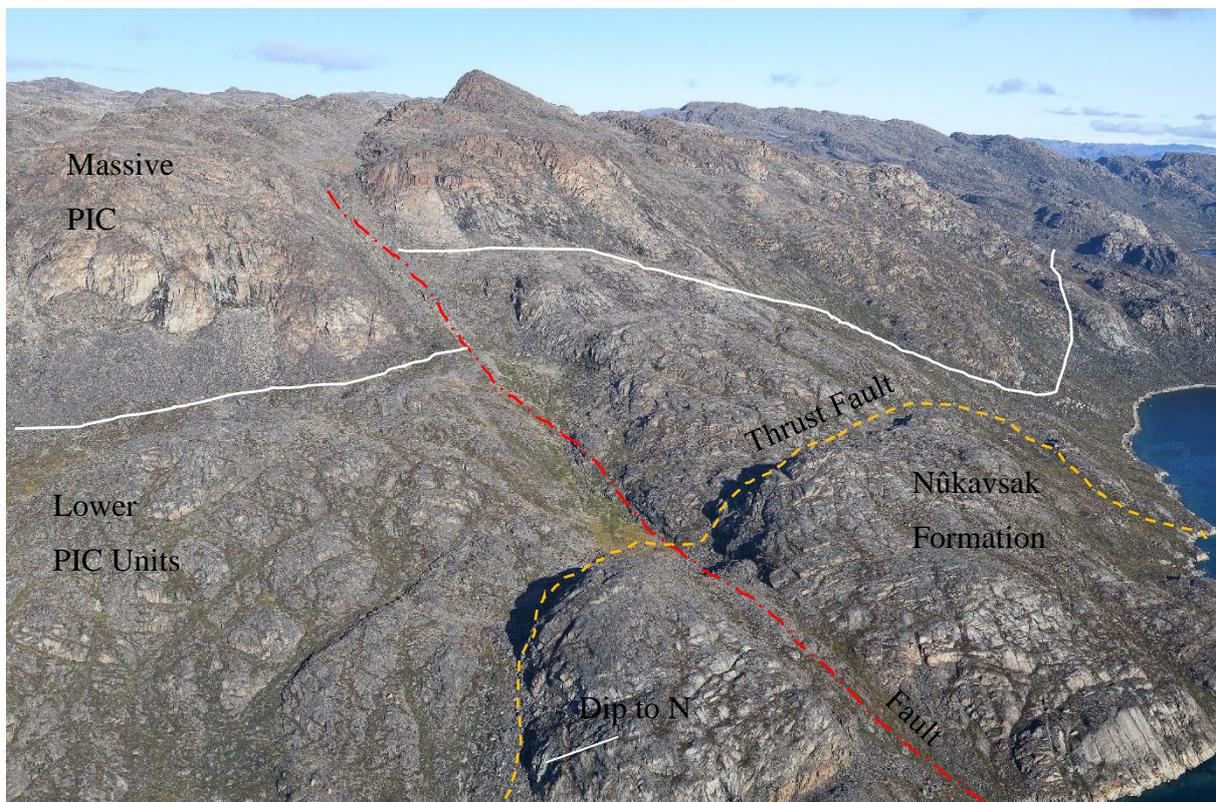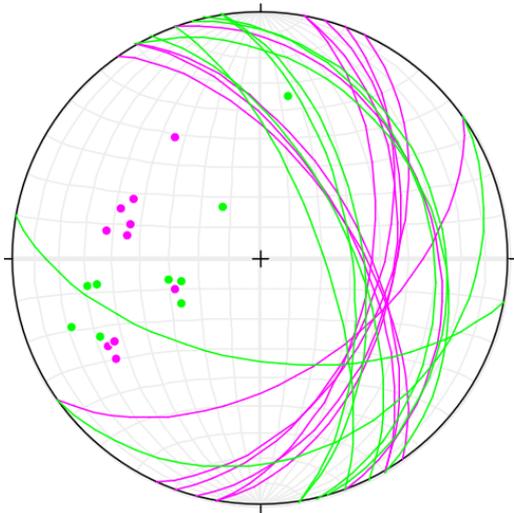
Open antiform plunging towards the east

Figure 7.36 – Thrust contact at Akuliaruseq, Akuliaruseq Photo: GEUS

On the southern coast of Akuliaruseq, at Assakaasut, a small outcrop of Nûkavsak Formation is visible (Fig. 7.34). The leucogranite layers in the Nûkavsak Formation dip 50-degrees to the north whereas the layering in the lower PIC Units dip 25-degrees to the south (Fig. 7.34). This change in foliation dip between the Nûkavsak Formation and the LPIC units indicates this is an isolated thrust contact, which is clear from the photogrammetry (Fig. 7.36).

7.7.2 Interpretations

Using cross sections and reflecting the geology to the north we can identify the main structures and their order of formation (Fig. 7.37).

Mode	Descriptions	Orientation of Fold Axial Trace
D1	D1 Thrust Boundary	
F2	F2 Open Synclines	N-S
F3	F3 Open Anticline	E-W

Figure 7.37 – Table of stages of major structures on Akuliaruseq and Amarortalik

From this we can identify the different phases of deformation and their associated strain regime (Fig. 7.38).

Phase	Associated structures	Strain Regime
D1	D1 Thrust System	Ductile thrusting E-W
D2	F2 Open folds	E-W Contraction
D3	F1 Open fold	N-S Contraction

Figure 7.38 – Table of stages of deformation on Akuliaruseq and Amarortalik

We interpret that the base PIC has deformed in an "eggbox" type manner, with 2 major fold structures perpendicular to each other (Fig. 7.34). This is a Type I interference pattern (Ramsay, 1967; Ramsay and Huber 1987). As previously noted, the wavelength of these folds is much larger than folds lower in the stratigraphy and they are more open in structure (Fig. 7.2D).
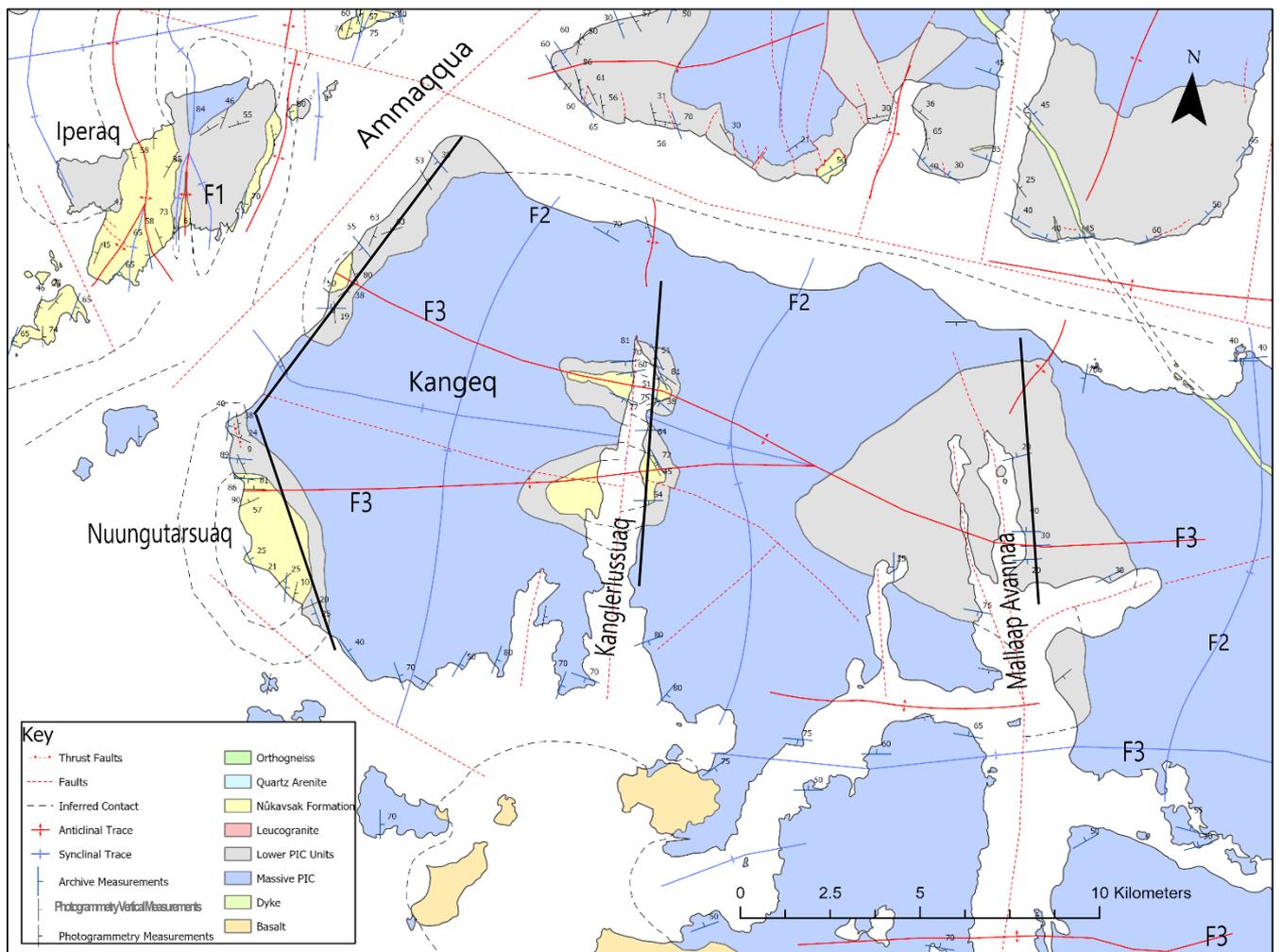
7.8 Kangeq

Figure 7.39 – Geological Map of Kangeq

7.8.1 Descriptions

The large peninsula in the south of the study area, Kangeq, is similar in map pattern to Akuliaruseq and Amarortalik with mostly PIC units cropping out with small, isolated outcrops of Nûkavsak Formation (Fig. 7.39).

However, on Kangeq the base PIC outcrops are sub-rounded in shape and elongated along a E-W axis (Fig. 7.39). Structural measurements show that the northern contacts dip to the north and the southern contacts dip to the south (Fig. 7.39). This implies the presence of an E-W orientated anticline, which can be mapped for around 25km (Fig. 7.39). Map pattern and structural measurements show that in the east the anticline is large and open, but to the west the anticline bifurcates into two small, tight anticlines (Fig. 7.39).

In the east at Mallaap Avannaa the anticline is evident as a large outcrop of Lower PIC Units which represents a 10km wide, symmetrical, open fold (Fig. 7.39). This is further supported

with measurements taken from the layers in the Lower PIC Units, which show a very cylindrical anticline (Fig. 7.39, Fig. 7.41). The fold cannot be mapped to the east, suggesting a gentle plunge under the surface (Fig. 7.39). Cross sections show that the LPIC units remain constant in thickness across the fold (Fig. 7.40). The fold is elongated to the N-S indicating that it is overprinted by a N-S trending fold with a similar open structure to the E-W fold, developing a fold interference pattern. This syncline has been eroded by the fjord (Fig. 7.39).
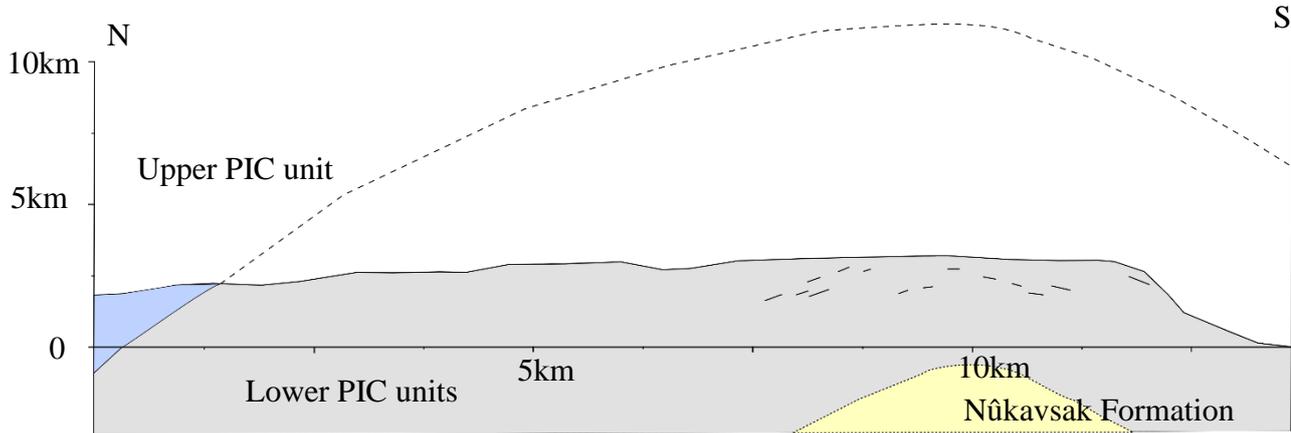
Figure 7.40 Kangeq anticline at Mallaap Avannaa, cross section and stereonet. Image taken directly from Stereoblend and digitised in Inkscape
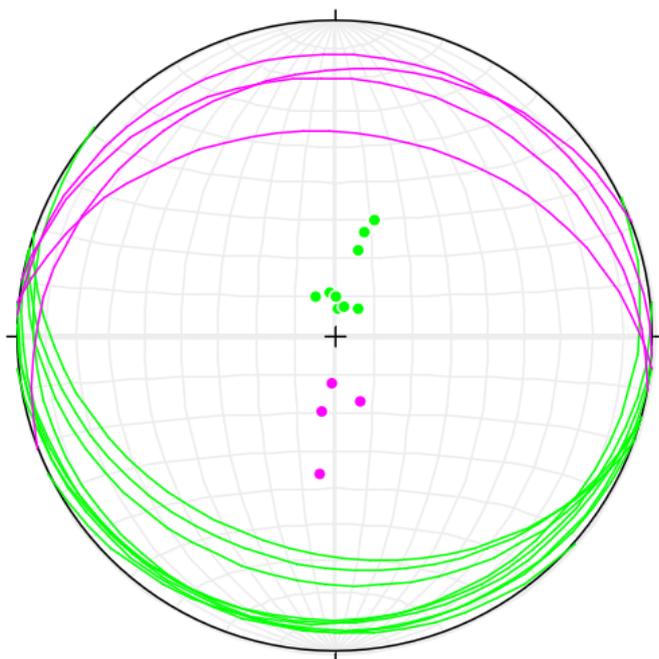
Figure 7.41 Stereonet of Kangeq anticline at Mallaap Avannaa n=13
Pink = North limb
Green = South limb

(Lambert projection)

To the west of at Mallaap Avannaa, in central Kangeq at Kangerlussuaq two rounded outcrops are formed of Lower PIC units with a central core of Nûkavsak Formation (Fig. 7.39). Leucocratic dykes within the units dip steeply away from each other highlighting the opposing limbs of two tight anticlines (Fig. 7.39, Fig. 7.42). This indicates a bifurcation of the anticlinal

84

axial trace as the axial trace moves from east to west, between Kangerlussuaq and Mallaap Avannaa (Fig. 7.39).

Cross sections show that the antiforms plunge towards each other with a steep synform in the centre (Fig. 7.42). The northern anticline is much tighter and has a steep sided "box" shape (Fig. 7.42). The Lower PIC units show significant variation in thickness between the northern and southern anticline (Fig. 7.42). The northern fold plunges steeply to the SE, whereas the southern fold plunges gently towards the E (Fi. 7.41, Fig. 7.42).

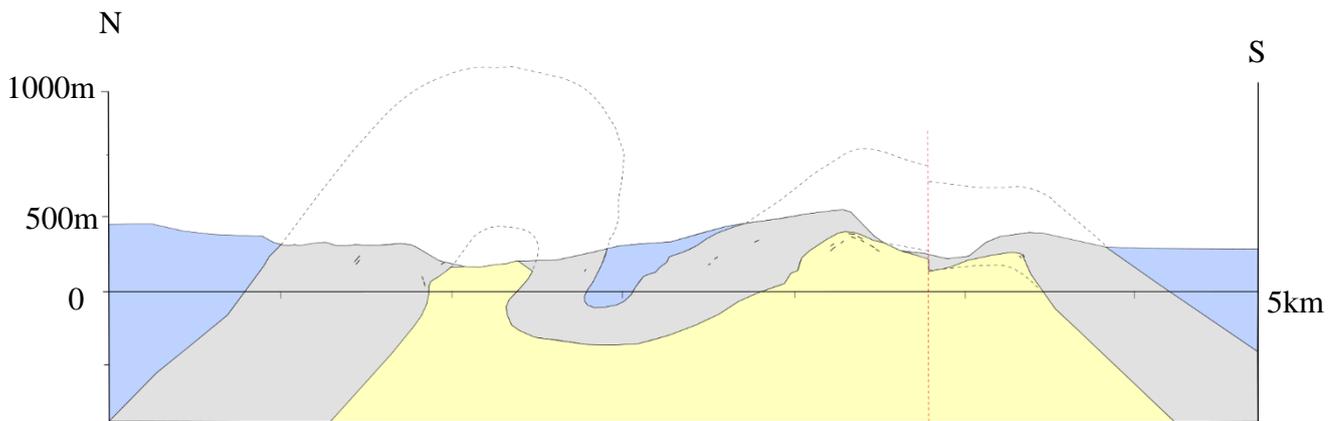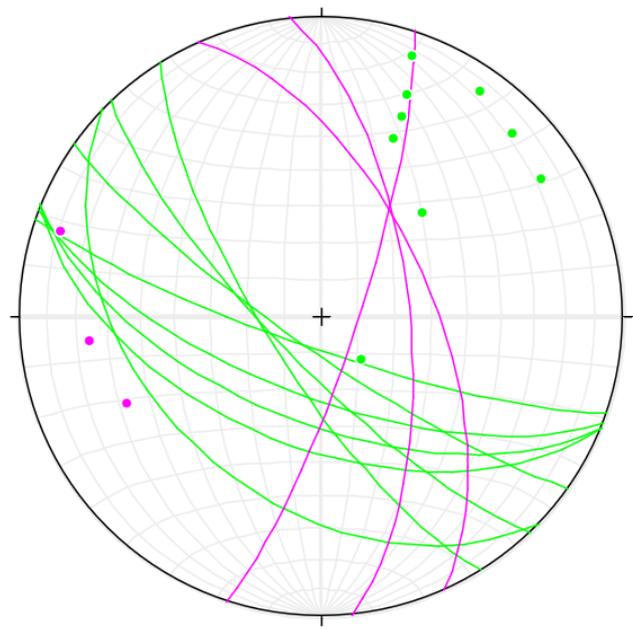Figure 7.42 - Kangeq anticline at Kangerlussuaq, cross section and Stereonet.

Figure 7.41 Stereonet of northern Kangeq anticline at Kangerlussuaq n=13 Pink = North limb Green = South limb
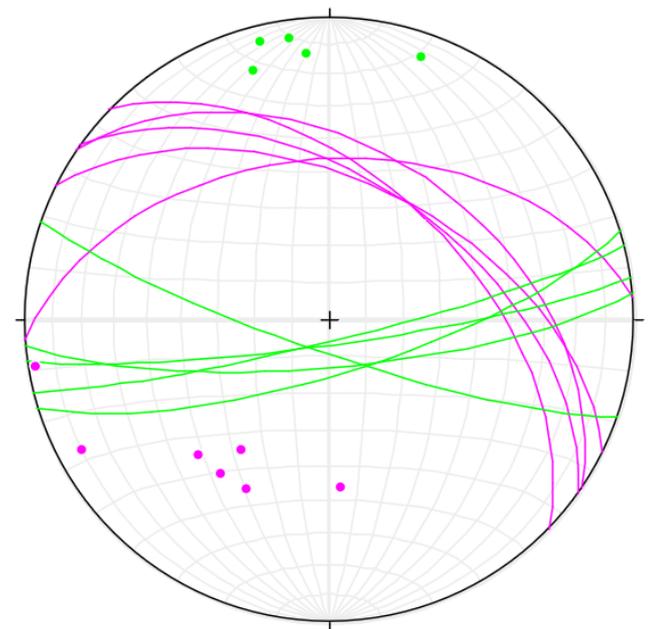
Figure 7.42 Stereonet of southern Kangeq anticline at Kangerlussuaq n=10 Pink = North limb Green = South limb

The southern limb of the anticline has been cut by a normal fault dipping to the south, which has an offset of around 50m (Fig. 7.43). The fault and the anticline were then eroded to form the valley system.

Figure 7.43 - Kangeq anticline at Kangerlussuaq, image taken looking east towards Mallaap Avannaa. Image: GEUS

East of Kangerlussuaq, on the east coast of Kangeq, there are again two rounded outcrops of Lower PIC Units with cores of Nûkavsak Formation (Fig. 7.39). Structural measurements show these outcrops are anticlinal cores and likely expose the continued axial traces of the anticlines at Kangerlussuaq (Fig. 7.39). The anticlines are much further apart than at Kangerlussuaq indicating they are plunging away from each other (Fig. 7.39; Fig. 7.41).

In the south east a large, asymmetrical antiform trends towards the WSW and, like in Kangerlussuaq, a box shape is highlighted by upright leucogranite dykes at Nuungutarsuaq (Fig. 7.44, Fig. 7.45). On the eastern limb of the fold the leucogranites dip gently to the south west and the lower PIC units thin (Fig. 7.44; Fig. 7.47).

Further up the east coast the northern anticline is exposed opposite Iperaq island, with a very small outcrop Nûkavsak Formation as the anticlinal core (Fig. 7.39). The anticline has an

asymmetric structure with varying thickness of Lower PIC Units (Fig. 7.44). Cross sections show that the two antiforms plunge eastwards, converging towards each other, with a deep syncline in the centre (Fig. 7.39; Fig. 7.44; Fig. 7.46).
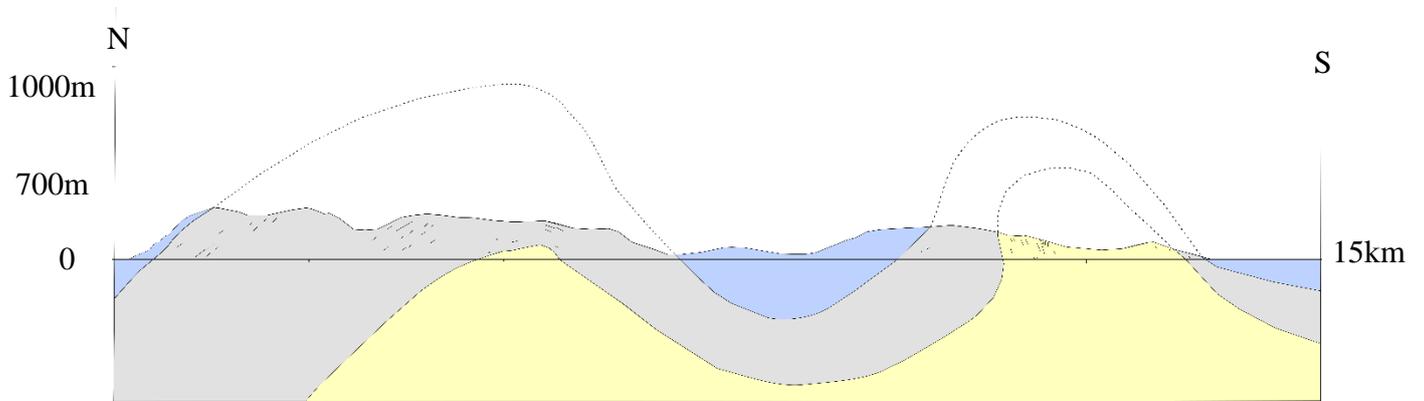
Figure 7.44 - Kangeq anticlines along the east coast of Kangeq, cross section and stereonets.

Figure 7.45 – Southern antiform of Kangeq anticline exposed at Nuungutarsuaq. Image: GEUS

Figure 7.46 Stereonet of northern Kangeq anticline along the east coast of Kangeq n=8

Pink = North limb Green = South limb

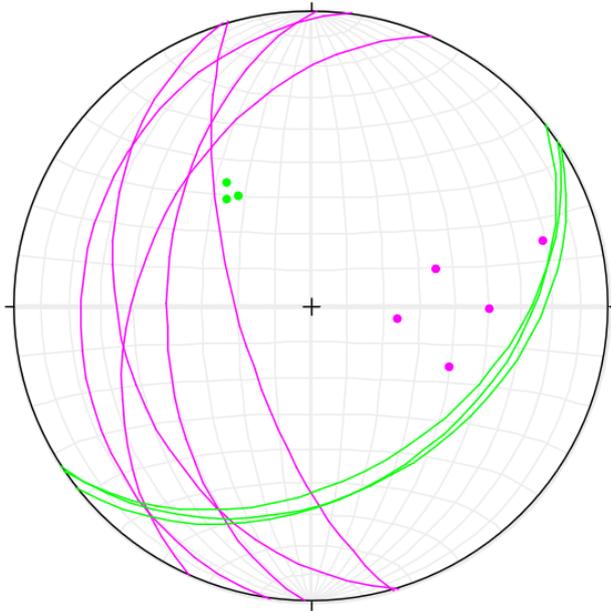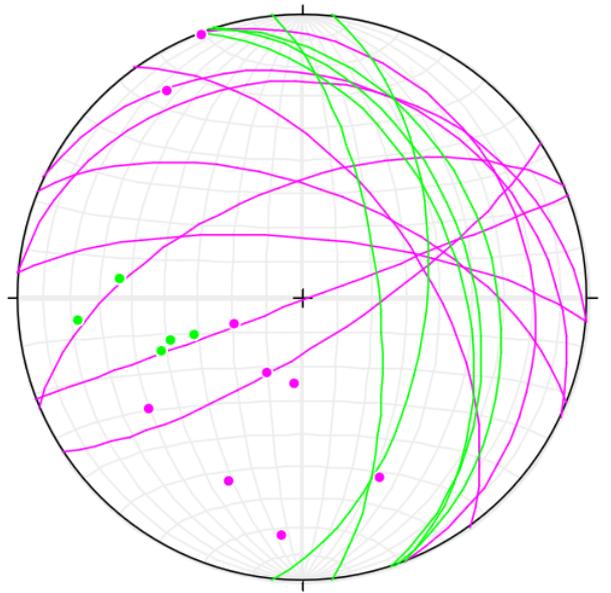Figure 7.47 Stereonet of southern Kangeq anticline along the east coast of Kangeq n=8

Pink = North limb Green = South limb

7.8.2 Interpretations

Using cross sections and reflecting on the geology to the north we can identify the main structures and their order of formation (Fig.7.48).

Mode	Descriptions	Orientation of Fold Axial Trace
F2	F2 Open Synclines	N-S
F3	Bifurcating Anticline F3	E-W

Figure 7.48 – Table of stages of deformation on Kangeq

From this we can identify the different phases of deformation and their associated strain regime. (Fig. 7.49)

Phase	Associated structures	Strain Regime
D2	F2 Folds	E-W Contraction
D3	F3 Box Folds	N-S Contraction

Figure 7.49 – Table of stages of deformation on Akuliaruseq and Amarortalik

On Kangeq, mapping reveals a large-scale bifurcating anticline with axial trace orientated E-W across the peninsular (Fig. 7.39). The anticline bifurcates towards the west, indicating strain developing on an E-W axis (Fig. 7.39). Detailed cross sections allow investigation into the structure of the anticlines and reveal a "box" like shape with steeply dipping limbs, much like the folds on Qaarsorsuatsiaq (Fig.7.40; Fig. 7.42; Fig. 7.44; Fig. 7.2E). We interpret that this shape has formed due to outwards verging thrust faults in the fold core - kink bands. This indicates late-stage reactivation of previous stress regime, localised intensification of folds where the late-stage normal faults converge.

The map pattern and structural measurements show that synclines trend N-S across the peninsula around 7.4km apart (Fig. 7.39). The map shows that the axial traces of the N-S synclines have been transported and bend towards the west along the axial traces of the E-W anticlines (Fig. 7.39). Therefore, the E-W folds (F3) overprint the N-S folds (F2), reflecting the age relationships and structural evolution seen in the geology to the north. The F1 N-S synclines and F3 E-W anticlines intersect perpendicular to each other, meaning that the base of the PIC can be visualised as almost eggbox in shape and a Type I Interference fold pattern

has developed (Ramsay, 1967; Ramsay and Huber 1987; Fig. 7.2E). Further south the archive maps show F3 folds continue along the fjord as far south as the contact of the PIC with the overlying basalts (Fig. 7.39).

7.9 Annertusoq and Iperaq
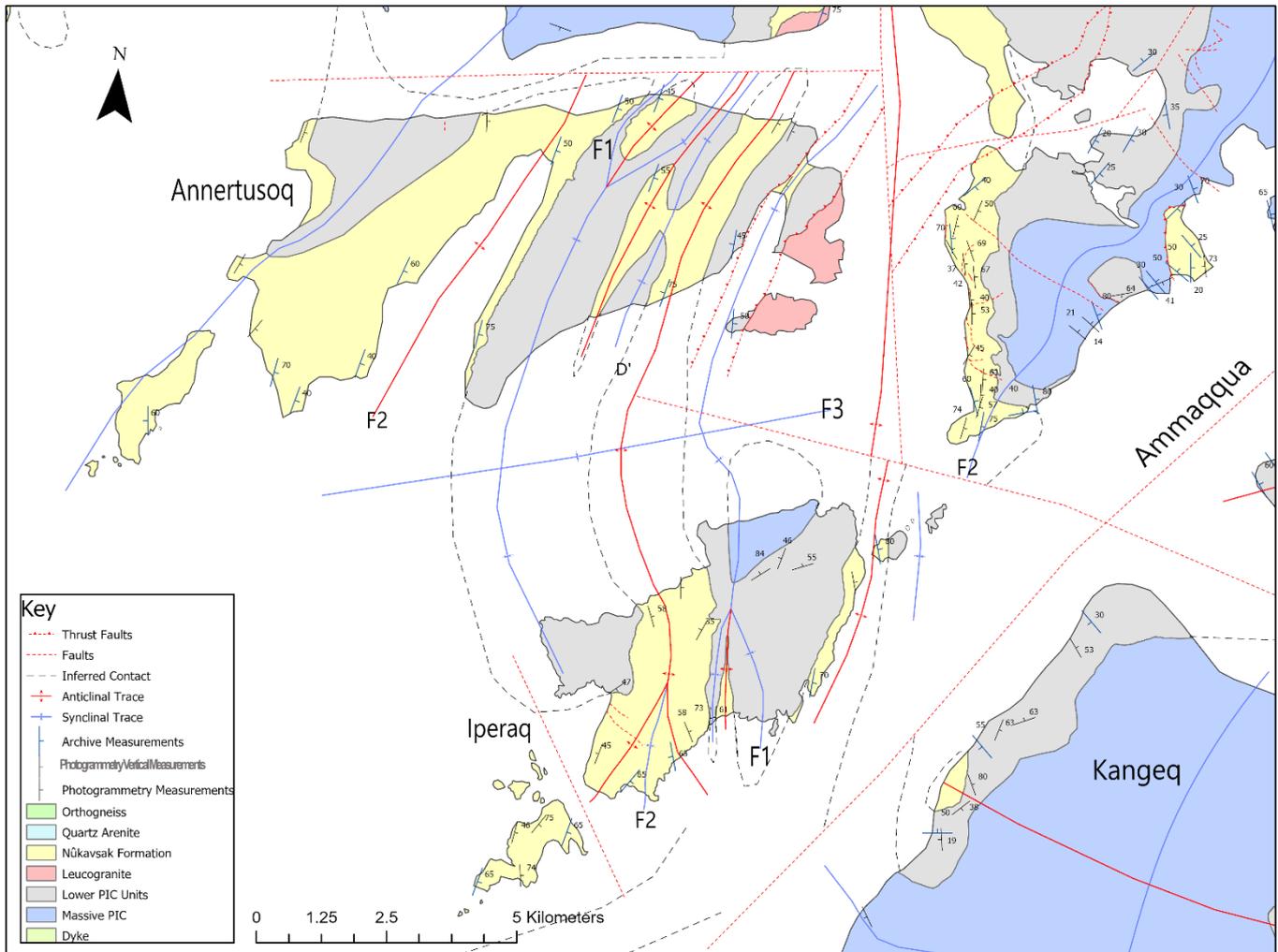
Figure 7.50 - Geological Map of Annertusoq

7.9.1 Descriptions

Directly to the west of Kangeq the islands of Annertusoq and Iperaq show a map pattern of predominantly Lower PIC Units and Nûkavsak Formation (Fig. 7.1; Fig. 7.50). The map pattern is like the outcropping geology of the NE of the area, in contrast to the geology of the nearby mainland (Fig. 7.50).

On Iperaq the outcrops consist of mainly N-S orientated strips of Lower PIC Units and Nûkavsak Formation with an isolated outcrop of Upper PIC Units in the north (Fig. 7.50). Structural measurements show that within the Nûkavsak Formation, the contacts dip outwards

implying the presence of an anticline (Fig. 7.50). Within the Lower PIC Units, the contacts dip outwards, implying the presence of a syncline (Fig. 7.50). Together with the map pattern this confirms there is a series of folds with axial traces orientated N-S (Fig. 7.50).

Within the Lower PIC outcrop, a small triangular shaped anomalous outcrop of Nûkavsak Formation appears to be structurally above the Lower PIC Units (Fig. 7.50; Fig. 7.51). However, using structural data, we can conclude that this is a Type II interference pattern, where an E-W orientated F1 Syncline has been folded by a N-S orientated F2 Anticline (Ramsay, 1967; Ramsay and Huber 1987; Fig. 7.2E; Fig. 7.52).
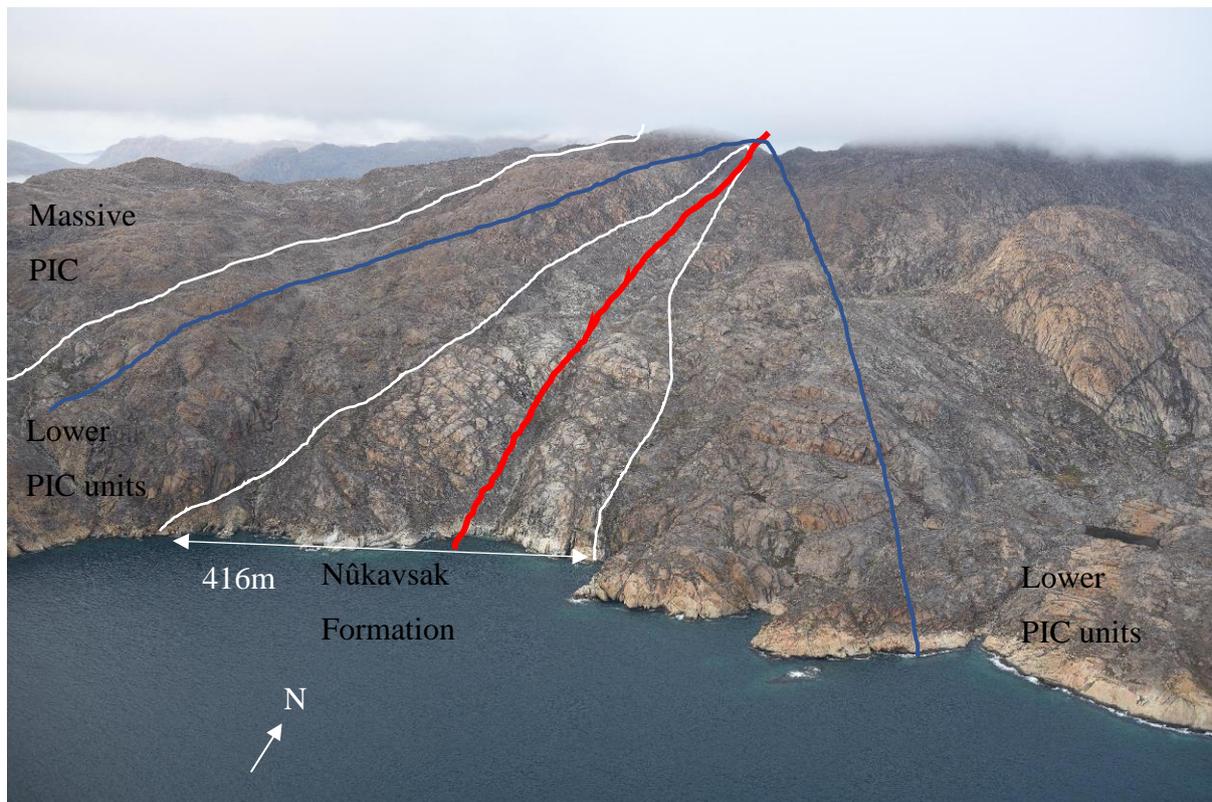
Figure 7.51 Paragneiss highlighting refolded fold structure at Iperaq Image: GEUS

On Annertusoq the map pattern is similarly formed of NE-SW orientated strips of Lower PIC Units and Nûkavsak Formation, with an outcrop of Leucogranite on the east coast (Fig. 7.50). Using structural measurements and constructing cross sections a series of tight F2 folds with N-S orientated axial traces is revealed (Fig. 7.50; Fig. 7.2E). A similar triangular outcrop of Nûkavsak Formation as on Iperaq reveals the same structural evolution of Type 2-fold interference patterns – so called "dome-crescent-mushroom style" interference patterns (Fig. 7.2E; Fig. 7.50).

91

On the east side of Annertusoq a repeated pattern of Lower PIC Units and Nûkavsak Formation cannot be explained by folding, as the Nûkavsak Formation would have to lie above the Lower PIC Units (Fig. 7.50). This indicates the presence of a N-S trending thrust fault which can be extrapolated to join a previously mapped thrust fault on Nutaarmiut (Fig. 7.50).
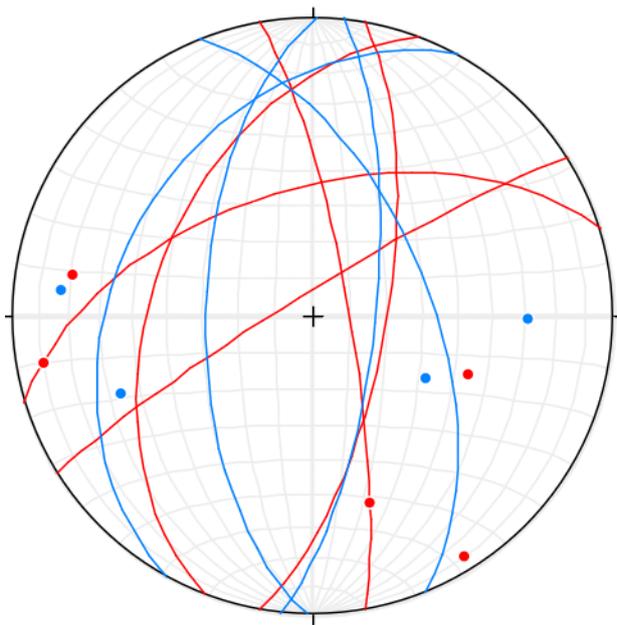
Figure 7.52 Stereonet of Iperaq East fold n=9

Red = East limb Blue = West limb

7.9.2 Interpretations

From the map pattern, structural measurements, and cross sections we can identify the main structures and their order of formation (Fig. 7.53).

Mode	Descriptions	Orientation of Fold Axial Trace
D1	Thrust Faults	
F1	F1 Synclines	E-W
F2	F2 Open Synclines	N-S
F3	F3 Syncline	E-W

Figure 7.53 – Table of major structures on Annertusoq and Iperaq

Although no large scale F3 folds can be mapped with photogrammetry, extrapolating the axial planes of the F2 folds between Annertusoq and Iperaq requires a significant bend along an E-W plane, indicating the presence of a large scale F3 fold (Fig. 7.50).

From this we can identify the different phases of deformation and their associated strain regime (Fig. 7.54).

Phase	Associated structures	Strain Regime
D1	Thrust Faults	Ductile thrusting E-W
	F1 Folds	Ductile thrusting E-W
D2	F2 Folds	E-W Contraction
D3	F3 Folds	N-S Contraction

Figure 7.54 – Table of stages of deformation on Annertusoq and Iperaq

This reflects a similar sequence of deformation to Akia, with an interpreted base thrust system verging towards the west (Fig 7.2E). It is noted that the map pattern on Annertusoq and Iperaq is distinctly different in scale and wavelength of folds to the surrounding larger islands (Fig 7.2E).

7.10 Ikeq Margin Thrust System

Figure 7.55 - Geological Map of Ikeq Margin Thrust System ArcGIS Pro

7.10.1 Descriptions

In the north east corner of the study area, to the NE of the Atilissuaq Dome Complex, are a series of small islands formed of outcrops of Lower PIC Units and Nûkavsak Formation (Fig. 7.1; Fig. 7.55). The map pattern is complex and highly deformed, but through the production of cross sections a picture of the sub surface geology has been developed (Fig. 7.2A).
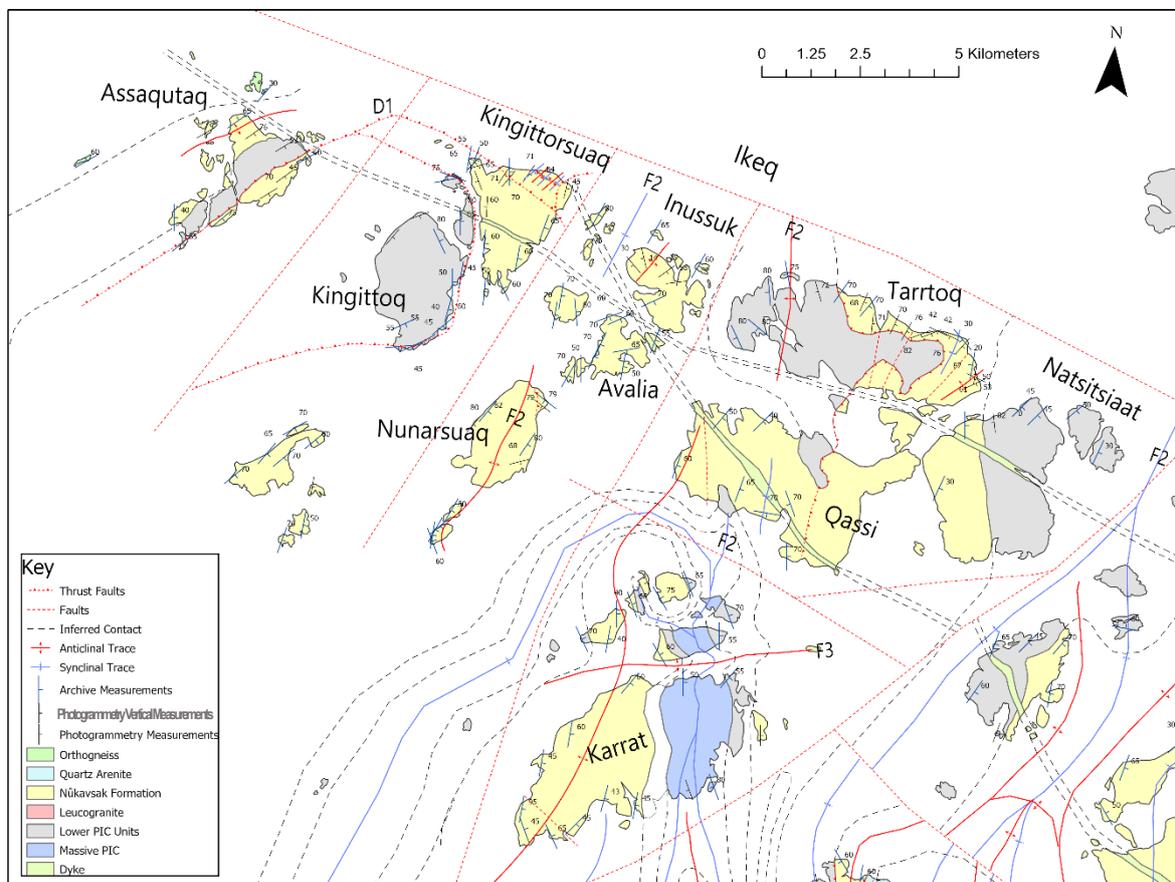
On the furthest West island, Assaqutaq, the map pattern shows a repeating sequence of Lower PIC Unit within Nûkavsak Formation (Fig. 7.55). All the units dip to the south east, so the Nûkavsak Formation is both up and down dip of the Lower PIC Units (Fig. 7.55). Effectively sandwiched between Lower PIC Units, contrasting the established stratigraphy (Fig. 7.2A). This shows that the repeated sequence must indicate the presence of a thrust contact down dip of the Nûkavsak Formation which has caused structural thickening (D1) (Fig. 7.2A).

To the east are the two islands of Kingittoq – outcropping Lower PIC Units – and Kingittorsuaq – outcropping Nûkavsak Formation (Fig. 7.55). On Kingittoq the leucogranite sheets show that the units on the east coast dip towards the east at around 65 degrees, and on the west coast of Kingittorsuaq the Nûkavsak Formation dips towards the west at around 60 degrees (Fig. 7.55). The narrow fjord between the two islands is only 20m across (Fig. 7.55). This stratigraphy places the Nûkavsak Formation on top of the Lower PIC Units, and so indicates the presence of a thrust between the islands (Fig. 7.55). The structural measurements in the units are parallel to the coastline indicating a curved contact, which can be extrapolated to connect with the thrust on Assaqutaq (D1) (Fig. 7.55). On the north coastline there are a series of very tight folds with axial traces orientated NE-SW with wavelengths no more than 10m (F2) (Fig. 7. 55).

Further east is the island of Inussuk, with the islands of Avalia and Nunarsuaq directly to the SW. These islands are all formed of Nûkavsak Formation and structural measurements from the leucogranite sheets show a series of NE-SW orientated folds (F2) (Fig. 7.55). These folds have a wavelength of about 50m (Fig. 7.55). On Nunarsuaq there is a very strong foliation in a NE-SW trend, with lots of small-scale flattened folds in the leucogranites (Fig. 7.56; Fig. 7.57).

To the east are three larger islands: Taartoq, Qassi and Natsitsiaat (Fig. 7.55). These are all formed of both Nûkavsak Formation and Lower PIC Units (Fig. 7.55). On the south coast of Qassi a small triangular outcrop of Lower PIC Units indicates the hinge zone of the Ikermiunnguaq Syncline (F2) (Fig. 7.55). On the north coast of Qassi a similar strangely shaped outcrop of Lower PIC Units crops out (Fig. 7.55). This outcrop can be extrapolated over onto Taartoq where the contact separates the west side - Lower PIC Units, from the east side -

Nûkavsak Formation (Fig. 7.55). The Lower PIC Units dip towards the SW and the Nûkavsak Formation dips to the SE (Fig. 7.55). The cross sections cannot explain this contact by folding as the Nûkavsak Formation is on top of the Lower PIC Units (Fig. 7.2A). This indicates a thrust along the contact between the two units (D1) (Fig. 7.55; Fig. 7.2A). With an open anticline with axial trace NE-SW in the Lower PIC Units (F2) (Fig. 7.55). On Natsitsiaat the Nûkavsak Formation crops out on the west coast, and the Lower PIC Units on the east coast (Fig. 7.55). Both units dip to the east and this indicates that the islands is on the west limb of a large F2 syncline orientated NE-SW in the fjord between Aappilatoq and Natsitsiaat, on the edge of the Atilissuaq Dome Complex (D1) (Fig. 7.55; Fig. 7.2A).

These islands are all clearly affected by a very strong overprinting NE-SW foliation which has reorientated fold axial traces and flattened the folds (D3).

Figure 7.56 – Tectonic deformation of Nûkavsak Formation and leucogranites on Nunarsuaq with axial planes marked. Photo: GEUS
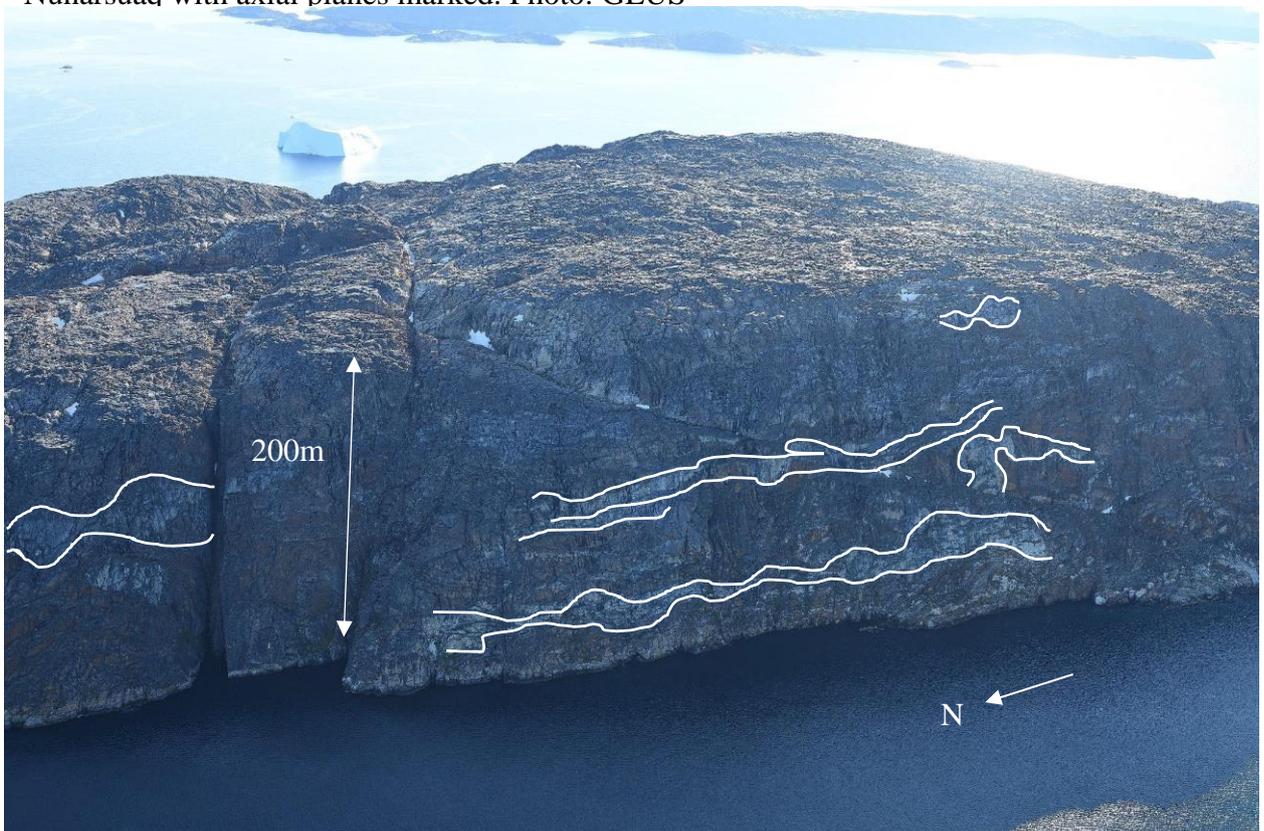
Figure 7.57 – Deformation of Nûkavsak Formation and leucogranites on Nunarsuaq showing intrusive geometries. Photo: GEUS

From the map pattern, structural measurements, and cross sections we can identify the main structures and their order of formation (Fig. 7.55; Fig. 7.2A)

From this we can identify the different phases of deformation and their associated strain regime. (Fig. 7.58).

Phase	Associated structures	Strain Regime
D1	Thrust Faults	Ductile thrusting E-W
D2	F2 NE-SW Folds	E-W Contraction
D3	NE-SW Foliation	Shear Zone

Figure 7.58 – Table of stages of deformation on Annertusoq and Iperaq

These islands are an area of intense deformation where thrusts have cut the surface. This indicates that the basal thrust is very close to the exposure level (Fig. 7.2A). After this, the area has been affected by a series of NE-SW orientated F2 folds, which have folded the thrust contacts (Fig. 7.55). Late-stage deformation of the NE-SW orientated shear zone has flattened and reorientated the fold axial traces, and further deformed the thrust contacts. F2 folds have been tightened and reorientated from N-S to NE-SW. This overprinting has removed any trace of F1 folds that can be found elsewhere in the mapping area. This all suggests the presence of an intense fold-thrust belt, likely related to the margins of the Tussaq Shear Zone outside of the mapping area which formed during D3 (GEUS report, Rosa et al 2017).

8. Discussion

From the production of the geological map a series of key questions have developed.

- What was the structural evolution of the host rocks and the intrusive complex? How does the intrusion emplacement event relate to deformation and timing?
- What is the intrusion geometry of the PIC?
- How far and from what depth has the PIC been displaced?
- What are good analogues for the PIC?
- How well has the photogrammetry technique worked?

Using the map pattern, structural measurements, and cross sections - as presented in Chapter 7 - we can discuss key interpretations and further work necessary to answer them.

8.1 Structural Evolution

We can summarise the main deformation phases, associated structures, and related strain regimes of deformation into 4 key phases of structural evolution. This is summarised as a table in Figure 8.1.

8.1.1 D1

In the first stages of deformation intense ductile thrusting developed. This is illustrated by thrust imbrication within an antiformal stack on Atilissuaq, around which the 20km wide Atilissuaq Dome developed as the PIC buckled over the top of the roof thrust around the dome. Isolated D1 thrust faults at the base of the PIC are exposed in the east on Nutaarmiut and Akuliaruseq, indicating that the base PIC is imbricated across the area.

A model for how original D1 structures developed is that associated E-W orientated open F1 folds formed synchronously with ductile thrusting and dome formation. F1 folds in the PIC are mapped on Nutaarmiut and Qaarsorsuatsiaq, indicating deformation occurred after emplacement. Towards the end of this phase intense horizontal shear at the base of the intrusion flattened F1 folds in the metasediment, forming recumbent isoclinal structures. This indicates an intense shearing event occurred below the PIC which produced the progressive evolution of the D1 structures. Transport direction was towards the WNW, highlighted by the cross sections and the vergence of folds and fold orientation, and during fieldwork from the stretching fabrics in the shear zone and kinematic indicators.

<u>8.1.2 D2</u>

In the secondary deformation phase, associated F2 folds overprint the F1 folds. These are a series of N-S orientated tight to close folds. These folds are mapped within the PIC and the base metasediments. This is highlighted as small-scale folds in the metasediments around 100m in wavelength by the map patterns in the west such as on Akia and Atilissuaq. Large scale 10km+ wavelength F2 folds such as the Ikermiunnguaq syncline and the Akornat Anticline formed in the east of the mapping area. Transport direction was again towards the W, highlighted by the cross sections and the vergence of folds and fold axial trace orientations.

The interaction between original D1 folds and D2 folds has led to the development of two types of interference patterns (Ramsay, 1967; Ramsay and Huber 1987).

- Type 1 "eggbox" style fold interference patterns within the upper PIC unit, where the twofold axial traces intersect at right angles to each other. For example, on Qaarsorsuatsiaq where N-S orientated detachment F2 folds overprint the original E-W orientated F1 folds.
- Type 2 "dome-crescent-mushroom" style interference patterns predominantly noted in the map pattern on small islands on the west coast such as Akia and Iperaq, and on a large scale within the Sanningasoq Fold in the east. Where an isoclinal F1 fold with axial trace orientated E-W is folded by an open F2 fold with axial trace orientated N-S.

Associated F2 anticlines show concentrations of leucogranite intruded into the fold cores and filling the hinge zone. During buckling as multilayers of varying competences are folded a space problem develops between hinges (Fossen, 2016). The passive emplacement of the leucocratic granite in the crest of F2 anticlines in this system is analogous to the common occurrence of microstructures such as quartz veins and other types of mineralisation in fold hinge zones in lower grade rocks (Fossen, 2016). The formation of the leucogranite by partial melting of the underlying metasediments indicates peak metamorphism in the late stages of D2 as maximum temperatures were reached.

<u>8.1.3 D3</u>

The axial trace orientations of F2 structures in the north east of the area show a 45° bend into a NE-SW orientation. This bend increases the further north along the axial trace. This is present across the Atilissuaq Dome complex, especially on the island of Aappilatoq. Along the Ikeq Margin Fold Thrust, mapping shows no trace of another orientated fold structures as they have been likely been flattened and reorientated. Transport Direction was to the NW as shown by

the vergence of folds, fold axial trace orientations and the intense foliation. This suggests that the Ikeq Margin Fold Thrust Belt is part of a much larger shear zone which represents a late bend around the western margin of the PIC. This aligns with the Tussaq Shear Zone, an area of intense ductile deformation and flattening outside of the mapping area (GEUS report, Rosa et al 2017).

F1 and F2 structures show a clear overprinting by folds with E-W axial trace orientation which progressively rotate into the Ikeq Margin Fold Thrust Belt. Overprinting can clearly be seen in the map patterns on Akia and the Sanningasoq Fold, as parallel stratigraphic contacts along F2 axial traces highlight bends in the contacts due to overprinting by the F3 hinges. Transport direction was to the W, as indicated in cross sections by the vergence of folds and the axial trace orientations (Fig. 7.2). In the west the wavelength of F3 structures is around 100m within the metasediments and in the east around 10km within the PIC. F3 structures have developed a large-scale Type 1 Ramsay interference pattern as perpendicular F2 N-S orientated fold axial traces are overprinted by F3 E-W orientated fold axial traces, especially prominent in the south such as on Kangeq. F3 folds are prone to bifurcation, both towards the E in the north and towards the W in the south on Kangeq.

8.1.4 Brittle Faulting

Across the area there are strong indications of extensional faulting, and reactivation of existing structures within the PIC. Several deep cut fjords are likely to be related to a series of faults trending SE-NW, such as the Akornat Fjord and the Ammaqqua Fjord (Fig. 7.1). On the island of Akuliaruseq the map pattern indicates offset between the Upper and Lower PIC Units, indicating potential reactivation of existing thrust structures as normal faulting.

8.1.5 Summary

Deformation Phase	Associated Structures	Major Structure Examples	Transport Direction	Strain Regime	Notes and interpretations
D1	Thrust imbrication	Atilissuaq Dome Complex Ikeq Margin Thrust System Annertusoq	WNW	Ductile thrusting	Minimal as basal thrust well below erosion level

	F1 Isoclinal folds with inverted limbs	Akia Iperaq Sanningasoq Fold Annertusoq		Intense horizontal shear	Rare in PIC
D2	F2 N-S large scale folds	Akornat Anticline Ikermiunnguaq Syncline Nutaarmiut Syncline Amarortalik Kangeq Atilissuaq Sanningasoq Fold Iperaq Annertusoq	W	E-W Contraction	Common
	Intrusion of Leucogranite	Akornat Anticline			Peak metamorphism reached
D3	Fold thrust Belt	Ikeq Margin Thrust System	NW		Strong overprinting NE-SW foliation
	F3 E-W Folds	Akia Akuliaruseq Kangeq Karrat Sanningasoq Fold Atilissuaq	W		Common

		Dome Complex			
Brittle Faulting	Large Scale SE-NW Faults	Ammaqqua Fault Kangeq		Extension	

Figure 8.1 – Table of structural evolution of the Prøven Igneous Complex within the Rinkian Fold-Thrust Belt

The presence of the thick, massive unit at the top of the PIC is strong evidence that the PIC was competent during deformation. This indicates that the PIC was emplaced well before intense deformation and high-grade metamorphism during the Rinkian, which displaced the intrusion progressively to the NW and W.

Further work would assess the progressive nature of deformation between D1 and D2, which indicates a period of intense horizontal shear.

8.2 Intrusion geometry and tectonic implications

The cross sections in Figure 7.2 show that the PIC is a tabular intrusion, with a minimum thickness of 3km. The change in dip of the fold envelope – steeper and deeper in the east - implies a steep ramp mid-way in the sub-surface that is shown qualitatively in the cross sections (Fig. 7.2). The PIC was mechanically strong and thick above the ductile metasediments during deformation. The dominant fold wavelength is related to layer thickness, layer rheology and competency contrasts between layers (Fossen, 2020).

Layer thickness can be estimated using the Biot (1961) equation which expresses the relationship between layer thickness and dominating wavelength.

$$\frac{L_d}{h} = 2\pi \left(\frac{\mu_L}{6\mu_M}\right)^{1/3}$$

Where h = layer thickness, Ld = dominating wavelength, μ= viscosity of L (layer) and matrix (m)

$$h = \frac{L_d}{2\pi} \left(\frac{6\mu_M}{\mu_L}\right)^{1/3}$$

Ld = 10km ~ 1km

μ_L = viscosity of granite = 3–6·1020 Pa·s.

μ_M = viscosity of migmatite =

Therefore, if Ld = 10km in the east

$$h = \frac{10}{2\pi} \left(\frac{6\mu_M}{\mu_L} \right)^{1/3}$$

Then

$$h = \frac{10}{2\pi} \left(\frac{6\mu_M}{4} \right)^{1/3}$$

$$h = n$$

And if Ld = 1km in the north west

$$h = \frac{1}{2\pi} \left(\frac{6\mu_M}{\mu_L} \right)^{1/3}$$

Then

$$h = \frac{1}{2\pi} \left(\frac{6\mu_M}{4} \right)^{1/3}$$

$$h =< n$$

The exact values of this equation are not essential, they are simply used to establish the relationship between parameters when $\mu_L > \mu_M$. In this instance the larger the value of Ld the larger the value of h. Therefore, as the dominating fold wavelength is longer in the east and shorter in the north west, the intrusion was thicker to the east and thinned towards the north west. This strongly implies the presence of multiple competent sheets in the east, and potentially only a singular sheet towards the north west (Fig. 8.2).

Further work on this would need to involve fieldwork/sample collection within the massive PIC for intrusion related structures which would help distinguish separate sheets that are only visible on outcrop scale. The ramp in the basement could also be modelled more accurately using an area balance.
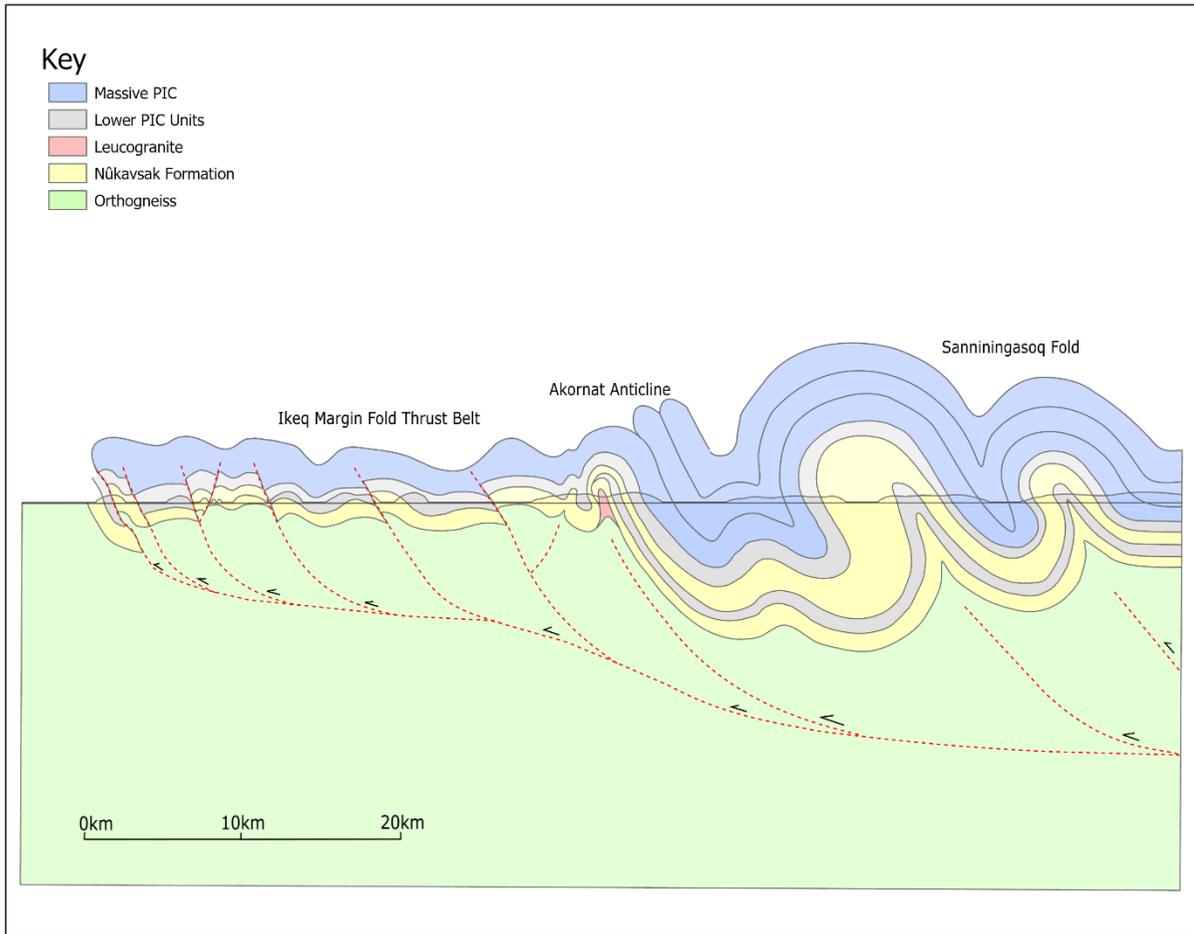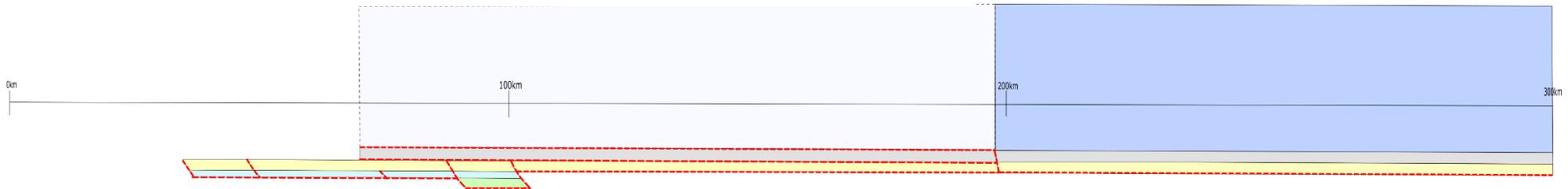
Figure 8.2 – Cross section with multiple sheets

Produced on Inkscape

Figure 8.3 – Partial reconstruction showing horizontal displacement

Produced on Inkscape

8.3 Displacement

The mapping highlights an intense shear zone at the base of the PIC which has displaced the intrusion progressively towards the WNW. Field evidence of enclaves of Nûkavsak Formation in the base PIC suggests an emplacement depth of no more than 10km. Recent partial restoration of Section Line B indicates at least 100km displacement of the PIC (Fig. 8.3).

Displacement at this magnitude implies that the PIC is likely has moved up through the crustal section. The ramps in the cross sections deepen the detachment to the east, suggesting that displacement is shallowly inclined to the east and that the PIC has moved up through the crustal section (Fig. 7.2). However, the field evidence of enclaves suggests that the PIC was emplaced at no more than 10km (Fig. 6.15).

The main evidence for this displacement, as shown in Chapter 7, is the repeated units of Lower PIC and Nûkavsak Formation within the core of the Sanningasoq Fold which all dip to the east. This repeated contact has been interpreted as a large thrust, which is also outcropping at Aappilatoq where the map pattern shows a similar repetition.

Potential alternative interpretations are that the duplicated section of Nûkavsak and LPIC, which previously led to the diagnosis of a thrust contact, could be due to multiple sheets of PIC being emplaced at the base of the complex with screen of metasediment between them. It also could be that not all the contacts within the Atilissuaq Dome are thrust duplications and represent a thick basin where turbidite material was deposited in sequence.

Further work on this would involve production of multiple partial restorations, a reassessment of the mapping and geochemistry work on the base shear zone. The distance of displacement is very important to understand as the original area of emplacement will help understand the location of the missing subduction zone indicated by the I-type granite.

8.4 Analogues

Recent geochemistry has reclassified the PIC as an I-type granite (Kokfelt et al, yet unpublished). This has reorientated tectonic models of the Rinkian orogen from a passive margin to a subduction related setting as part of a volcanic arc. The PIC intrusion is a pyroxene-bearing granitic rock and so defined as charnockite which usually form in a range of high-pressure settings (Frost & Frost, 2008). Ongoing work at the University of Bochum on mineral assemblages in the PIC suggests that peak metamorphism occurred at a pressure of maximum 5 kilobars within the paragneiss, implying a depth of 10-15km (Laura Bramm, unpublished

data 2021). The actual depth of emplacement is still uncertain but is likely to be a similar depth within a low-pressure system. A potential analogue for the PIC in terms of scale would be the Cordillera Blanca Batholith in Peru. The Cordillera is a similar scale granite intrusion at 60km+ diameter and just one of several large-scale granitic intrusions in South America due to the subducting plate I-type tectonic setting (Petford & Atherton, 1996). However, the Cordillera has not been metamorphosed at high grade to form a charnockite. The PIC represents a much lower pressure system where charnockite has formed at shallow depth with high temperatures and continental collision has occurred. The Himalayan charnockites are well exposed and the major Gangdese batholith contains charnockites to the east, which are evidence for a convergent plate margin in a similar setting to the PIC (Zhang et al, 2010).

8.5 Photogrammetry technique

The photogrammetry technique has allowed for years of fieldwork to be bypassed in months, reducing the need for extensive field seasons without compromising on quality. Over 40,000 images, each 50-60MB of data, were taken in a weeklong field season in August 2018. A typical 2-month field season for GEUS along with the additional expense of collating the map, however this map will cost GEUS around half of that.

Mapping relies heavily on the quality of each individual photo which can be affected by weather conditions, alignment of the camera etc. Weather can affect light and cloud levels, but there is generally enough light on the photos to identify layering etc, whereas in some flight lines environmental factors such as a low cloud base, glare from sunlight on the lens and snow cover obscures higher cliffs. As the data collection was limited to the specific time frame of a single week, the method always will be dependent on the weather and further controls that effect the group during that week such as illness, transport problems etc. The system works best on non-vegetated terrain and gently dipping landscapes. For some places, such as cliffs, it is the only way of mapping features. The entire system relies on the quality of the original photos, so waiting for a weather window may be necessary.

However, during the acquisition period of 2018 luckily most days were very good weather and there were no unexpected incidents. Only half a day of fieldwork was lost due to bad weather.

Geological field work is still essential with this method and cannot be removed altogether as a good understanding of the existing stratigraphy is essential. The system is great for large scale, outcrop size and above features, and for measuring planar fabrics such as strike and dip. Data cannot be collected on linear fabrics such as stretching directions and kinematic indicators

There are a few limitations to the software, such as only two photos can be viewed at once, so flicking between photos to map round a corner can be difficult. It also takes a while for the user to get used to using the software and the technical side to things, zooming in and out can be very frustrating and drawing polylines can initially be very confusing. Polylines are drawn directly into the 3D space, so they are draped like a ribbon and the cursor always needs to remain on the land surface. The programme does not know where the surface is and as this is a visual aspect to things which is determined by the user, human error can play quite a strong role here when getting used to using the software and a lot of polylines initially created had to be redrawn. However, with only a few days of training, most novices can engage with the software (Sørensen & Dueholm, 2018). When tracing a plane, the polyline needs to be drawn as accurately as possible in order to the software to calculate accurate geological measurements. Clearly this is harder to do on the software than in the field at an outcrop, but the programme allows measurements to be taken in inaccessible locations such as dangerous coastal areas, cliffs and steep ground. It also allows large quantities of data to be calculated at once, and you can easily flick back and forth between locations 1000s of kilometres apart. A weeks' worth of fieldwork allows for years' worth of contact and structural data to be collected.

At the photogeological lab, the nature of the system means that areas can be revisited multiple times by multiple different people. This allows peer review of mapping and represents a potential increase in mapping quality. The map produced in this study has been reviewed by GEUS staff and some contacts slightly redrawn for the official survey map.

Further work could involve the inclusion of other data gathering such as Lidar. The system itself could be more user friendly as it is hard to extract strike and dip data from each polyline. In addition, the software interface requiring 3D glasses and multiple screens is hard to get used to and requires an expensive setup which resulted in data collection for this study necessitating an expensive two month stay in Copenhagen.

9. Conclusion

The Prøven Igneous Complex is a tabular sheet intrusion of hypersthene granite, emplaced into Paleoproterozoic sedimentary rocks on the margin of the Archean age Rae Craton. The photogrammetry technique used in this study has allowed years of work on a geological survey map to be bypassed in months, with massively reduced costs and likely an increase in quality of mapping. Cross sections produced suggest the intrusion is likely to be made up of multiple sheets, thinning in thickness and number to the north west. After emplacement, the intrusion was deformed by a complex 4 stage structural evolution within the Rinkian orogenic belt. This includes a progressive displacement to the north west along an intense shear zone at the base of the PIC. Partial restoration of cross sections suggests this displacement was likely over 100km, from an emplacement depth of around 1015km, which suggests relatively little movement of the intrusion up-section. The intrusion also deformed, forming a series of strongly non-cylindrical folds in the ductile migmatitic sedimentary units below the buckling PIC.

Together with geochemical work by GEUS this study has added new constraints to Paleoproterozoic plate boundaries within the Rinkian. The geochemistry suggests that the PIC intrusion is most likely to be an arc complex (Kokfelt, yet unpublished). The structural reconstructions in this study suggest that the PIC intrusion underwent the same 5 phase progressive deformation as the host rock. The overall system was high temperature and medium pressure deformation with underlying thrusts verging towards the NW. This study adds to work by GEUS which suggests that the Rinkian foreland is to the East, implying a subduction boundary in Baffin Bay (Guarnieri, yet unpublished).

10. Bibliography

Biot, M.A., Ode, H., Roever, W.L., 1961. Experimental verification of the theory of folding of stratified viscoelastic media. Geological Society of America Bulletin, 72(11), pp.1621-1631.

Connelly, J.N., Thrane, K., Krawiec, A.W., Garde, A.A., 2006. Linking the Palaeoproterozoic Nagssugtoqidian and Rinkian orogens through the Disko Bugt region of West Greenland. Journal of the Geological Society, 163(2), pp.319-335.

Connelly, J.N., van Gool, J.A. and Mengel, F.C., 2000. Temporal evolution of a deeply eroded orogen: the Nagssugtoqidian Orogen, West Greenland. Canadian Journal of Earth Sciences, 37(8), pp.1121-1142.

Corrigan, D., Pehrsson, S., Wodicka, N. and De Kemp, E., 2009. The Palaeoproterozoic Trans-Hudson Orogen: a prototype of modern accretionary processes. Geological Society, London, Special Publications, 327(1), pp.457-479.

Escher, A. & Pulvertaft, T.C.R., 1968. The Precambrian rocks of the Upernavik-Kraulshavn area (72–74 15¢ N), West Greenland. Rapport Grønlands geologiske Undersøgelse, 15, pp.11-14.

Escher, A., Pulvertaft, T.C.R., Watt, W.S., 1976. Rinkian mobile belt of West Greenland. Geology of Greenland, 102, p.119.

Escher, J.C., Thorning, L. and Pulvertaft, T.C.R., 1995. Geologic Map of Greenland: 1: 2,500,000. Grønlands Geologiske Undersøgelse.

Escher, J.C. & Stecher, O., 1978. Precambrian geology of the Upernavik–Red Head region (72 15′–75 15′ N), northern West Greenland. Rapport Grønlands Geologiske Undersøgelse, 90, pp.23-26.

Escher J.C. & Stecher, O., 1980. Field work on Precambrian granites andmetasediments in the Søndre Upernavik–Kuvdlorssuaq region (72°00'–74°40'N), northern West Greenland. Rapport Grønlands GeologiskeUndersøgelse,100,38–41.

Escher J.C., 1981. (Compiler) Geologisk kort over Grønland, 1:100 000 Tasiussaq 73 V.1 Syd, Grønlands Geologiske Underøgelse, Copenhagen.

Escher, J.C. and Nielsen, T.F.D., 1983. Archaean gneisses and supracrustal rocks of the Tingmiarmiut region, South-East Greenland. Rapport Grønlands Geologiske Undersøgelse, 115, pp.79-82.

Escher J. C., Pulvertaft T. C. R. Stecher, O. (1967, 1978, 1979) Geological maps of Upernavik Isfjord, 1:40 000 (Geological Survey of Greenland, Copenhagen).

Fossen H., 2016. Structural geology. Cambridge University Press.

Frost, B.R. & Frost, C.D., 2008. On charnockites. Gondwana Research, 13(1), pp.30-44.

Garde A. A., Grocott J., Thrane K., Connelly J. N., 2003. Reappraisal of the Rinkian fold belt in central West Greenland: Tectonic evolution during crustal shortening and linkage with the Nagssugtoqidian Orogen. European Union of Geosciences Meeting, Geophysical Research Abstracts CD

Garde, A.A. & Pulvertaft, T.C.R., 1976. Age relations of the Precambrian Mârmorilik marble Formation, central West Greenland. Geological Survey of Greenland Report,80,49–53

Garde, A.A. 1978. The Lower Proterozoic Maarmorilik Formation east of Mârmorilik, West Greenland. Meddelelser om Grønland,200,1–71

Grocott J., McCaffrey K.J.W, Garde A.A, Thrane K., Hand M., Connelly J. 2004 Regional-scale horizontal flow of the mid-lower crust: the northern Nagssugtoqidian-Rinkian collisional orogenic system, West Greenland. Channel flow, Ductile Extrusion and Exhumation of Lower-mid Crust in Continental Collision Zones. December 2004 Geological Society of London

Grocott, J. & Pulvertaft, T.C.R. 1990. The Early Proterozoic Rinkian belt ofcentral West Greenland. In: Lewry, J.F. & Stauffer, M.R. (eds) The EarlyProterozoic Trans-Hudson Orogen of North America. Geological Associationof Canada, Special Paper, 37, 443–463

Grocott, J. & McCaffrey, K.J., 2017. Basin evolution and destruction in an Early Proterozoic continental margin: the Rinkian fold–thrust belt of central West Greenland. Journal of the Geological Society, 174(3), pp.453-467.

Grocott, J. & Vissers, R.L.M. 1984. Field mapping of the early Proterozoic KarratGroup on Svartenhuk Halvø, central West Greenland. Geological Survey ofGreenland Report,120,25–31.

Guarnieri, P., Partin, C.A Rosa. D. 2016. Paleovalleys at the basal unconformity of the Paleoproterozoic Karrat Group, West Greenland Geological Survey of Denmark and Greenland Bulletin, 35 (2016), pp. 63-66

Henderson, G. & Pulvertaft, T.C.R. 1967. The stratigraphy and structure of the Precambrian rocks of the Umanak area, West Greenland. Meddelelser fraDansk Geologisk Forening,17,1–20

Henderson, G. & Pulvertaft, T.C.R. 1987: Geological Map of Greenland, 1:10 0000, Mârmorilik 71 V.2 Syd, Nûgâtsiaq 71 V.2 Nord, Pangnertôq 72 V.2 Syd. Descriptive text. 72 pp., 8 plates. Copenhagen: Geological Survey of Greenland.

Hoffman, P.F., 1988. United plates of America, the birth of a craton: Early Proterozoic assembly and growth of Laurentia. Annual Review of Earth and Planetary Sciences, 16(1), pp.543-603.

Hoffman, P.F. 1990. Dynamics of the tectonic assembly of north-east Laurentia in geon 1.8 (1.9–1.8 Ga). Geoscience Canada , 17, 222–226.

Escher, J.C. and Stecher, O., 1978. Precambrian geology of the Upernavik–Red Head region (72 15′–75 15′ N), northern West Greenland. Rapport Grønlands Geologiske Undersøgelse, 90, pp.23-26.

Kalsbeek, F., Pulvertaft, T.C.R. and Nutman, A.P., 1998. Geochemistry, age and origin of metagreywackes from the Palaeoproterozoic Karrat Group, Rinkian belt, West Greenland. Precambrian Research, 91(3-4), pp.383-399.

Lewry, J.F., 1990. The Trans-Hudson Orogen: extent, subdivision, and problems. The Early Proterozoic Trans-Hudson Orogen of North America, pp.1-14.

Nielsen, T.F.D., 1990. Melville Bugt dyke swarm: A major 1645 Ma alkaline magmatic event in west Greenland. In International dyke conference. 2 (pp. 497-505).

Partin, C.A., Bekker, A., Corrigan, D., Modeland, S., Francis, D. and Davis, D.W., 2014. Sedimentological and geochemical basin analysis of the Paleoproterozoic Penrhyn and Piling groups of Arctic Canada. Precambrian Research, 251, pp.80-101.

Petford, N. and Atherton, M., 1996. Na-rich partial melts from newly underplated basaltic crust: the Cordillera Blanca Batholith, Peru. Journal of petrology, 37(6), pp.1491-1521.

Ramsay, J.G. and Huber, M.I., 1987. Modern structural geology. Folds and Fractures, 2, pp.309-700.

Ramsay, J.G., 1967. Folding and fracturing of rocks. Mc Graw Hill Book Company, 568.

Rosa, D., Dewolfe, M., Guarnieri, P., Kolb, J., LaFlamme, C., Partin, C., Salehi, S., Vest Sørensen, E., Thaarup, S. and Thrane, K., 2016. Architecture and mineral potential of the Paleoproterozoic Karrat Group, West Greenland. Danmarks og Grønlands Geologiske Undersøgelse Rapport, 12, p.98.

Rosa, D., Dewolfe, M., Guarnieri, P., Kolb, J., LaFlamme, C., Partin, C., Salehi, S., Sørensen, E.V., Thaarup, S., Thrane, K. & Zimmermann, R. 2017: Architecture and mineral potential of

the Paleoproterozoic Kar-rat Group, West Greenland – Results of the 2016 Season. Danmarks og Grønlands Geologiske Undersøgelse Rapport 2 017/5, 98 pp.

Rosa, D., Dewolfe, M., Guarnieri, P., Kolb, J., LaFlamme, C., Partin, C., Salehi, S., Sørensen, E.V., Thaarup, S., Thrane, K. & Zimmermann, R. 2017: Architecture and mineral potential of the Paleoproterozoic Kar-rat Group, West Greenland – Results of the 2017 Season. Danmarks og Grønlands Geologiske Undersøgelse Rapport 2018/19

Sanborn-Barrie, M., Thrane, K., Wodicka, N. and Rayner, N., 2017. The Laurentia–West Greenland connection at 1.9 Ga: new insights from the Rinkian fold belt. Gondwana Research, 51, pp.289-309.

Sørensen, E.V. and Guarnieri, P., 2017. Remote geological mapping using 3D photogrammetry: an example from Karrat, West Greenland. Geological Survey of Denmark and Greenland Bulletin, pp.63-66.

Sørensen, E.V. and Dueholm, M., 2017. Analytical procedures for 3D mapping at the Photogeological Laboratory of the Geological Survey of Denmark and Greenland. Geological Survey of Denmark and Greenland Bulletin, pp.99-104.

St-Onge, M.R., Van Gool, J.A., Garde, A.A. and Scott, D.J., 2009. Correlation of Archaean and Palaeoproterozoic units between northeastern Canada and western Greenland: constraining the pre-collisional upper plate accretionary history of the Trans-Hudson orogen. Geological Society, London, Special Publications, 318(1), pp.193-235.

Thompson, M.M., 1952. Development of photogrammetry in the U.S. Geological Survey, Bulletin 2 (2). Topographic Division, USGS, Washington, D.C

Thrane, K., Baker, J., Connelly, J. and Nutman, A., 2005. Age, petrogenesis and metamorphism of the syn-collisional Prøven Igneous Complex, West Greenland. Contributions to Mineralogy and Petrology, 149(5), pp.541-555.

Thrane, K. and Connelly, J.N., 2006. Zircon geochronology from the Kangaatsiaq–Qasigiannguit region, the northern part of the 1.9–1.8 Ga Nagssugtoqidian orogen, West Greenland. Geological Survey of Denmark and Greenland (GEUS) Bulletin, 11, pp.87-100.

Thrane, K., Connelly, J.N., Garde, A.A., Grocott, J. and Krawiec, A.W., 2003, April. Linking the Palaeoproterozoic Rinkian and Nagssugtoqidian belts of central West Greenland:

implications of new U-Pb and Pb-Pb zircon ages. In EGS-AGU-EUG Joint Assembly (p. 9275).

Van Kranendonk, M.J., St-Onge, M.R. and Henderson, J.R., 1993. Paleoproterozoic tectonic assembly of Northeast Laurentia through multiple indentations. Precambrian Research, 63(3-4), pp.325-347.

Whalen, J.B., Wodicka, N., Taylor, B.E. and Jackson, G.D., 2010. Cumberland batholith, Trans-Hudson Orogen, Canada: petrogenesis and implications for Paleoproterozoic crustal and orogenic processes. Lithos, 117(1-4), pp.99-118.

Wodicka, N., St-Onge, M.R., Corrigan, D., Scott, D.J. and Whalen, J.B., 2014. Did a proto-ocean basin form along the southeastern Rae cratonic margin? Evidence from U-Pb geochronology, geochemistry (Sm-Nd and whole-rock), and stratigraphy of the Paleoproterozoic Piling Group, northern Canada. Bulletin, 126(11-12), pp.1625-1653.

Zhang, Z., Zhao, G., Santosh, M., Wang, J., Dong, X. and Shen, K., 2010. Late Cretaceous charnockite with adakitic affinities from the Gangdese batholith, southeastern Tibet: evidence for Neo-Tethyan mid-ocean ridge subduction? Gondwana Research, 17(4), pp.615-631.